Advances in Iridium-Catalyzed C-H Borylation Enabled by 2,2'-Dipyridylarylmethane Ligands

By

Margaret Rose Jones

Dissertation

Submitted to the Faculty of the

Graduate School of Vanderbilt University

in partial fulfillment of the requirements

for the degree of

DOCTOR OF PHILOSOPHY

in

CHEMISTRY

August 13th, 2021

Nashville, Tennessee

Nathan D. Schley, Ph.D. (Advisor)

Jeffrey N. Johnston, Ph.D.

Timothy P. Hanusa, Ph.D.

Paul E. Laibinis, Ph.D.

Dedicated to my future self;
Whenever you are lost, may you always find the strength to get back up, recognize your progress, and persevere. Whenever you are triumphant, may you find the humility, discipline, and curiosity to acknowledge your beginnings.

“If you know the way broadly, you will see it in all things”
– Miyamoto Musashi

ACKNOWLEDGMENTS

There are a number of people who have played an integral role in my success and ability to maintain my sanity during my years in graduate school. First and foremost, I would like to recognize and thank my advisor, Dr. Nathan Schley. When I first began my graduate school journey, organometallic chemistry was merely a side interest of mine, as I considered myself more traditionally organic focused; I am grateful to have taken Nathan's organometallics course and completed a rotation in his lab during my first semester at Vanderbilt. It was then that I found I not only had a deep interest for the projects in the group, but also truly enjoyed Nathan's mentorship style. I appreciated that he was always willing to come into lab to demonstrate proper technique or reaction setup and was always available to discuss project ideas or explain unfamiliar concepts, however, he also allowed me an incredible degree of freedom to explore my own ideas and learn independently. I always felt supported and encouraged to advance my own understanding and was constantly impressed by the depth of his knowledge. None of this work would have been possible without his guidance, expertise, and support.

Completing my degree in the Schley lab was a particularly special experience, as I had the opportunity to be one of the founding two grad student cohorts of the group. While we did not have any senior students to guide our journey through grad school, I am thankful to have had Ben Mueller, Scott Chapp, Caleb Jones, and Caleb Fast around the lab learning alongside me. While our small group was constantly working on divergent project ideas, there were always things to learn from each of them. I appreciate our unique experience and am excited to see all of their projects grow and expand with Nathan's research program in future years. Similarly, I can't wait to see how our little cohort of founding Schley-guys advance in our personal lives and careers; I have the utmost faith in the success of each one of them. I also would like to acknowledge Trey Carter and Griffin Perry, who joined the group more recently. Both of them have already demonstrated incredible skill, work ethic, and passion for chemistry, and make for excellent additions to the group.

While there were no senior students around the Schley lab when I was a younger student, I was fortunate to have had the opportunity to connect with and learn from older graduate students during my rotations in the labs of Dr. Gary Sulikowski and Dr. Jeffrey

Johnston in my first year. Both research programs generate excellent chemists, and I consider these rotations to have been incredibly supportive in the development of my organic synthesis skillset. I would like to particularly thank Dr. Robert Davis and Dr. Thomas Struble, who each acted as my mentors during these rotations and taught me a number of valuable concepts and lab techniques. I also am grateful to have befriended Dr. Jeanette Bertron of the Lindsley lab during our time in graduate school, as she is not only a skilled organic chemist but also a great friend and confidant.

I am incredibly grateful for the support of my loving husband, Harley, and our adorable pup, Cora. Despite the roller coaster of moods that comprised my graduate experience, these two were always by my side, making sure I felt loved, supported, happy, and fed. These past few years have certainly been rough at times, but these two made it much easier and always kept me moving forward. I also would like to thank my dad, who fostered my curiosity from a young age, has always supported me, and always encouraged me to work hard for what I want. My brothers, Nick, Dan, and Sam have always provided a source of healthy competition, as we encourage each other to progress in our own lives and careers into adulthood. I love each one of you and am glad to call each of you family.

My success in graduate school, and in life, has also been greatly supported by my wonderful training partners and coaches at Artista Brazilian Jiu Jitsu, as well as the broader community within the sport of Jiu Jitsu. Through the sport I have gained confidence, resilience, and discipline, attributes which transcend the mats and play a crucial role in my success in other areas of life, including my research. Most importantly, I have been fortunate to meet incredible people through training, friends of all backgrounds and walks of life, who always are there to encourage me to work my hardest, celebrate each other's wins, and support me even when I feel like I can't get back up. Thank you for your never-ending support, it is difficult to imagine that I could've persevered through the herculean task of a Ph.D. without the stress relief and support I've gained from training.

TABLE OF CONTENTS

LIST OF TABLES

LIST OF FIGURES

CHAPTER 1

Advances in Transition Metal Catalyzed C-H Borylation: Ligand Platforms for Increasingly Active or Selective Catalysts

1.1 Introduction

The direct functionalization of C-H bonds has garnered considerable attention in recent decades as a means of rapid elaboration of feedstock chemicals. Hydrocarbons, particularly saturated hydrocarbons, though widely abundant and low cost as components of crude oil, have long been considered inert due to the high bond energies and low acidity of unactivated C-H bonds.[1] Borrowing from the sophisticated specificity of enzymatic systems, the development of a vast arsenal of efficient and highly site-selective methods for direct C-H functionalization of organic molecules to generate higher value products is considered a “Holy Grail” in synthetic chemistry.[2,3] Nature has accomplished the feat of selective and efficient C-H functionalization at ambient temperatures through oxygenases, such as cytochrome P450s, inspiring the development of analogous and broadly applicable molecular organometallic catalysts. Originating with the stoichiometric activation of inert carbon-hydrogen bonds at late transition metals, organometallic C-H functionalization has since evolved to promote a diverse array of catalytic bond constructions, ranging from the repurposing of low-value materials to the late-stage derivatization of privileged organic molecules. While far less intricate than the complex molecular recognition of enzymatic systems, design of increasingly active or selective catalysts has been largely driven by the introduction of ligand platforms which facilitate tuning of the chemical environment about the metal center.

C-H functionalization is widely attractive as an environmentally benign and economical synthetic tool, owing to reduction in need for toxic reagents, minimization of byproduct generation, elimination of unnecessary synthetic steps, and the potential to provide routes to previously inaccessible products.[4] Among desirable transformations to emerge from studies of C-H activation is the direct borylation of C-H bonds, which provides a method of preparing synthetically versatile organoborane products directly from aryl, heteroaryl, and alkyl precursors.[5] Extensive work over the past several

decades has led to the development of relatively mature sp^2 C–H borylation methodology, with modern strategies aimed at addressing a host of issues in usability, functional-group tolerance, and selectivity.[6–9] The corresponding borylation of aliphatic sp^3 C–H bonds remains relatively underdeveloped, limited by harsh reaction conditions, a requirement for catalysis in neat substrate, and incomplete conversion of the diboron reagent. The ultimate goal of achieving highly active and selective catalysts for the industrially viable application of sp^3 C-H functionalization still remains, though significant progress has been accomplished in recent years.

1.2 Overview of Transition Metal Mediated C-H Activation and Functionalization

The reactivity of hydrocarbons has long been demonstrated using both organometallic and non-metallic reagents. Classical C-H activation methods involve electrophilic or free radical mechanisms, rendering this chemistry poorly selective, and not readily amenable to development of catalytic processes.[10,11] Shortcomings of methodologies that relied on radical intermediates generated an impetus to develop concerted C-H oxidative addition processes at low valent transition metals, a mode of C-H activation which would enable control and tunability of these parameters for a wide range of substrate types.[1,12] Originally, this transformation was considered infeasible for both stoichiometric and catalytic processes due to proposed thermodynamic instability of the metal(alkyl)hydride with respect to alkane reductive elimination.[1] With the proper choice of supporting ligand sets however, organometallic systems capable of intermolecular, stoichiometric C-H oxidative activation were identified beginning in the early 1980s.[2,3,11,12] Eventually, these pioneering studies fostered the evolution of a wealth of catalytic processes for the direct functionalization of hydrocarbons.

1.2.1 Generation of Metal-Alkyl and -Aryl Complexes by C-H Activation

Early evidence for activation of both aryl and alkyl C-H bonds by oxidative addition was noted by H-D exchange with D_2O using the Pt(II) salts K_2PtCl_4 and Na_2PtCl_4, marking a pivotal discovery in the field (**Figure 1.1**).[1,13,14] Comparison of the H-D exchange rate across aromatic substrates bearing substituents of varied electronic character shows no marked influence across substituent types, indicating exchange by oxidative addition rather than an electrophilic substitution mechanism.[13] Shilov and

coworkers have also illustrated the use of these Pt(II) salts in the functionalization of alkanes to alkyl halides and alcohols, with the addition of $[Pt(IV)Cl_6]^{2-}$ as an oxidant (**Figure 1.2**).[12,15,16] Later mechanistic study of this work confirmed the involvement of oxidative addition and proton abstraction either directly from the sigma-bound complex or from the alkane upon addition to the metal center, producing an alkyl-Pt complex.[17–19] While this method is catalytic in Pt(II), the need for stoichiometric Pt(IV) oxidant precludes this functionalization from further application.

Figure 1.1: *H/D exchange of hydrocarbons with D_2O/CH_3COOD catalyzed by Pt(II) salts*

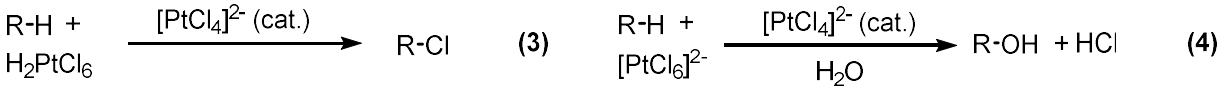

Figure 1.2: *C-H activation and functionalization by Pt(II) salts*

Cases involving the cyclometallation of alkyl- or aryl-containing coordinated groups were among the earliest observations of C-H activation, lending greater credence to speculation of an oxidative addition mechanism.[12] Select influential works demonstrating intramolecular C-H oxidative addition via cyclometalation at late transition metal complexes are displayed in **Figure 1.3**. Square planar d^8 iridium complexes, such as Vaska's complex, were shown to undergo ortho cyclometalation of sp^2 C-H bonds of aryl phosphine[20,21] (1) or diazobenzene[22] (2) ligands to yield an isolable σ-aryl complex. Initial examples of sp^3 C-H bond activation to generate metallocycles were similarly demonstrated in the case of methyl phosphines[23] (3) or metal alkyls[24] (4). In each case an oxidative mechanism is indicated by the resultant octahedral metal hydride complex, or the loss of a hydride equivalent in the case of (4). For a more comprehensive treatment of cyclometalation examples, mechanisms, and outlooks, please see the following review.[25]

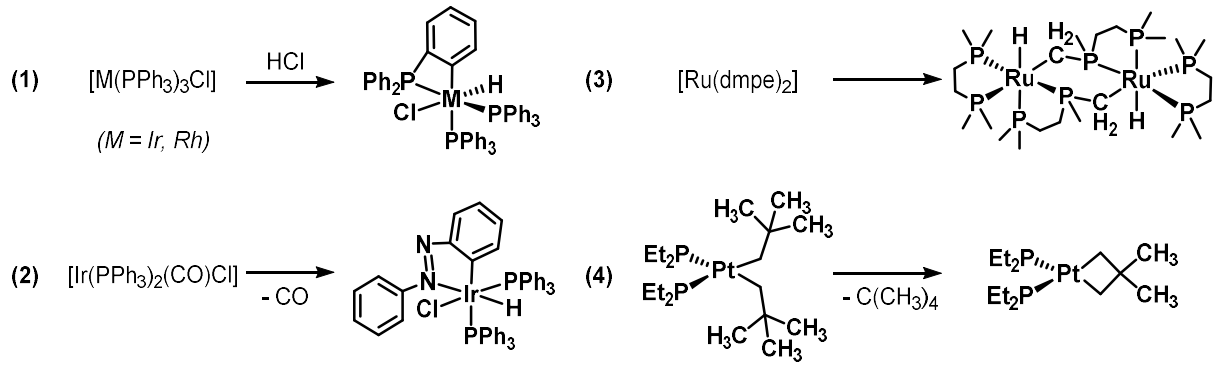

Figure 1.3: *Early literature examples of C-H activation by ligand ortho-cyclometalation*

Seminal examples of intermolecular C-H bond activation to give isolable organometallic compounds were reported in the early 1980s at pentamethylcyclopentadienyl (Cp*) complexes of iridium and rhodium, soon followed by several other second- and third- row late transition metal complexes.[3] The general reaction requires initial activation of the metal complex via dissociation or reductive elimination of a spectator ligand, promoted either thermally or by photolysis. From the resultant low-valent, coordinatively unsaturated metal species, oxidative addition of inert C-H bonds occurs readily to give the corresponding metal(alkyl)hydride product (**Figure 1.4**).

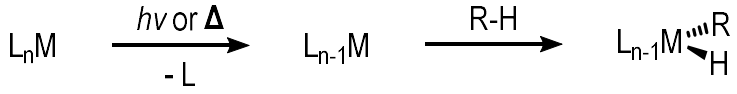

Figure 1.4: *General scheme for stoichiometric oxidative addition of C-H bonds*

This process was first observed at iridium by the Bergman and Graham groups using $[Cp^*IrH_2(PMe_3)]$[10,26] and $[Cp^*Ir(CO)_2]$[27], respectively. The analogous rhodium complex, $[Cp^*RhH_2(PMe_3)]$, was also described.[28,29] In each of these examples, photolytic loss of either dihydrogen or CO gives a reactive 16 electron Ir(I) or Rh(I) intermediate, which then undergoes oxidative addition of the hydrocarbon solvent to generate [Cp*LM(H)(R)] (**Figure 1.5**). Hydrocarbon solvents demonstrated to undergo C-H activation include simple arenes, and branched, linear, and cyclic alkanes Competition experiments of C-H activation at Cp*Ir and Cp*Rh complexes revealed general trends in rate consistent with preference for formation of stronger metal-carbon bond, rather than expected proclivity towards reaction with weaker C-H bonds.[27,30,31]

This is demonstrated by the superior rate of activation of stronger sp^2 C-H bonds versus sp^3 C-H bonds, and by the 10-50 fold rate of primary C-H activation relative to reaction of secondary C-H bonds (**Figure 1.6**).[28]

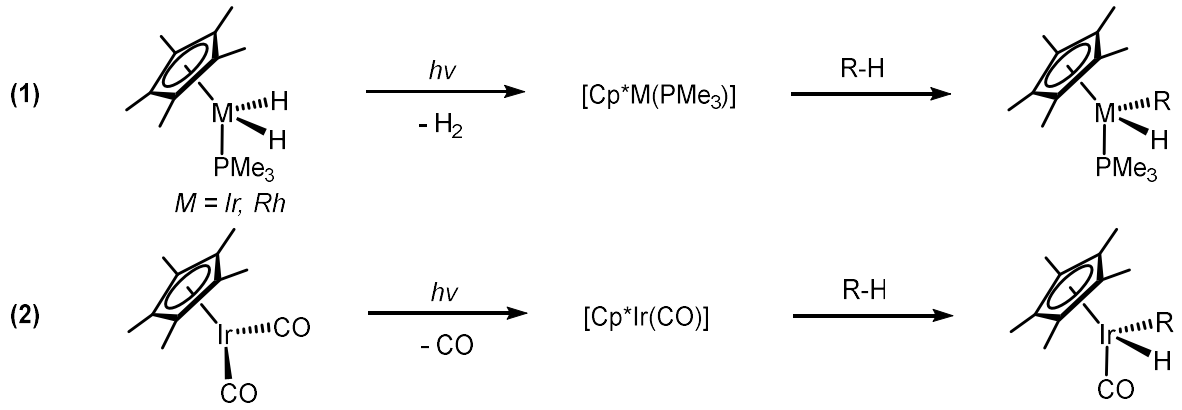

Figure 1.5: *C-H activation at Cp*Ir and Cp*Rh complexes*

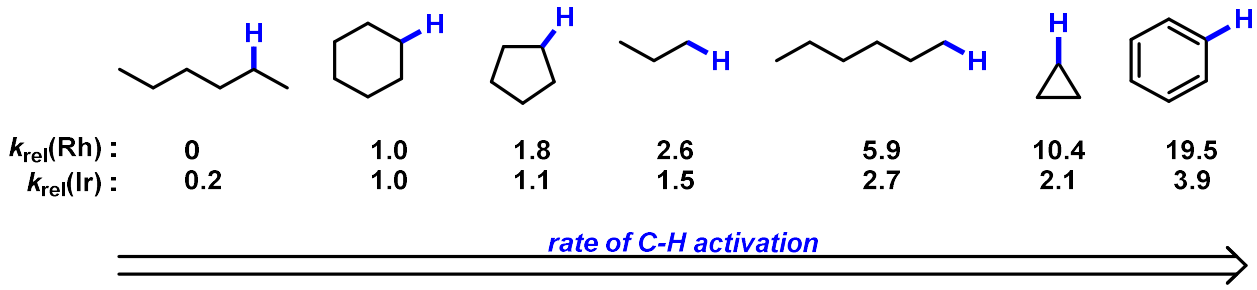

Figure 1.6: *Relative rates of C-H activation at Cp*Ir and Cp*Rh complexes*

1.2.2 Transition Metal Mediated C-H Functionalization

Incredible strides in C-H oxidative addition allowing for the preparation of σ-alkyl and -aryl complexes enabled the development of homogenous organometallic catalysts for the functionalization of unactivated hydrocarbons. Further elaboration of organic molecules from the generated M-C species can be envisioned utilizing reagents which effect elementary organometallic transformations. Additions of olefins or carbonylation can be achieved through subsequent migratory insertion, beta elimination can provide dehydrogenated products from alkane substrates, sigma metathesis could generate coupled products, or treatment with an oxidant can facilitate a host of redox functionalizations through reductive elimination pathways.[2,32] Functionalization by

reductive elimination can be further classified as non-oxidative (wherein the coupling reagent acts as the oxidant), oxidative (requiring an external oxidant), or dehydrogenative (C-H + X-H → C-X + H_2).[32] A generalized overview of potential reaction types involving C-H functionalization is presented in **Figure 1.7.**

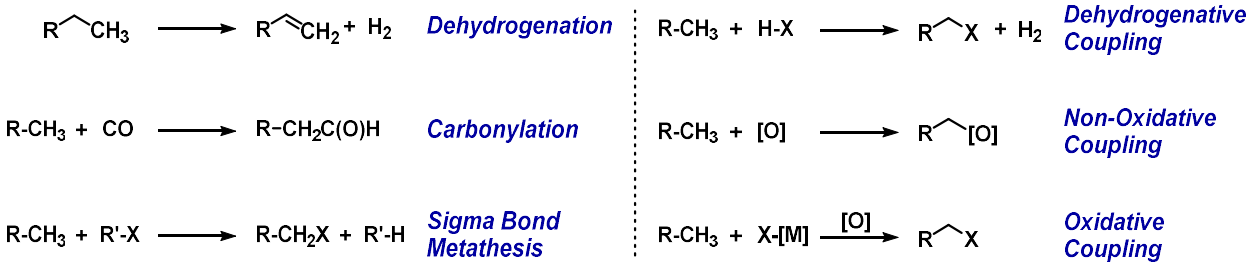

Figure 1.7: *Classification of types of C-H functionalization reactions*

Although metal-mediated activation of both sp^2 and sp^3 C-H bonds have been explored contemporaneously, the direct functionalization of unactivated alkanes has lagged in development by comparison. The functionalization of alkane feedstocks, particularly methane, is highly sought after for purposes of liquifying methane for transport, preparation of higher order hydrocarbons, and improved economy of fine chemical production.[2,3,12,16,33] Despite the sp^3 bond constituting the weaker of these two C-H bonds, alkanes present a prominent challenge to C-H functionalization due to their far lower acidity, low polarity, and preferential reactivity of functionalized products over alkane substrate. Methods of sp^3 C-H activation also selectively distinguish between similarly unreactive C-H bonds elsewhere in organic substrates or of solvent.[5]

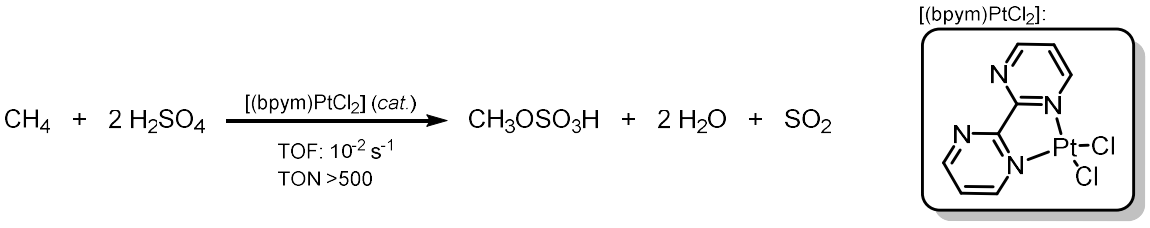

Figure 1.8: *Pd-catalyzed conversion of methane to methyl bisulfate*

The Shilov chemistry detailed previously (section 1.2.1; **Figure 1.2**) represented a seminal advance in metal catalyzed alkane functionalization, facilitating the chlorination of unactivated hydrocarbons. However, while this reaction is catalytic in Pt

(II), the requirement for stoichiometric Pt (IV) precludes its application. Successive efforts have sought alternative oxidants as a means to render Shilov-type functionalization of methane industrially viable. With a shift towards the use of a bipyrimidine-supported Pt(II) catalyst and SO_3/H_2SO_4 as an oxidant, Periana and coworkers later adapted this method for the conversion of methane to methyl bisulfate (**Figure 1.8**).[34]

An additional class of C-H functionalization unique to alkane substrates is beta-dehydrogenation to generate olefin products. Iridium complexes for reactions of this type were originally described by the laboratories of both Crabtree and Felkin, yielding olefin products with remarkably high catalyst turnover (**Figure 1.9**).[35–37] The use of homogenous catalysts affords improved control over selectivity of dehydrogenation, with kinetic selectivity for terminal functionalization of linear alkanes.[35] Unfortunately, practical application of dehydrogenation remains limited by secondary isomerization of the α-olefin product, granting a mixture of internal alkenes.[38] This has been largely addressed by improved catalyst design involving the use of pincer ligands, use of hydrogen acceptor additives, or pairing dehydrogenation to additional processes (i.e. metathesis).[2,16]

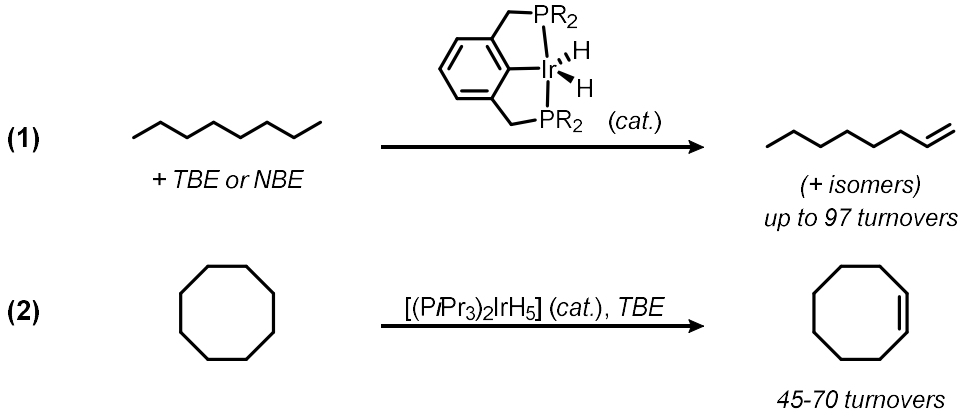

Figure 1.9: *High turnover dehydrogenation catalyzed by* ***(1)*** *[(PCP)IrH$_2$] (R = tBu or iPr) or* ***(2)*** *[(PiPr$_3$)$_2$IrH$_5$]. TBE = t-butylethylene, NBE = norbornene*

In the late 60s and 70s, concurrently with Shilov chemistry, the application of C-H activation to Pd(II) catalyzed oxidative C-C bond formations was also investigated, through treatment of unactivated arenes with CO or olefins. Fujiwara and coworkers reported the $Pd(OAc)_2$ catalyzed olefination of arenes to generate vinylarene products.

In this reaction, $Cu(OAc)_2$ is used as an oxidant to facilitate turnover of the reduced Pd center.[39,40] Similarly, the Fujiwara group also demonstrated Pd-catalyzed direct C-H carboxylation of both arenes and alkanes from CO (**Figure 1.10**).[41,42] Ru catalysts, first described by Murai and coworkers, have been employed in analogous arene oxidative C-H olefinations, however, this method requires the use of substrates containing ortho-chelating functionality for both reactivity and site selectivity.[43,44] Many oxidative C-H functionalization methods have been developed since, aiming to incorporate not only carbon but various other elements such as heteroatoms, halogens, and main group Lewis acids into unactivated hydrocarbons. Currently, the field offers expansive solutions for the diverse functionalization of C-H bonds, influenced greatly by these inceptive works.

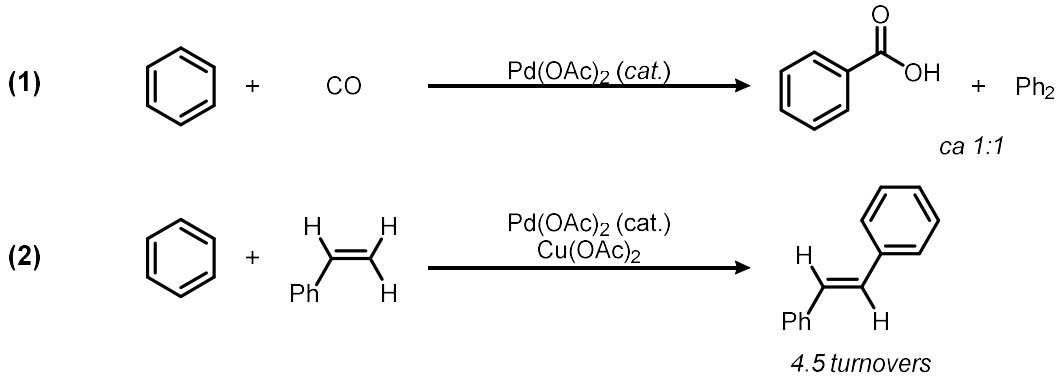

Figure 1.10: *Pd-catalyzed C-H carboxylation* ***(1)*** *and olefination* ***(2)*** *of benzene*

1.2.3 Emergence of C-H Borylation

One of many oxidative functionalization methods to arise from the study of C-H cleavage by homogenous transition metal complexes is the direct borylation of hydrocarbons. C-H borylation enables the synthetically efficient preparation of versatile organoborane products from hydrocarbons with reliable regioselectivity. Earlier well-established methods, such as hydroboration and Miyaura borylation of organohalides, have resulted in widespread use of organoboranes as intermediates in the synthesis of complex molecules (**Figure 1.11**).[45,46] In contrast to these alternative preparations, C-H borylation provides a direct, sustainable route to organoborane products, bypassing the

necessity for their synthesis through multistep transformations and hazardous halogenated reagents.

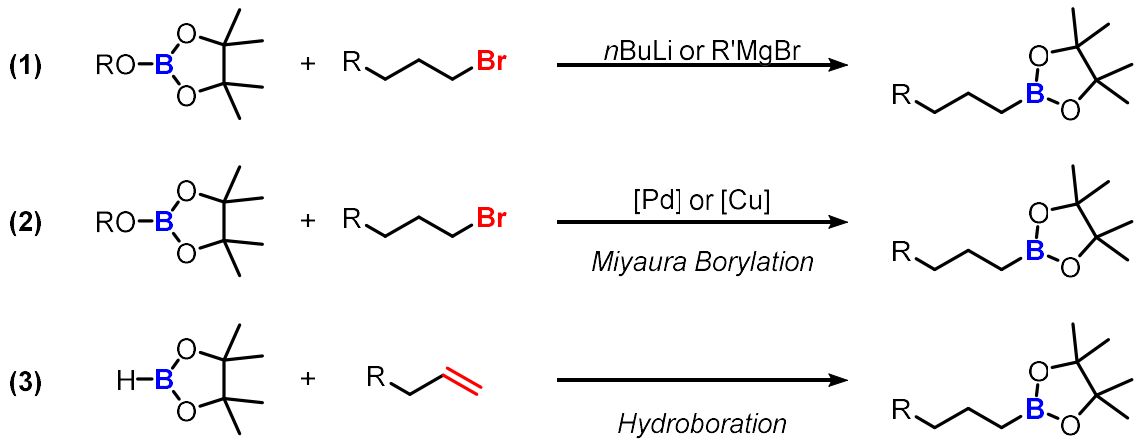

Figure 1.11: *Methods of organoborane synthesis;* ***(1)*** *Metal-halogen exchange* ***(2)*** *Miyaura borylation of alkyl halides* ***(3)*** *hydroboration of olefins.*[45,46]

Canonical transition metal-boryl complexes were originally prepared from Wilkinsons catalyst, [$RhCl(PPh_3)_3$], and catecholborane (HBcat), soon followed by the first report of a tris-boryl complex derived of [(Ind)Ir(cod)] and HBcat.[47,48] Stoichiometric C-H borylation by transition metal-boryl complexes was first realized using [$CpFe(CO)_2Bcat$], generating phenyl-Bcat from benzene solvent upon irradiation with UV light (**Figure 1.12**).[49] Later, Cp* σ-boryl complexes of W, Ru, and Re were also shown to effect the direct borylation of hydrocarbon solvent under photochemical conditions, following the liberation of a CO ligand (**Figure 1.13**).[50,51] Organoplatinum complexes, reminiscent of classical Shilov examples of C-H activation, also exhibit reactivity with diboron reagents to generate a bis-boryl platinum species and organoborane.[52] Archetypal C-H activation complexes, [$Cp^*IrH(R)(PMe_3)$], were later used to demonstrate borylation of a σ-alkyl or σ-aryl with pinacolborane (HBpin), yielding metal-boryl and organoborane products (**Figure 1.14**).[53] These stoichiometric findings would represent individual steps relevant to the inception of catalytic systems, allowing for turnover under appropriate conditions.

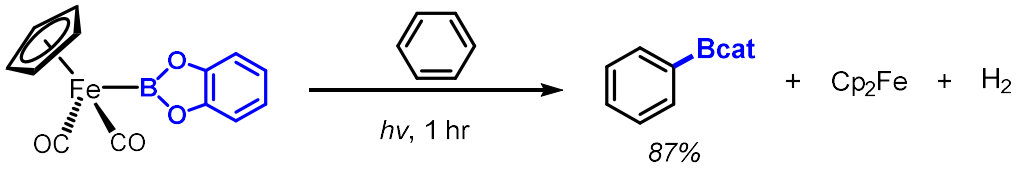

Figure 1.12: *C-H borylation of benzene solvent from [CpFe(CO)$_2$(Bcat)]*[49]

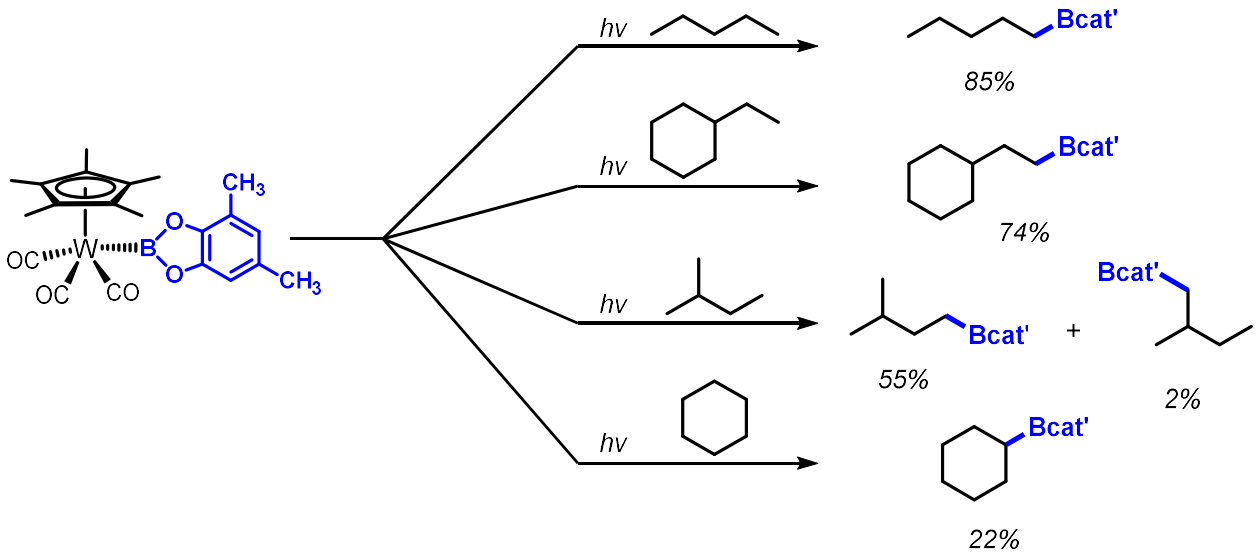

Figure 1.13: *C-H borylation of alkanes by [Cp*W(CO)$_3$(Bcat')]*[50]

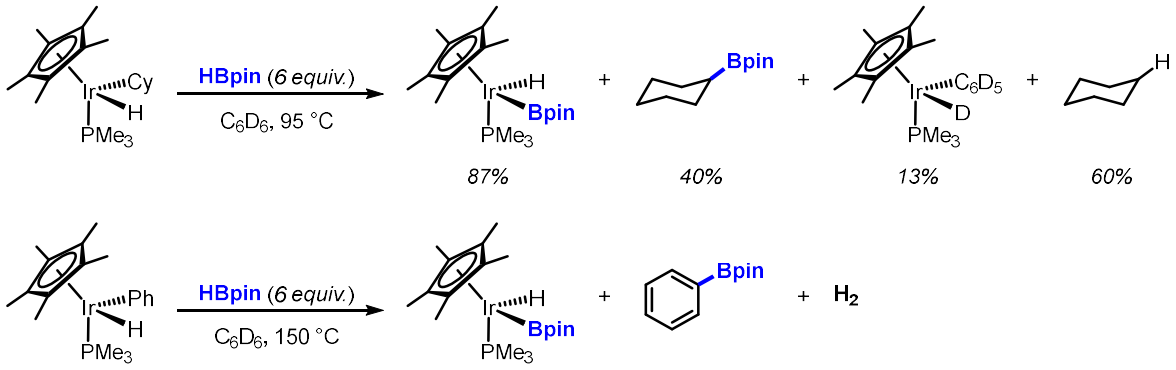

Figure 1.14: *Generation of organoboranes by treatment of Cp*Ir -alkyl and -aryl complexes with HBpin*[53]

Primary reports of thermal catalytic C-H borylation were demonstrated soon after, which made use of transition metal Cp* catalysts and either HBpin or B_2pin_2 as the borylating agent. Catalytic arene and alkane C-H borylation were both accomplished near the turn of the century by the Smith and Hartwig groups, respectively.[51,53–55] Soon

after, a transition to 4,4′-bipyridine (bipy) or 1,10- phenanthroline (Phen) supported iridium catalysts gave reduced temperatures, more accessible catalysts, and improved scope. While a number of catalysts derived from these examples have exhibited success, ligand systems for catalytic C-H borylation remain largely based upon these diimine backbones of bipy and phen. Extensive work over the past several decades has led to the development of relatively mature sp^2 C–H borylation methodology for many classes of arene and heteroarene substrates, with modern methods offering a host of strategies to address issues of usability, functional-group tolerance, and selectivity. While the corresponding borylation of aliphatic sp^3 C–H bonds is also continuously evolving, methods for this more challenging reaction remain relatively underdeveloped.

1.3 Transition Metal Catalyzed sp^2 C-H Borylation

1.3.2 Overview of seminal sp^2 C-H borylation catalysts and ligand types

In 1999, Smith and coworkers reported the cardinal example of catalytic arene C-H borylation, the borylation of benzene solvent from pinacolborane (HBpin) catalyzed by 17 mol% [Cp*IrH(PMe_3)(Bpin)] (**Figure 1.15**).[53] Requisite to this discovery was the transition to pinacol borylating reagents, as borane substitution was determined to have a profound effect on both rate of B-C bond formation and catalyst speciation. The Rh analogue, [Cp*Rh(C_6Me_6)], was later found to give a marked improvement in turnover number when used as pre-catalyst, as well as effective borylation of arenes in cyclohexane solvent (**Figure 1.16**).[55–57] Exploration of substrate scope with the Cp*Ir and Cp*Rh catalysts revealed higher yields and faster reaction rate with electron deficient arene substrates.[56] While both Ir and Rh display this trend in reactivity, Cp*Ir pre-catalysts display more pronounced rate differences in competition experiments of equimolar amounts of monosubstituted arene and toluene.[56]

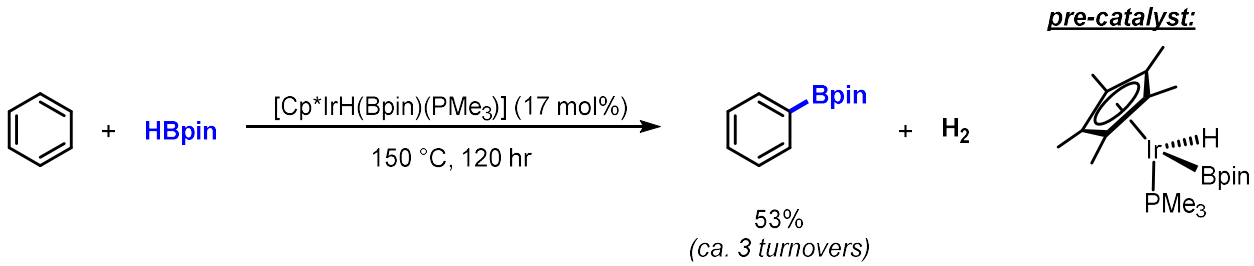

Figure 1.15: *Cp*Ir catalyzed borylation of benzene*[53,55]

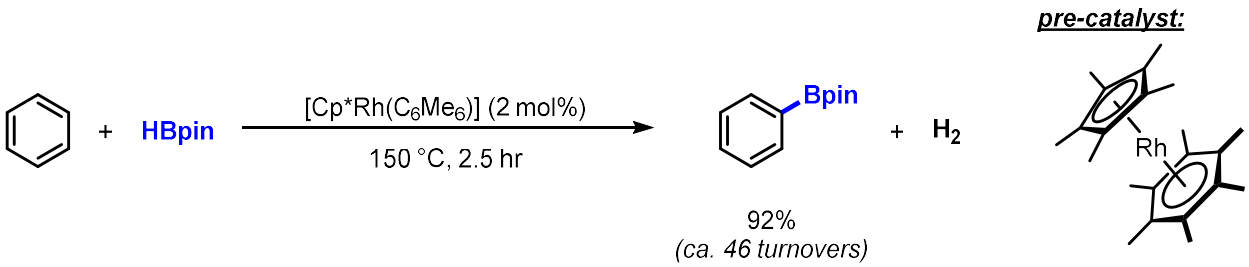

Figure 1.16: *Cp*Rh catalyzed borylation of benzene*[53,54]

Further exploration of iridium pre-catalysts was instrumental in the application of additional ligand types for the modulation of catalyst features as well as improved conditions for the C-H borylation reaction. Smith and coworkers pioneered the use of [(Ind)Ir(cod)] and [(Mes)Ir(Bpin)$_3$] pre-catalysts, which, in conjunction with various phosphine ligands, produced a dramatic improvement in catalytic activity and selectivity relative to earlier Cp* catalysts. Use of these pre-catalysts along with bis(diphenylphosphino)ethane (dppe) permitted the borylation of multiple arenes in excellent yields, with tolerance for alkyl, alkoxy, ester, and halogen substituents.[54] The intermediacy of an Ir(III) species was also demonstrated in this work through the preparation and study of the complexes *fac*-[(PMe)$_3$Ir(Bpin)$_3$] and [(PMe)$_4$Ir(Bpin)].[54] Later studies of phosphino iridium boryl complexes display the necessity of appropriate P:Ir ratio in the generation of active species for the borylation reaction. Tuning of steric demand about bis-phosphine ligands through use of 1,2-bis(diisopropyl-phosphino)ethane (dippe) minimized the formation of catalytically inactive phosphine-bridged iridium dimers as observed with dmpe.[58] Similarly, slight excesses of monodentate phosphines have been noted as detrimental to borylation yields through sequestration of iridium in the form of coordinatively saturated species.

Analogous iridium (I) cod pre-catalysts were studied concurrently by the Hartwig group in concert with substituted dipyridyl ligands.[59,60] Use of the pre-catalyst/ligand combination of [(cod)IrCl]$_2$/2,2'-bipyridine (bpy) permitted C-H borylation of a suite of substituted arenes from HBpin at far milder temperatures than previous reports, ranging from room temperature to 80 °C. Further improvement came from the use of [(coe)$_2$IrCl]$_2$ (coe = η^2-cyclooctene) along with di-*tert*-butyl-2,2'-bipyridine (dtbpy), enabling the borylation of benzene with exceedingly high catalyst turnover (as high as 8000 TOs) using B$_2$pin$_2$ as the boron source (**Figure 1.17**).[59] Subsequent studies of Ir (I) precursors

focused on varying the anionic ligand to allow for more facile catalyst activation, resulting in the application of [(cod)IrOMe]$_2$/dtbpy to C-H borylation of arenes and heteroarenes with a stoichiometric ratio of B_2pin_2:substrate.[60]

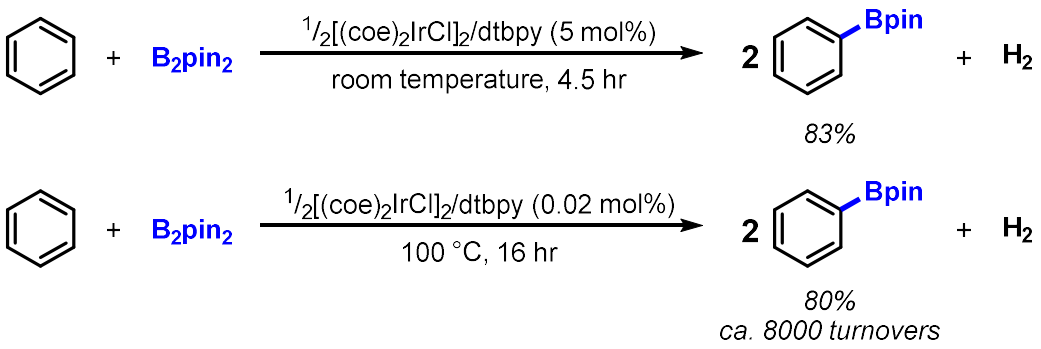

Figure 1.17: *High turnover borylation of benzene by [(coe)$_2$IrCl]$_2$/dtbpy*[59]

The success of original Cp*Ir and Rh catalysts encouraged the pursuit of analogous facially coordinated monoanionic ligands. Hydrotris(pyrazolyl)borate (Tp) iridium and rhodium catalysts were found to effect the C-H borylation of arenes, either from the preformed TpM complex or by *in-situ* generation of the active catalyst from KTp and [(cod)MCl]$_2$.[61] Alternatively, pincer-supported catalysts, pre-generated from monoanionic meridional ligand complexation, have also been shown to catalyze the C-H borylation of arenes. Bis(oxazolinyl)phenyl (phebox) iridium compounds readily undergo C-H activation for the preparation of isolable σ-aryl complexes and were shown to catalyze the borylation of arenes in modest yields.[62] POCOP-pincer iridium catalysts investigated by Ozerov and coworkers provide remarkable turnover numbers exceeding 20,000 for the borylation of benzene from HBpin.[63] These works suggest the importance of catalyst geometry, tunability, and accessibility in the C-H borylation reaction.

In recent years, numerous advances by way of catalyst development for arene C-H borylation have been realized. Comprehensive studies have investigated parameters involved in reaction scalability, high throughput screening, and catalytic efficiency.[64] Significant study of inherent selectivity trends and development of directed borylation methods have also been undertaken, described in further detail in Ch. 3.[9,32,65,66] Conditions which enable pairing to additional transformations in one-pot syntheses[67–76], as well as use in total syntheses[77–80] have also demonstrated both the versatility of organoborane products and utility of the Ir/dtbpy catalyst.

1.3.3 Mechanism of sp^2 C-H borylation by Diimine Ir Catalysts

The accepted mechanism of diimine/Ir catalyzed C-H borylation of arenes proceeds via the Ir^{III}/Ir^{V} cycle depicted in (**Figure 1.18**). Catalyst activation is proposed to involve initial coordination of the diimine ligand and oxidative addition of the boron reagent to an Ir^{I} precatalyst, generating Ir^{III} tris boryl complex **A**. Isolation of [(dtbpy)Ir(Bpin)$_3$] and identification as the catalyst resting state was accomplished by the Hartwig group (**Figure 1.18**).[81] **A** is speculated to undergo rate-limiting oxidative addition to aryl C-H bonds, giving Ir^{V} complex **B**. Product organoborane is expelled by reductive elimination, and the corresponding iridium hydride **C** is recycled by reaction with another equivalent of boron reagent. For arene substrates, both B_2pin_2 and HBpin can act as effective borylating agents; when B_2pin_2 is used, HBpin byproduct re-enters the catalytic cycle to form a second equivalent of organoborane and dihydrogen.[8,82]

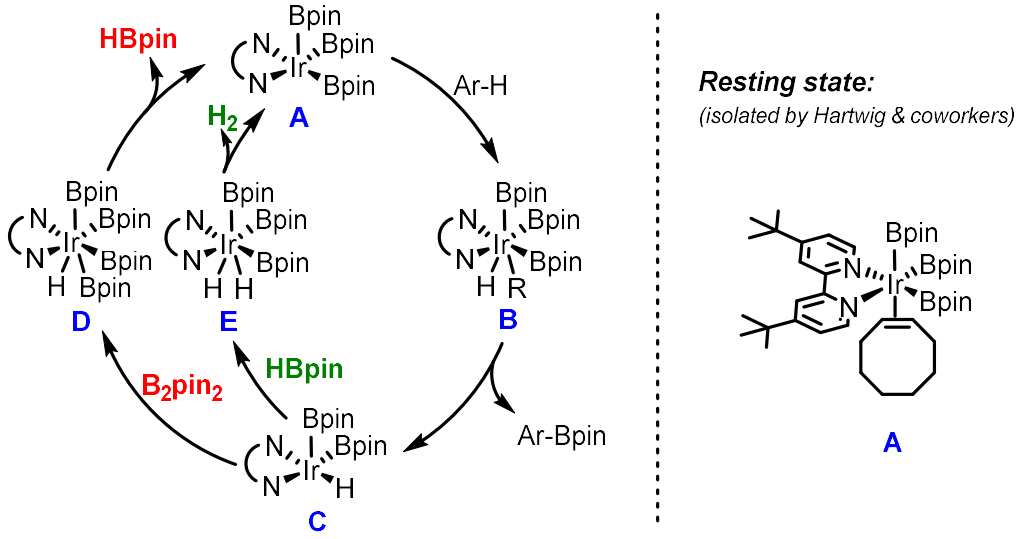

Figure 1.18: *General mechanism for the Ir-catalyzed C-H borylation of arenes and heteroarenes from B_2pin_2 or HBpin (left); Isolated resting state **A** (right)*

With the established general mechanism in mind, continued development of increasingly active catalysts has focused on ligand modifications which either provide desirable electronic and steric features or mitigate catalyst decomposition. One such pathway has been demonstrated in the case of bipyridine ligand borylation; ortho borylation of bpy sterically inhibits metal coordination resulting in an inactive catalyst.[83,84] Notably, the use of dtbpy rather than unsubstituted bpy provides a more

active, electron-rich alternative while also impeding ligand borylation, maintaining greater concentrations of active catalyst.[60] Comparison of dtbpy and me$_4$phen showed that dtbpy is more prone to ligand dissociation and gives shorter catalyst lifetime, despite the nearly identical electronics of the resulting tris-boryl complexes.[84] It has also been remarked that use of conformationally rigid ligands, such as me$_4$phen, is vital to catalyst speciation by disfavoring k^1 ligand binding or complete dissociation (**Figure 1.19**). This effect has been observed as more important to catalyst function than electron richness of the ligand.[64]

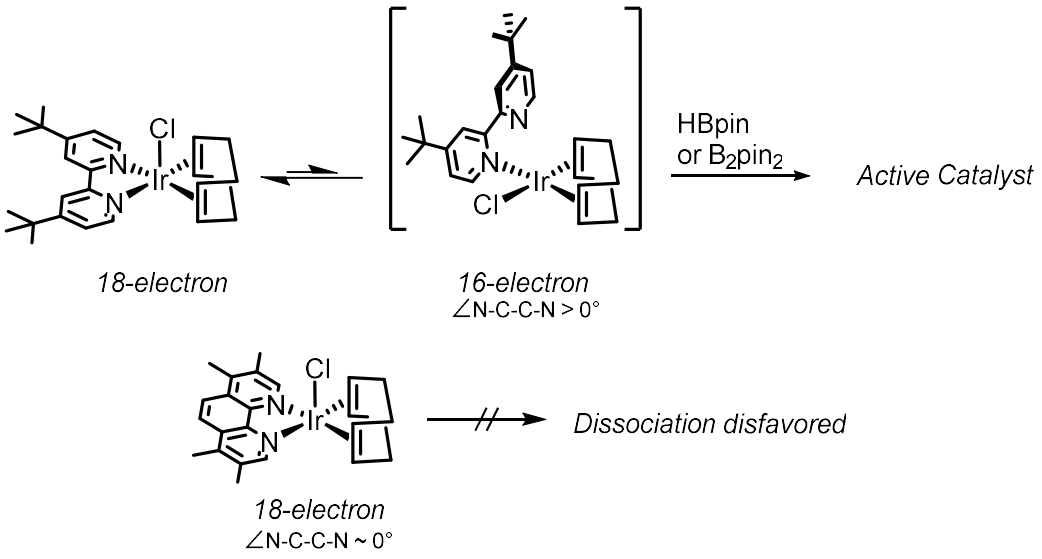

Figure 1.19: *Comparison of binding modes and catalyst lifetime using dtbpy and Me$_4$phen*[64,84]

1.4 Transition Metal Catalyzed sp^3 Borylation

The corresponding catalytic borylation of unactivated sp^3 C-H bonds presents unique challenges to catalyst activity and chemoselectivity. Despite near-simultaneous initial reports of sp^2 and sp^3 C-H borylation catalysts, aliphatic borylation remains largely underdeveloped by comparison. Practical application of the sp^3 borylation reaction is predicated on the design of accessible catalysts which promote scalable, selective, and sustainable functionalization of C-H bonds.[2] The synthetic versatility of organoborane products and exceptional selectivity for terminal C-H bonds[85] distinctly afforded by borylation catalysts implicates such methods as advantageous for the elaboration of feedstock chemicals or late stage functionalization of complex molecules.

Limitations which currently preclude such application of existing C-H borylation catalysts include requirement for solvent quantities of substrate, incomplete economy of the boron reagent, poor functional group tolerance, and necessity for high temperatures in order to achieve reasonable reaction rates. Challenges to atom-economy of sp^3 borylation can be attributed to the near thermoneutral conversion of pinacolborane to alkyboronate and dihydrogen, though the reaction is overall both kinetically and thermodynamically favored.[5] Alkane borylation also suffers a kinetic disadvantage—metal-mediated C-H bond cleavage has long been acknowledged to occur at much slower rate for alkyl C-H bonds respective to aryl C-H bonds, represented in the relative rates of aryl and alkyl borylation.[26,30] As a result, alkane C-H borylation requires more forcing conditions to achieve high yields on an acceptable time scale.

1.4.1 Catalysts for Unactivated sp^3 C-H Borylation

Reminiscent of stoichiometric alkane borylation by tungsten and iron -boryl complexes,[49,50] [Cp*Re(CO)$_3$] was reported by Chen and Hartwig to effect the photochemical borylation of simple alkanes and ethers from B_2pin_2, marking the earliest example of catalytic sp^3 C-H borylation.[51] Use of this catalyst affords 95% yield of *n*-pentyl-Bpin over 56 hours, respective to the B_2pin_2 reagent; oxidation of the HBpin byproduct was observed under the reaction conditions, precluding the borylation of a second equivalent of *n*-pentane (**Figure 1.20**).

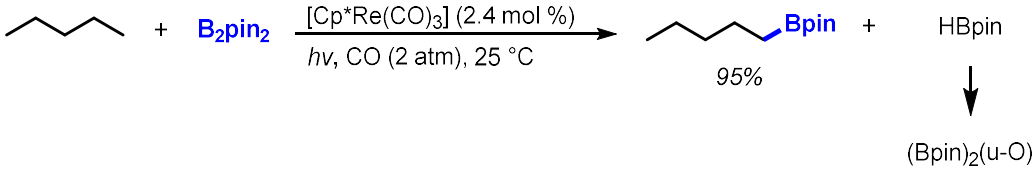

Figure 1.20: *Rhenium-catalyzed photochemical borylation of pentane*

Soon after, methods for thermal C-H borylation were realized with the use of Cp*Ir and Rh catalysts.[55,86] [Cp*Rh(C_6Me_6)] was found to promote the borylation of *n*-octane from B_2pin_2 at 150 °C with a yield of 88% relative to total boron, generating H_2 as a byproduct. As observed previously in stoichiometric and photochemical C-H borylation examples, the terminal product of C-H borylation, 1-octylboronate ester, was formed with high regiospecificity. While [Cp*Ir(C_2H_4)$_2$] and [Cp*IrH_4] also catalyzed this transformation, higher catalyst loadings, reaction times, and temperatures were

necessary to achieve modest yields of organoborane product (**Figure 1.21**).[55] Exploration of functional group tolerance with the Cp*Rh catalyst revealed successful regioselective C-H borylation of ether, amine, acetal, and fluorine containing substrates.[86]

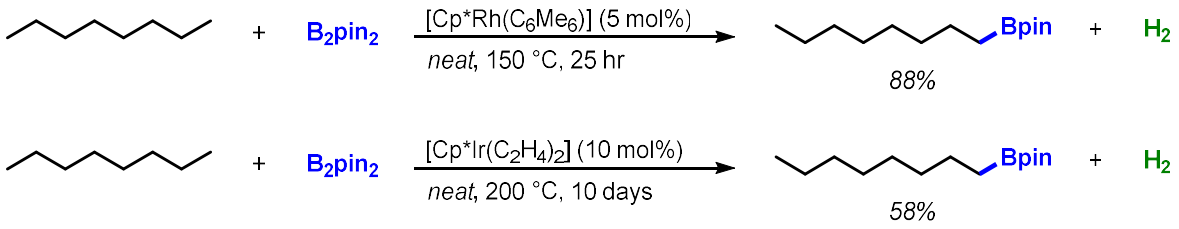

Figure 1.21: *Cp* iridium and rhodium catalyzed thermal borylation of n-octane. Yields reported based on boron*

To date [Cp*Rh(C_6Me_6)] remains one of the most active catalysts for unactivated sp^3 C-H borylation. Superior activity of this catalyst was exemplified in the borylation of polypropylenes. Subsequent hydroxylation resulted in polymers incorporated with 1-2% hydroxymethyl groups relative to total methyl groups, suggesting utility in the challenging preparation of polar-functionalized polymers.[87] Application of the Cp*Rh catalyst has also proven successful in the borylation of methane, allowing for near-quantitative conversion of B_2pin_2 to methyl-Bpin and turnover numbers approaching 100. Compared to other systems, Cp*Rh operates with high selectivity for monoborylation of methane rather than diborylation or cyclic alkane solvent borylation (**Figure 1.22**).[88]

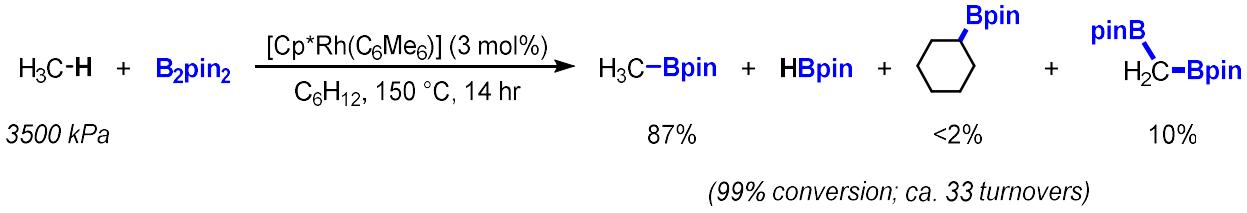

Figure 1.22: *Borylation of methane in cyclohexane by [Cp*Rh(C_6Me_6)]*

Shortly following initial Cp*Rh examples, in 2006 Murphy and Hartwig disclosed the use of ruthenium catalysts for alkane C-H borylation from B_2pin_2.[89] 1 mol% [Cp*$RuCl_2$]$_2$ afforded 98% octyl-Bpin from *n*-octane, yield relative to B_2pin_2, over 48 hours at 150 °C (**Figure 1.23**). Uniquely, Ru-catalyzed borylation was found to occur in

higher yields for alkanes than for arene substrates. Further study indicated that the presence of arene actually inhibits alkyl C-H borylation, postulated to be due to formation of an off-cycle η^6-arene complex (**Figure 1.24**).

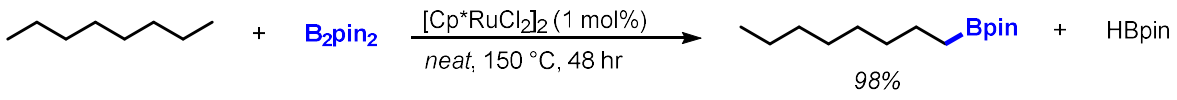

Figure 1.23: *Cp*Ru catalyzed thermal borylation of n-octane*

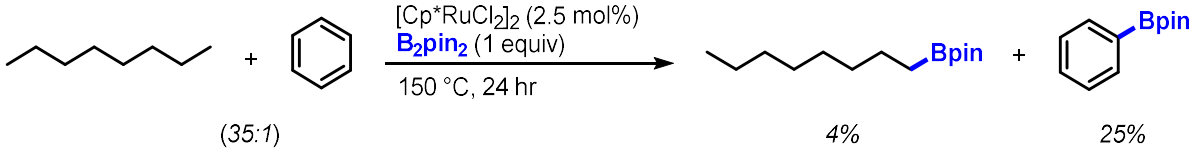

Figure 1.24: *Inhibition of Cp*Ru catalyzed borylation of n-octane by presence of arene*

Following a period of stagnant development of alkane borylation, a transition to 3,4,7,8-tetramethyl-1,10-phenanthroline (Me_4phen)-supported iridium catalysts allowed C–H borylation at lower temperatures in the range of 100–120 °C.[90,91] The C-H borylation of *n*-octane in the presence of Me_4phen and $[(cod)Ir(OMe)]_2$ gives the product 1-octylboronate ester in an 88% yield with respect to the B_2pin_2 reagent (**Figure 1.25**). Along with reduced temperature requirements, the Me_4phen/Ir system contributed a more accessible catalyst with modest improvements in scope. This system has been studied extensively by Hartwig and others and has become the benchmark for sp^3 borylation of unactivated substrates.

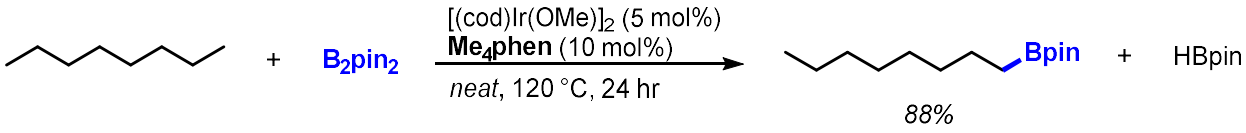

Figure 1.25: *Borylation of n-octane using $[(cod)Ir(OMe)]_2$/Me_4phen catalyst; yield reported based on 1 equivalent of B_2pin_2.*[91]

Distinctively, the Me_4phen/Ir catalyst enables the borylation of secondary C-H bonds, a feature noted during attempted borylation of *n*-octane in THF solvent.[91] A combination of Me_4phen and $[(Mes)Ir(Bpin)_3]$ catalyzed the C-H borylation of various cyclic ethers with strong selectivity for functionalization at the position β to oxygen

(**Figure 1.26**). Liskey and Hartwig proposed an O→B interaction between an Ir-boryl and substrate during C-H activation as the origin of this β selectivity. A following report detailed the analogous borylation of acyclic ether and amine substrates, occurring preferentially at ethyl chain lengths (**Figure 1.26**).[90] Application of the Me_4phen/Ir catalyst to the borylation of cyclopropane[92], alkylsilane[93,94], and branched alkane[95] substrates has further demonstrated the unique reactivity and versatility of this platform.

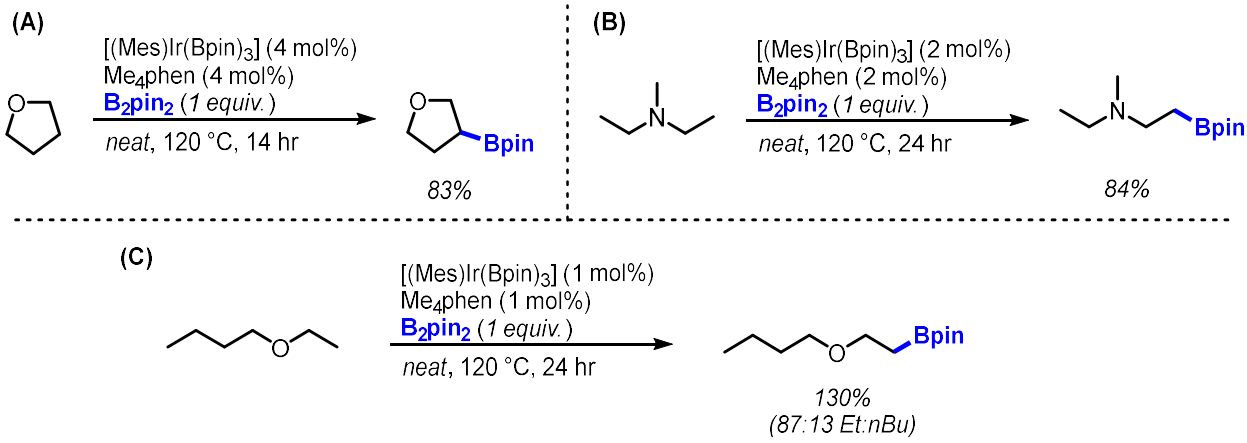

Figure 1.26: *Me_4phen/Ir Catalyzed borylation of (A) cyclic ethers, (B) linear amines, and (C) linear ethers; yields were reported based on 1 equivalent of B_2pin_2 reagent.*

The switch in iridium precursor from $[(cod)Ir(OMe)]_2$ to $[(Mes)Ir(Bpin)_3]$ was key to improvement in yield and reduced catalyst loadings for alkane borylation. Along with choice of metal pre-catalyst, subtle differences in ligand structure and properties have been demonstrated to have a profound effect on catalyst activity. Very few successful ligands have been identified which deviate from the phen or bipy core structures, though the facially coordinating tris(pyrazolyl)borate (Tp) gives iridium catalysts which borylate *n*-octane in yields ranging from 76-120%, relative to B_2pin_2.[96] In a survey of N,N'-coordinating ligands for *n*-octane borylation, use of Me_4phen provided far superior product yield even when compared to unsubstituted phenanthroline (**L2**) and to dtbpy (**L6**), the standard for arene borylation (**Figure 1.27**).[91]

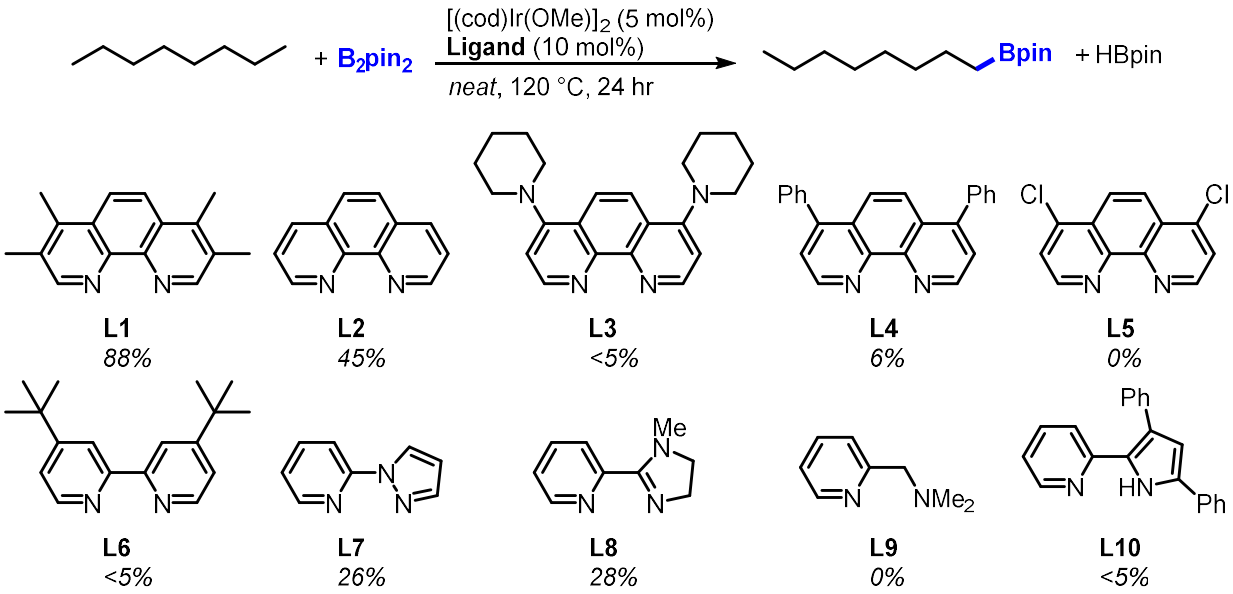

Figure 1.27: *Survey of N-N Ligands for the borylation of n-octane; yields were reported based on 1 equivalent of* B_2pin_2.[91]

Computational treatment of alkane borylation by Sakaki and coworkers suggests electron-donating ligands with strong trans-influence will produce a highly active iridium catalyst.[97] A library of phen derivatives was later synthesized and explored to ascertain the effect of ligand substitution and electronic features on the resulting catalyst.[98] Modulation of the 4 and 7 substituents of phen to generate more electron-rich iridium complexes resulted in more active catalysts for THF borylation, similar to prior observations in arene borylation.[60,64] Substitution of the 3 and 8 positions with either Me or Mes provided substantial increases in rate (**Figure 1.28**), despite minimal difference in electron density at the metal center. DFT study of the 3,8-substitutents illuminated possible stabilizing C-H···O interactions between phen and a boryl ligand in the transition state.

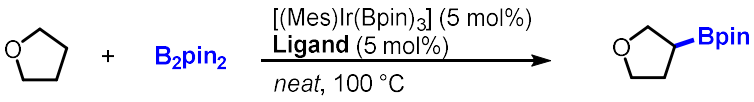

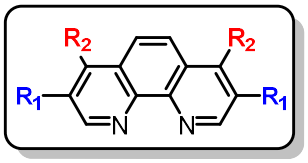

R_1	R_2	Yield	TON	TOF (h^{-1})
H	H	42%	8.0	1.7
H	Cl	15%	3.0	0.28
H	CH_3	23%	4.5	0.82
H	CH_2TIPS	55%	11	0.38
H	Pyrrolidine	33%	6.6	0.53
CH_3	H	100%	20	0.63
CH_3	Cl	23%	4.6	0.23
CH_3	**CH_3**	**103%**	**21**	**0.86**
CH_3	CH_2TIPS	137%	27	1.2
CH_3	Pyrrolidine	89%	18	0.74
Mes	H	97%	20	1.3
Mes	Cl	28%	5.6	1.0
Mes	CH_3	99%	20	2.3
Mes	CH_2TIPS	70%	14	2.1

Figure 1.28: *Survey of phen ligand derivatives for the borylation of THF; yields were reported based on 1 equivalent of B_2pin_2.*[91]

Very recently, an advanced understanding of the effects of phen ligand substitution on properties of the resulting catalyst enabled the discovery of a platform for the borylation of limiting alkane in inert solvent. Oeschger and Hartwig achieved aliphatic C-H borylation without need for excess substrate using 2-methylphenanthroline (2-mphen) and $[(cod)Ir(OMe)]_2$ (**Figure 1.29**), noting a substantial rate acceleration of nearly two orders of magnitude compared to Me_4phen.[98] Alkyl borylation was demonstrated in broad scope and organoborane products were further derivatized, highlighting the value of reduced substrate excess to both catalyst function and synthetic economy. Their work was published shortly after our own initial report of the 2,2'-dipyridylarylmethane/Ir catalyst detailed in chapter 4.

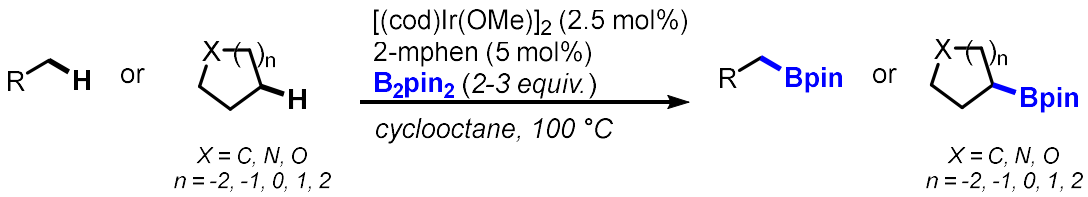

Figure 1.29: *Alkyl C-H borylation of a single equivalent of substrate in cyclooctane catalyzed by 2-mphen/$[(cod)IrOMe]_2$.*[99]

1.4.2 Mechanism of sp^3 C-H Borylation by phen/Ir Catalysts

The accepted catalytic cycle for sp^3 C-H borylation mirrors that proposed for arene borylation. A general catalytic cycle for iridium-catalyzed C–H borylation with diimine ligands, such as Me_4phen, has been significantly informed by mechanistic studies published by Hartwig, Sakaki, and their respective co-workers (**Figure 1.30**).[81,90,98,100,101] Catalyst activation is proposed to generate the 5-coordinate trisboryl Ir complex **A**. This species has been identified as the catalyst resting state in arene borylation.[81] Computational treatments of sp^3 C–H borylation also support an oxidative addition mechanism for C–H cleavage,[90,97,102] though a σ-bond metathesis mechanism has not been rigorously excluded.[103] The resulting iridium diboryl monohydride **C** is presumed to react with B_2pin_2 to regenerate **A** and extrude HBpin. Under conditions where B_2pin_2 has been fully consumed, the byproduct HBpin is proposed to supplant B_2pin_2 in the catalytic cycle, with dihydrogen serving as the terminal byproduct.[101]

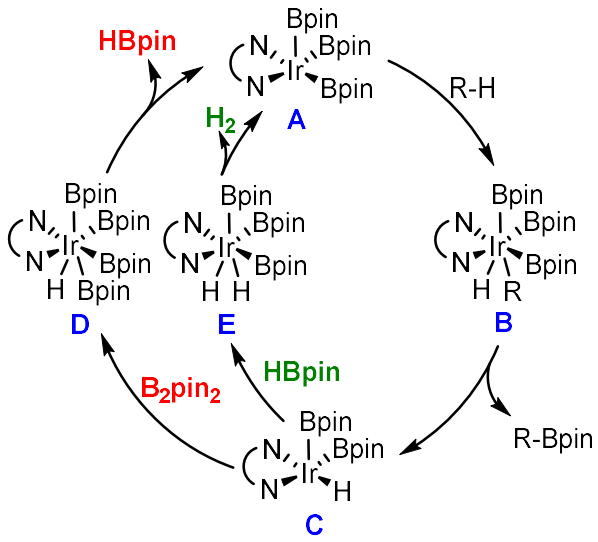

Figure 1.30: *General mechanism for sp^3 C-H borylation by diimine/Ir catalysts*

An analogous oxidative addition/reductive elimination Ir(III)/Ir(V) process has been detailed for sp^3 C-H borylation by Cp*Rh and Cp*Ir catalysts.[55,100,103–105] Alternatively, evidence for a boron-assisted sigma bond metathesis pathway was published by Webster and Hartwig.[103] It is likely that these two reaction pathways are similar in energy, and can be separately accessed by variation of catalyst features.

Notably, both cases indicate the importance of catalyst geometry in potential interaction of a metal-boryl and the incoming C-H bond.

1.4.3 Current Challenges in sp^3 C-H Borylation

Existing challenges to alkane borylation can be broadly delineated into two categories: (1) the need for excess molar quantities of neat substrate and (2) poor economy of the diboron reagent. With few recent exceptions, a catalyst for sp^3 borylation which operates on aliphatic substrate as limiting reagent or which effectively consumes both equivalents of B_2pin_2 has yet to be achieved. Resolution of these issues would largely address specific ongoing problems of functional group tolerance, harsh reaction conditions, usability, and atom economy.

Achieving high reactivity while maintaining selectivity in undirected C–H functionalization is an intrinsic challenge to any approach, owing to the number of C–H bonds in a typical substrate. This challenge is amplified when reactions are conducted with a small excess of substrate in organic solvent, because the rate of substrate borylation is likely to be diminished and competitive borylation of the solvent must be avoided. Relative performance and chemoselectivity of Cp*Rh, Cp*Ru, and Me_4phen/Ir catalysts is exemplified by their respective borylations of methane in cyclohexane solvent, with success of Cp*Rh catalysts owed to selective monoborylation and mitigation of competitive secondary borylation (**Figure 1.31**).[88]

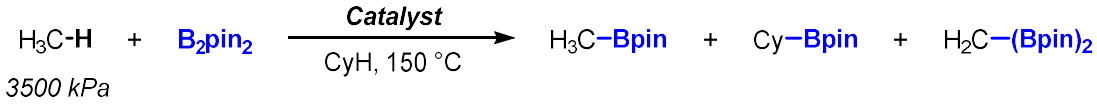

Catalyst	*Yield**	*H_3CBpin : CyBpin*	*H_3CBpin : H_2C(Bpin)$_2$*
[Cp*Rh(C_6Me_6)]	99%	59:1	9:1
Me_4phen/[(Mes)Ir(Bpin)$_3$]	45%	3:1	4:1
[Cp*RuCl$_2$]$_2$	67%	83:1	21:1

**Yield represents combined yield of all borylated products*

Figure 1.31: *Borylation of methane in cyclohexane solvent by [Cp*Rh(C_6Me_6)], Me_4phen/[(Mes)Ir(Bpin)$_3$], and [Cp*RuCl$_2$]$_2$.*[88]

Traditional systems for the borylation of *n*-alkanes, including both Cp*Rh/Ir[51,53,55]and (diimine)Ir,[91,94] perform quite poorly in solvent. Catalysts have been developed for the sp^3 borylation of activated (including benzylic, cyclopropane, and

alkylsilane substrates)[92–94,106] or directed substrates.[106–111] However, the C–H borylation of unactivated alkyl substrates in solvent was largely unaddressed prior to recent work by the Hartwig group[99] and ourselves.[112] In both cases, successful catalysis in cycloalkane solvents reflects the intrinsic selectivity of iridium sp^3 C–H borylation catalysts for methyl C–H bonds over methylene C–H bonds. Substantial limitations remain for both systems, however, leaving space for the development of improved catalysts for sp^3 C–H borylation chemistry in solvent.

The second major challenge is the complete incorporation of the diboron reagent B_2pin_2 into organoborane product; C–H Borylation with B_2pin_2 comprises two separate but analogous catalytic reactions. In the first reaction, shown in **(1)**, B_2pin_2 is consumed to give 1 equivalent of product and 1 equivalent of HBpin. In the second **(2)**, the byproduct HBpin serves as the borylating agent to produce H_2 as the terminal byproduct of C–H cleavage, along with a second equivalent of organoborane. Early Cp*Rh/Ir examples of alkane sp^3 borylation catalyze both reactions to different extents, exhibiting complete consumption of B_2pin_2, as well as conversion of byproduct HBpin into H_2 in select cases.[51,53,55,86] Although the Me_4phen/Ir system for sp^3 C–H borylation is capable of effecting the reaction depicted in **(1)** at lower temperatures (approximately 100–120 °C), poor conversion of HBpin by this catalyst system has given rise to the convention of reporting alkane borylation yields relative to molar equivalents of B_2pin_2.[91] Thus, a system that produces 2 equivalents of alkyl boronate from 1 equivalent of B_2pin_2 is often reported as achieving 200% yield.

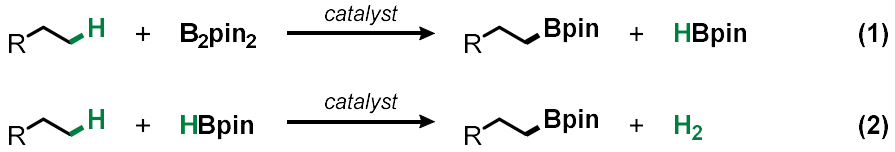

Figure 1.32: *Consumption of boron equivalents from B_2pin_2*

Since the vast majority of alkane borylation systems use B_2pin_2 as the limiting reagent, conversion of the HBpin byproduct of **(1)** is an important goal for the atom economy of the process. Especially in the case of simple, unactivated hydrocarbon substrates, the diboron reagent can be more valuable than the substrate. The challenges to HBpin utilization likely stem both from differences in the thermodynamic

driving force[5] for equations **(1)** and **(2)** and from kinetic challenges arising from distinct elementary steps in the two catalytic cycles.[101] For instance, although the (diimine)Ir trisboryl species A is the presumed resting state of the catalytic reaction associated with **(1)**, the role of A and the identity of the resting state are less clear when HBpin is used. At a minimum, HBpin consumption requires the extrusion of molecular dihydrogen – either by reductive elimination of an iridium dihydride intermediate such as E or by σ-bond metathesis of an iridium hydride with an equivalent of HBpin.[101]

Although significant strides have been made towards both the efficient utilization of the diboron reagent and the functionalization of stoichiometric quantities of substrate, no catalytic system yet offers a complete solution. Further development is still needed for sp^3 C-H borylation catalysis to overcome its longstanding limitations. Success has been demonstrated in the sp^3 C-H borylation of unactivated substrates through careful construction of catalysts through the dimension of ligand design for tuning of desirable features. It is clear that ligand optimization will play an important role moving forward in the development of increasingly active catalysts.

1.4 Conclusions

The field of C-H bond activation, and consequently, catalytic C-H borylation has progressed remarkably since its seminal advance. Notable innovations have been made in the realms of mild and sustainable conditions, catalyst usability, turnover, scope, and selectivity for both sp^2 and sp^3 C-H borylation. While the borylation of arene and substrates has witnessed substantially more development than the corresponding alkane borylation reaction, advances in atom-economy, scope, and substrate quantity continue to be achieved. It is clear that further development is still needed for sp^3 C–H borylation catalysis to overcome its longstanding limitations. Further success can be accessed through meticulous cultivation of ligand frameworks, which provide a strategy for the continued development of highly active or site-selective catalysts for C-H borylation. We expect that design and optimization of novel, tunable ligand platforms will be key to success in this sphere moving forward.

Portions of this chapter have been adapted with permission from Jones, M.R., Schley, N.D.; Ligand-Driven Advances in Iridium-Catalyzed sp^3 C–H Borylation: 2,2'-Dipyridylarylmethan. Synlett 2021; 32(09): 845-850. DOI: 10.1055/a-1344-1904 Georg Thieme Verlag KG Copyright 2021

1.5 References

(1) Crabtree, R. H. The Organometallic Chemistry of Alkanes. *Chem. Rev.* **1985**, *85* (4), 245–269.

(2) Goldberg, K. I.; Goldman, A. S. Large-Scale Selective Functionalization of Alkanes. *Acc. Chem. Res.* **2017**, *50* (3), 620–626..

(3) Arndtsen, B. A.; Bergman, R. G.; Mobley, T. A.; Peterson, T. H. Selective Intermolecular Carbon-Hydrogen Bond Activation by Synthetic Metal Complexes in Homogeneous Solution. *Acc. Chem. Res.* **1995**, *28* (3), 154–162.

(4) Wencel-Delord, J.; Glorius, F. C–H Bond Activation Enables the Rapid Construction and Late-Stage Diversification of Functional Molecules. *Nat. Chem.* **2013**, *5* (5), 369–375.

(5) Mkhalid, I. A. I.; Barnard, J. H.; Marder, T. B.; Murphy, J. M.; Hartwig, J. F. C−H Activation for the Construction of C−B Bonds. *Chem. Rev.* **2010**, *110* (2), 890–931.

(6) Hartwig, J. F. Borylation and Silylation of C–H Bonds: A Platform for Diverse C–H Bond Functionalizations. *Acc. Chem. Res.* **2012**, *45* (6), 864–873.

(7) Ros, A.; Fernández, R.; Lassaletta, J. M. Functional Group Directed C–H Borylation. *Chem. Soc. Rev.* **2014**, *43* (10), 3229–3243..

(8) Xu, L.; Wang, G.; Zhang, S.; Wang, H.; Wang, L.; Liu, L.; Jiao, J.; Li, P. Recent Advances in Catalytic C−H Borylation Reactions. *Tetrahedron* **2017**, *73* (51), 7123–7157..

(9) Kuroda, Y.; Nakao, Y. Catalyst-Enabled Site-Selectivity in the Iridium-Catalyzed C–H Borylation of Arenes. *Chem. Lett.* **2019**, *48* (9), 1092–1100.

(10) Janowicz, A. H.; Bergman, R. G. Activation of C-H Bonds in Saturated Hydrocarbons on Photolysis of $(\eta^5\text{-}C_5Me_5)(PMe_3)IrH_2$. *J Am Chem Soc.* **1983**, *105:12*.

(11) Crabtree, R. H. Organometallic Alkane CH Activation. *J. Organomet. Chem.* **2004**, *689* (24), 4083–4091.

(12) Shilov, A. E.; Shul'pin, G. B. Activation of C−H Bonds by Metal Complexes. *Chem. Rev.* **1997**, *97* (8), 2879–2932.

(13) Garnett, J. L.; Hodges, R. J. Homogeneous Metal-Catalyzed Exchange of Aromatic Compounds. Isotopic Hydrogen Labeling Procedure. *J. Am. Chem. Soc.* **1967**, *89* (17), 4546–4547.

(14) Gol'dshleger, N. F.; Tyabin, M. B.; Shilov, A. E.; Shteinman, A. A. Activation of Saturated Hydrocarbons-Deuterium-Hydrogen Exchange in Solutions of Transition Metal Complexes. *Zh Fiz Khim* **1969**, *43* (8), 2174.

(15) Gol'dshleger, N. F.; Eskova, V. V.; Shteinman, A. A.; Shilov, A. E. Gol'dshleger, N.F., Es'Kova, V.V., Shteinman, A.A. and Shilov, A.E., 1972. Reactions of Alkanes in Solutions of Chloride Complexes of Platinum. Russ. J. Phys. Chem, 46, Pp.785-786. *Zh Fiz Khim* **1972**, *46*, 785–786.

(16) Hartwig, J. F. Evolution of C–H Bond Functionalization from Methane to Methodology. *J. Am. Chem. Soc.* **2016**, *138* (1), 2–24.

(17) Labinger, J. A.; Herring, A. M.; Lyon, D. K.; Luinstra, G. A.; Bercaw, J. E.; Horvath, I. T.; Eller, K. Oxidation of Hydrocarbons by Aqueous Platinum Salts: Mechanism and Selectivity. *Organometallics* **1993**, *12* (3), 895–905.

(18) Luinstra, G. A.; Labinger, J. A.; Bercaw, J. E. Mechanism and Stereochemistry for Nucleophilic Attack at Carbon of Platinum(IV) Alkyls: Model Reactions for Hydrocarbon Oxidation with Aqueous Platinum Chlorides. *J. Am. Chem. Soc.* **1993**, *115* (7), 3004–3005.

(19) Labinger, J. A.; Bercaw, J. E. Understanding and Exploiting C–H Bond Activation. *Nature* **2002**, *417* (6888), 507–514.

(20) Bennett, M. A.; Milner, D. L. Bennett, M. A., and D. L. Milner. Chlorotris (Triphenylphosphine) Iridium (I): An Example of Hydrogen Transfer to a Metal from a Co-Ordinated Ligand. *Chem. Comm.* **1967**, 12, 581-582.

(21) Keim, W. New σ-Bonded Rhodium(I) Complexes Containing a Metal—Carbon Bond. I. *J. Organomet. Chem.* **1968**, *14* (1), 179–184.

(22) Bruce, M. I.; Goodall, B. L.; Stone, F. G. A.; Thomson, B. J. Cyclometallation Reactions. IX. 2-(Phenylazo)Phenyl Complexes of Iridium(III). *Aust. J. Chem.* **1974**, *27* (10), 2135–2138.

(23) Chatt, J.; Davidson, J. M. 154. The Tautornerism of Arene and Ditertiary Phosphine Complexes of Ruthenium(0), and the Preparation of New Types of Hydrido- Complexes of Ruthenium(II). *J. of the Chem. Soc.* **1965**, 843-855.

(24) Foley, P.; Whitesides, G. M. Thermal Generation of Bis(Triethylphosphine)-3,3-Dimethylplatinacyclobutane from Dineopentylbis (Triethylphosphine) Platinum(II). *J. Am. Chem. Soc.* **1979**, *101* (10), 2732–2733.

(25) Bruce, M. I. Cyclometalation Reactions. *Angew. Chem. Int. Ed. Engl.* **1977**, *16* (2), 73–86.

(26) Janowicz, A. H.; Bergman, R. G. Carbon-Hydrogen Activation in Completely Saturated Hydrocarbons: Direct Observation of M + R-H --> M(R)(H). *J. Am. Chem. Soc.* **1982**, *104* (1), 352–354.

(27) Hoyano, J. K.; McMaster, A. D.; Graham, W. A. G. Activation of Methane by Iridium Complexes. *J. Am. Chem. Soc.* **1983**, *105* (24), 7190–7191.

(28) Periana, R. A.; Bergman, R. G. Oxidative Addition of Rhodium to Alkane Carbon-Hydrogen Bonds: Enhancement in Selectivity and Alkyl Group Functionalization. *Organometallics* **1984**, *3* (3), 508–510.

(29) Jones, W. D.; Feher, F. J. The Mechanism and Thermodynamics of Alkane and Arene Carbon-Hydrogen Bond Activation in $(C_5Me_5)Rh(PMe_3)(R)H$. *J. Am. Chem. Soc.* **1984**, *106* (6), 1650–1663.

(30) Jones, W. D.; Hessell, E. T. Photolysis of Tp'Rh(CN-Neopentyl)(η^2-PhN:C:N-Neopentyl) in Alkanes and Arenes: Kinetic and Thermodynamic Selectivity of [Tp'Rh(CN-Neopentyl)] for Various Types of Carbon-Hydrogen Bonds. *J. Am. Chem. Soc.* **1993**, *115* (2), 554–562.

(31) Jones, W. D.; Feher, F. J. Alkane Carbon-Hydrogen Bond Activation by Homogeneous Rhodium(I) Compounds. *Organometallics* **1983**, *2* (4), 562–563.

(32) Wedi, P.; van Gemmeren, M. Arene-Limited Nondirected C−H Activation of Arenes. *Angew. Chem. Int. Ed.* **2018**, *57* (40), 13016–13027.

(33) Jia, C.; Kitamura, T.; Fujiwara, Y. Catalytic Functionalization of Arenes and Alkanes via C−H Bond Activation. *Acc. Chem. Res.* **2001**, *34* (8), 633–639.

(34) Periana, null; Taube, null; Gamble, null; Taube, null; Satoh, null; Fujii, null. Platinum Catalysts for the High-Yield Oxidation of Methane to a Methanol Derivative. *Science* **1998**, *280* (5363), 560–564.

(35) Baudry, D.; Ephritikhine, M.; Felkin, H.; Zakrzewski, J. The Selective Conversion of N-Pentane into Pent-1-Ene via Trihydrido(Trans -Penta-1,3-Diene)Bis(Triarylphosphine)Rhenium. *J. Chem. Soc. Chem. Commun.* **1982**, *0* (21), 1235–1236.

(36) Crabtree, R. H.; Mellea, M. F.; Mihelcic, J. M.; Quirk, J. M. Alkane Dehydrogenation by Iridium Complexes. *J. Am. Chem. Soc.* **1982**, *104* (1), 107.

(37) Burk, M. J.; Crabtree, R. H. Selective Catalytic Dehydrogenation of Alkanes to Alkenes. *J. Am. Chem. Soc.* **1987**, *109* (26), 8025–8032.

(38) Liu, F.; Pak, E. B.; Singh, B.; Jensen, C. M.; Goldman, A. S. Dehydrogenation of N-Alkanes Catalyzed by Iridium "Pincer" Complexes: Regioselective Formation of α-Olefins. *J. Am. Chem. Soc.* **1999**, *121* (16), 4086–4087.

(39) Fujiwara, Y.; Moritani, I.; Danno, S.; Asano, R.; Teranishi, S. Aromatic Substitution of Olefins. VI. Arylation of Olefins with Palladium(II) Acetate. *J. Am. Chem. Soc.* **1969**, *91* (25), 7166–7169.

(40) Moritanl, I.; Fujiwara, Y. Aromatic Substitution of Styrene-Palladium Chloride Complex. *Tetrahedron Lett.* **1967**, *8* (12), 1119–1122.

(41) Fujiwara, Y.; Jintoku, T.; Uchida, Y. Palladium(II)-Mediated Carboxylation of Cyclohexane with CO via C-H Bond Activation. *New Journal of Chemistry* **1989**, *13* (10–11), 649–650.

(42) Jintoku, T.; Fujiwara, Y.; Kawata, I.; Kawauchi, T.; Taniguchi, H. Palladium-Catalyzed Synthesis of Aromatic Acids from Carbon Monoxide and Aromatic Compounds via the Aromatic C-H Bond Activation. *J. Organomet. Chem.* **1990**, *385* (2), 297–306.

(43) Murai, S.; Kakiuchi, F.; Sekine, S.; Tanaka, Y.; Kamatani, A.; Sonoda, M.; Chatani, N. Efficient Catalytic Addition of Aromatic Carbon-Hydrogen Bonds to Olefins. *Nature* **1993**, *366* (6455), 529–531.

(44) Kakiuchi, F.; Murai, S. Catalytic C−H/Olefin Coupling. *Acc. Chem. Res.* **2002**, *35* (10), 826–834.

(45) Onak,T. Organoborane Chemistry (Academic Press, New York, **1975**).

(46) Brown, H.C. Organic Synthesis via Boranes (Wiley, New York, **1975**).

(47) Nguyen, P.; Blom, H. P.; Westcott, S. A.; Taylor, N. J.; Marder, T. B. Synthesis and Structures of the First Transition-Metal Tris(Boryl) Complexes: Iridium Complexes (η^6-Arene)Ir($BO_2C_6H_4$)$_3$. *J. Am. Chem. Soc.* **1993**, *115* (20), 9329–9330.

(48) Burgess, K.; Van der Donk, W. A.; Westcott, S. A.; Marder, T. B.; Baker, R. T.; Calabrese, J. C. Reactions of Catecholborane with Wilkinson's Catalyst: Implications for Transition Metal-Catalyzed Hydroborations of Alkenes. *J. Am. Chem. Soc.* **1992**, *114* (24), 9350–9359.

(49) Waltz, K. M.; He, X.; Muhoro, C.; Hartwig, J. F. Hydrocarbon Functionalization by Transition Metal Boryls. *J. Am. Chem. Soc.* **1995**, *117* (45), 11357–11358.

(50) Waltz, K. M.; Hartwig, J. F. Selective Functionalization of Alkanes by Transition-Metal Boryl Complexes. *Science* **1997**, *277* (5323), 211–213.

(51) Chen, H.; Hartwig, J. F. Catalytic, Regiospecific End-Functionalization of Alkanes: Rhenium-Catalyzed Borylation under Photochemical Conditions. *Angew. Chem. Int. Ed.* **1999**, *38* (22), 3391–3393.

(52) Iverson, C. N.; Smith, M. R. Reactivity of Organoplatinum Complexes with $C_6H_4O_2B$-$BO_2C_6H_4$: Syntheses of a Platinum Diboryl Complex with, and without,

Metathesis of Boron-Boron and Metal-Carbon Bonds. *J. Am. Chem. Soc.* **1995**, *117* (15), 4403–4404.

(53) Iverson, C. N.; Smith, M. R. Stoichiometric and Catalytic B−C Bond Formation from Unactivated Hydrocarbons and Boranes. *J. Am. Chem. Soc.* **1999**, *121* (33), 7696–7697.

(54) Cho, J.-Y.; Tse, M. K.; Holmes, D.; Maleczka, R. E.; Smith, M. R. Remarkably Selective Iridium Catalysts for the Elaboration of Aromatic C-H Bonds. *Science* **2002**, *295* (5553), 305–308.

(55) Chen, H.; Schlecht, S.; Semple, T. C.; Hartwig, J. F. Thermal, Catalytic, Regiospecific Functionalization of Alkanes. *Science* **2000**, *287* (5460), 1995–1997.

(56) Cho, J. Y.; Iverson, C. N.; Smith, M. R. Steric and Chelate Directing Effects in Aromatic Borylation. *J. Am. Chem. Soc.* **2000**, *122* (51), 12868–12869.

(57) Tse, M. K.; Cho, J.-Y.; Smith, M. R. Regioselective Aromatic Borylation in an Inert Solvent. *Org. Lett.* **2001**, *3* (18), 2831–2833.

(58) Chotana, G. A.; Britt A. Vanchura, I. I.; Tse, M. K.; Staples, R. J.; Robert E. Maleczka, J.; Milton R. Smith, I. I. I. Getting the Sterics Just Right: A Five-Coordinate Iridium Trisboryl Complex That Reacts with C–H Bonds at Room Temperature. *Chem. Commun.* **2009**, No. 38, 5731–5733.

(59) Ishiyama, T.; Takagi, J.; Ishida, K.; Miyaura, N.; Anastasi, N. R.; Hartwig, J. F. Mild Iridium-Catalyzed Borylation of Arenes. High Turnover Numbers, Room Temperature Reactions, and Isolation of a Potential Intermediate. *J. Am. Chem. Soc.* **2002**, *124* (3), 390–391.

(60) Ishiyama, T.; Takagi, J.; Hartwig, J. F.; Miyaura, N. A Stoichiometric Aromatic C-H Borylation Catalyzed by Iridium(I)/2,2′-Bipyridine Complexes at Room Temperature. *Angew. Chem. Int. Ed.* **2002**, *41* (16), 3056–3058.

(61) Murata, M.; Odajima, H.; Watanabe, S.; Masuda, Y. Aromatic C–H Borylation Catalyzed by Hydrotris(Pyrazolyl)Borate Complexes of Rhodium and Iridium. *Bull. Chem. Soc. Jpn.* **2006**, *79* (12), 1980–1982.

(62) Ito, J.; Kaneda, T.; Nishiyama, H. Intermolecular C–H Bond Activation of Alkanes and Arenes by NCN Pincer Iridium(III) Acetate Complexes Containing Bis(Oxazolinyl)Phenyl Ligands. *Organometallics* **2012**, *31* (12), 4442–4449.

(63) Press, L. P.; Kosanovich, A. J.; McCulloch, B. J.; Ozerov, O. V. High-Turnover Aromatic C–H Borylation Catalyzed by POCOP-Type Pincer Complexes of Iridium. *J. Am. Chem. Soc.* **2016**, *138* (30), 9487–9497.

(64) Preshlock, S. M.; Ghaffari, B.; Maligres, P. E.; Krska, S. W.; Maleczka, R. E.; Smith, M. R. High-Throughput Optimization of Ir-Catalyzed C–H Borylation: A

Tutorial for Practical Applications. *J. Am. Chem. Soc.* **2013**, *135* (20), 7572–7582.

(65) Haldar, C.; Emdadul Hoque, M.; Bisht, R.; Chattopadhyay, B. Concept of Ir-Catalyzed CH Bond Activation/Borylation by Noncovalent Interaction. *Tetrahedron Lett.* **2018**, *59* (14), 1269–1277.

(66) Hartwig, J. F.; Larsen, M. A. Undirected, Homogeneous C–H Bond Functionalization: Challenges and Opportunities. *ACS Cent. Sci.* **2016**, *2* (5), 281–292.

(67) Maleczka, Robert E.; Shi, F.; Holmes, D.; Smith, M. R. C−H Activation/Borylation/Oxidation: A One-Pot Unified Route to Meta-Substituted Phenols Bearing Ortho-/Para-Directing Groups. *J. Am. Chem. Soc.* **2003**, *125* (26), 7792–7793.

(68) Murphy, J. M.; Tzschucke, C. C.; Hartwig, J. F. One-Pot Synthesis of Arylboronic Acids and Aryl Trifluoroborates by Ir-Catalyzed Borylation of Arenes. *Org. Lett.* **2007**, *9* (5), 757–760.

(69) Tajuddin, H.; Shukla, L.; Maxwell, A. C.; Marder, T. B.; Steel, P. G. “One-Pot” Tandem C−H Borylation/1,4-Conjugate Addition/Reduction Sequence. *Org. Lett.* **2010**, *12* (24), 5700–5703.

(70) Pei, X.; Zhou, G.; Li, X.; Xu, Y.; C. Panicker, R.; Srinivasan, R. Sterically Controlled C–H/C–H Homocoupling of Arenes via C–H Borylation. *Org. Biomol. Chem.* **2019**, *17* (23), 5703–5707.

(71) Kikuchi, T.; Nobuta, Y.; Umeda, J.; Yamamoto, Y.; Ishiyama, T.; Miyaura, N. Practical Synthesis of Pinacolborane for One-Pot Synthesis of Unsymmetrical Biaryls via Aromatic C–H Borylation–Cross-Coupling Sequence. *Tetrahedron* **2008**, *64* (22), 4967–4971.

(72) Liskey, C. W.; Liao, X.; Hartwig, J. F. Cyanation of Arenes via Iridium-Catalyzed Borylation. *J. Am. Chem. Soc.* **2010**, *132* (33), 11389–11391.

(73) Partridge, B. M.; Hartwig, J. F. Sterically Controlled Iodination of Arenes via Iridium-Catalyzed C–H Borylation. *Org. Lett.* **2013**, *15* (1), 140–143.

(74) Kallepalli, V. A.; Gore, K. A.; Shi, F.; Sanchez, L.; Chotana, G. A.; Miller, S. L.; Maleczka, R. E.; Smith, M. R. Harnessing C–H Borylation/Deborylation for Selective Deuteration, Synthesis of Boronate Esters, and Late Stage Functionalization. *J. Org. Chem.* **2015**, *80* (16), 8341–8353..

(75) Robbins, D. W.; Hartwig, J. F. Sterically Controlled Alkylation of Arenes through Iridium-Catalyzed C-H Borylation. *Angew. Chem.* **2013**, *125* (3), 967–971.

(76) Murphy, J. M.; Liao, X.; Hartwig, J. F. Meta Halogenation of 1,3-Disubstituted Arenes via Iridium-Catalyzed Arene Borylation. *J. Am. Chem. Soc.* **2007**, *129* (50), 15434–15435.

(77) Feng, Y.; Holte, D.; Zoller, J.; Umemiya, S.; Simke, L. R.; Baran, P. S. Total Synthesis of Verruculogen and Fumitremorgin A Enabled by Ligand-Controlled C–H Borylation. *J. Am. Chem. Soc.* **2015**, *137* (32), 10160–10163.

(78) Yuan, C.; Liu, B. Total Synthesis of Natural Products via Iridium Catalysis. *Org. Chem. Front.* **2017**, *5* (1), 106–131.

(79) Liao, X.; Stanley, L. M.; Hartwig, J. F. Enantioselective Total Syntheses of (−)-Taiwaniaquinone H and (−)-Taiwaniaquinol B by Iridium-Catalyzed Borylation and Palladium-Catalyzed Asymmetric α-Arylation. *J. Am. Chem. Soc.* **2011**, *133* (7), 2088–2091.

(80) Zhou, S.; Jia, Y. Total Synthesis of (−)-Goniomitine. *Org. Lett.* **2014**, *16* (12), 3416–3418.

(81) Boller, T. M.; Murphy, J. M.; Hapke, M.; Ishiyama, T.; Miyaura, N.; Hartwig, J. F. Mechanism of the Mild Functionalization of Arenes by Diboron Reagents Catalyzed by Iridium Complexes. *J. Am. Chem. Soc.* **2005**, *127* (41), 14263–14278.

(82) Wright, J. S.; Scott, P. J. H.; Steel, P. G. Iridium-Catalysed C−H Borylation of Heteroarenes: Balancing Steric and Electronic Regiocontrol. *Angew. Chem. Int. Ed.* **2021**, *60* (6), 2796–2821.

(83) Sadler, S. A.; Tajuddin, H.; Mkhalid, I. A. I.; Batsanov, A. S.; Albesa-Jove, D.; Cheung, M. S.; Maxwell, A. C.; Shukla, L.; Roberts, B.; Blakemore, D. C.; Lin, Z.; Marder, T. B.; Steel, P. G. Iridium-Catalyzed C–H Borylation of Pyridines. *Org. Biomol. Chem.* **2014**, *12* (37), 7318–7327.

(84) Oeschger, R. J.; Larsen, M. A.; Bismuto, A.; Hartwig, J. F. Origin of the Difference in Reactivity between Ir Catalysts for the Borylation of C–H Bonds. *J. Am. Chem. Soc.* **2019**, *141* (41), 16479–16485.

(85) Wei, C. S.; Jiménez-Hoyos, C. A.; Videa, M. F.; Hartwig, J. F.; Hall, M. B. Origins of the Selectivity for Borylation of Primary over Secondary C−H Bonds Catalyzed by Cp*-Rhodium Complexes. *J. Am. Chem. Soc.* **2010**, *132* (9), 3078–3091.

(86) Lawrence, J. D.; Takahashi, M.; Bae, C.; Hartwig, J. F. Regiospecific Functionalization of Methyl C−H Bonds of Alkyl Groups in Reagents with Heteroatom Functionality. *J. Am. Chem. Soc.* **2004**, *126* (47), 15334–15335.

(87) Bae, C.; Hartwig, J. F.; Boaen Harris, N. K.; Long, R. O.; Anderson, K. S.; Hillmyer, M. A. Catalytic Hydroxylation of Polypropylenes. *J. Am. Chem. Soc.* **2005**, *127* (2), 767–776.

(88) Cook, A. K.; Schimler, S. D.; Matzger, A. J.; Sanford, M. S. Catalyst-Controlled Selectivity in the C–H Borylation of Methane and Ethane. *Science* **2016**, *351* (6280), 1421–1424.

(89) Murphy, J. M.; Lawrence, J. D.; Kawamura, K.; Incarvito, C.; Hartwig, J. F. Ruthenium-Catalyzed Regiospecific Borylation of Methyl C−H Bonds. *J. Am. Chem. Soc.* **2006**, *128* (42), 13684–13685.

(90) Li, Q.; Liskey, C. W.; Hartwig, J. F. Regioselective Borylation of the C–H Bonds in Alkylamines and Alkyl Ethers. Observation and Origin of High Reactivity of Primary C–H Bonds Beta to Nitrogen and Oxygen. *J. Am. Chem. Soc.* **2014**, *136* (24), 8755–8765.

(91) Liskey, C. W.; Hartwig, J. F. Iridium-Catalyzed Borylation of Secondary C–H Bonds in Cyclic Ethers. *J. Am. Chem. Soc.* **2012**, *134* (30), 12422–12425.

(92) Liskey, C. W.; Hartwig, J. F. Iridium-Catalyzed C–H Borylation of Cyclopropanes. *J. Am. Chem. Soc.* **2013**, *135* (9), 3375–3378.

(93) Ohmura, T.; Torigoe, T.; Suginome, M. Catalytic Functionalization of Methyl Group on Silicon: Iridium-Catalyzed C(Sp^3)–H Borylation of Methylchlorosilanes. *J. Am. Chem. Soc.* **2012**, *134* (42), 17416–17419.

(94) Ohmura, T.; Torigoe, T.; Suginome, M. Functionalization of Tetraorganosilanes and Permethyloligosilanes at a Methyl Group on Silicon via Iridium-Catalyzed C(Sp^3)–H Borylation. *Organometallics* **2013**, *32* (21), 6170–6173.

(95) Ohmura, T.; Torigoe, T.; Suginome, M. Iridium-Catalysed Borylation of Sterically Hindered C(Sp^3)–H Bonds: Remarkable Rate Acceleration by a Catalytic Amount of Potassium t-Butoxide. *Chem. Commun.* **2014**, *50* (48), 6333–6336.

(96) Murphy, J. M. The Synthesis of Organoboron Compounds by Metal-Catalyzed Carbon-Hydrogen Borylation of Alkanes and Arenes. Ph.D., Yale University, United States - Connecticut, **2009**.

(97) Zhong, R.-L.; Sakaki, S. Sp3 C–H Borylation Catalyzed by Iridium(III) Triboryl Complex: Comprehensive Theoretical Study of Reactivity, Regioselectivity, and Prediction of Excellent Ligand. *J. Am. Chem. Soc.* **2019**, *141* (25), 9854–9866.

(98) Larsen, M. A.; Oeschger, R. J.; Hartwig, J. F. Effect of Ligand Structure on the Electron Density and Activity of Iridium Catalysts for the Borylation of Alkanes. *ACS Catal.* **2020**, *10* (5), 3415–3424.

(99) Oeschger, R.; Su, B.; Yu, I.; Ehinger, C.; Romero, E.; He, S.; Hartwig, J. Diverse Functionalization of Strong Alkyl C–H Bonds by Undirected Borylation. *Science* **2020**, *368* (6492), 736–741.

(100) Zhong, R.-L.; Sakaki, S. Methane Borylation Catalyzed by Ru, Rh, and Ir Complexes in Comparison with Cyclohexane Borylation: Theoretical Understanding and Prediction. *J. Am. Chem. Soc.* **2020**, *142* (39), 16732–16747.

(101) Tamura, H.; Yamazaki, H.; Sato, H.; Sakaki, S. Iridium-Catalyzed Borylation of Benzene with Diboron. Theoretical Elucidation of Catalytic Cycle Including Unusual Iridium(V) Intermediate. *J. Am. Chem. Soc.* **2003**, *125* (51), 16114–16126.

(102) Ahn, S.; Sorsche, D.; Berritt, S.; Gau, M. R.; Mindiola, D. J.; Baik, M.-H. Rational Design of a Catalyst for the Selective Monoborylation of Methane. *ACS Catal.* **2018**, *8* (11), 10021–10031.

(103) Webster, C. E.; Fan, Y.; Hall, M. B.; Kunz, D.; Hartwig, J. F. Experimental and Computational Evidence for a Boron-Assisted, σ-Bond Metathesis Pathway for Alkane Borylation. *J. Am. Chem. Soc.* **2003**, *125* (4), 858–859.

(104) Hartwig, J. F.; Cook, K. S.; Hapke, M.; Incarvito, C. D.; Fan, Y.; Webster, C. E.; Hall, M. B. Rhodium Boryl Complexes in the Catalytic, Terminal Functionalization of Alkanes. *J. Am. Chem. Soc.* **2005**, *127* (8), 2538–2552.

(105) Kawamura, K.; Hartwig, J. F. Isolated Ir(V) Boryl Complexes and Their Reactions with Hydrocarbons. *J. Am. Chem. Soc.* **2001**, *123* (34), 8422–8423.

(106) Shi, Y.; Gao, Q.; Xu, S. Chiral Bidentate Boryl Ligand Enabled Iridium-Catalyzed Enantioselective C(Sp^3)–H Borylation of Cyclopropanes. *J. Am. Chem. Soc.* **2019**, *141* (27), 10599–10604.

(107) Yamamoto, T.; Ishibashi, A.; Suginome, M. Boryl-Directed, Ir-Catalyzed C(Sp^3)–H Borylation of Alkylboronic Acids Leading to Site-Selective Synthesis of Polyborylalkanes. *Org. Lett.* **2019**, *21* (16), 6235–6240.

(108) Cho, S. H.; Hartwig, J. F. Iridium-Catalyzed Borylation of Secondary Benzylic C–H Bonds Directed by a Hydrosilane. *J. Am. Chem. Soc.* **2013**, *135* (22), 8157–8160.

(109) Reyes, R. L.; Sato, M.; Iwai, T.; Sawamura, M. Asymmetric Synthesis of α-Aminoboronates via Rhodium-Catalyzed Enantioselective C(Sp3)–H Borylation. *J. Am. Chem. Soc.* **2020**, *142* (1), 589–597.

(110) Kawamorita, S.; Murakami, R.; Iwai, T.; Sawamura, M. Synthesis of Primary and Secondary Alkylboronates through Site-Selective C(Sp3)–H Activation with Silica-Supported Monophosphine–Ir Catalysts. *J. Am. Chem. Soc.* **2013**, *135* (8), 2947–2950. https://doi.org/10.1021/ja3126239.

(111) Mita, T.; Ikeda, Y.; Michigami, K.; Sato, Y. Iridium-Catalyzed Triple C(Sp 3)–H Borylations: Construction of Triborylated Sp 3 -Carbon Centers. *Chem. Commun.* **2013**, *49* (49), 5601–5603.

(112) Jones, M. R.; Fast, C. D.; Schley, N. D. Iridium-Catalyzed Sp3 C–H Borylation in Hydrocarbon Solvent Enabled by 2,2′-Dipyridylarylmethane Ligands. *J. Am. Chem. Soc.* **2020**, *142* (14), 6488–6492.

CHAPTER 2

2,2'-Dipyridylarylmethane Ligands: Perspectives in Metal Coordination and Catalysis, Optimized Syntheses, and Derivatization

2.1 Introduction

Design of increasingly active or selective catalysts through innovation of unconventional ligand platforms has the potential to revolutionize contemporary methods of C-H functionalization. Current challenges to iridium-catalyzed C-H borylation, ranging from selectivity and scope to atom economy and catalyst efficiency, may be remedied through the development of reimagined ligands. We envisioned that the core structure 2,2'-dipyridylarylmethane would contribute a tunable framework, enabling the preparation of ligand derivatives which could address existing limitations to alkane borylation as well as selective catalysts for arene borylation.

We identified the 2,2'-dipyridylarylmethane as a suitable manifold which conserves the diimine backbone of contemporary dtbpy or Me_4phen ligands while also allowing for incorporation of substituents that project out of the N−M−N plane.[1,2] With the established general mechanism in mind[3–5], we hypothesized that a facial, tridentate, monoanionic ligand might serve as a substitute for the diimine and one boryl ligand in the resting state structure, providing a binding mode analogous to that of Cp* (**Figure 2.1**). We anticipated that dipyridylarylmethane derivatives would undergo cyclometalation readily at iridium to confer a κ^3-binding mode, a coordination mode which has been observed for complexes of palladium and nickel.[6,7] As a result of the high trans influence of boryl and σ-aryl ligands, dipyridylarylmethane derivatives would be expected to favor a geometry with an open site mutually cis to the boryl ligands and trans to the σ-aryl. Facial coordination would warrant modulation of catalyst steric and electronic parameters through substitution on the cyclometalated ring. Additionally, cyclometalation of the aryl ring under the reaction conditions would allow the use of the same pre-catalysts previously found to be effective alongside diimine or phosphine ligands.[8–10]

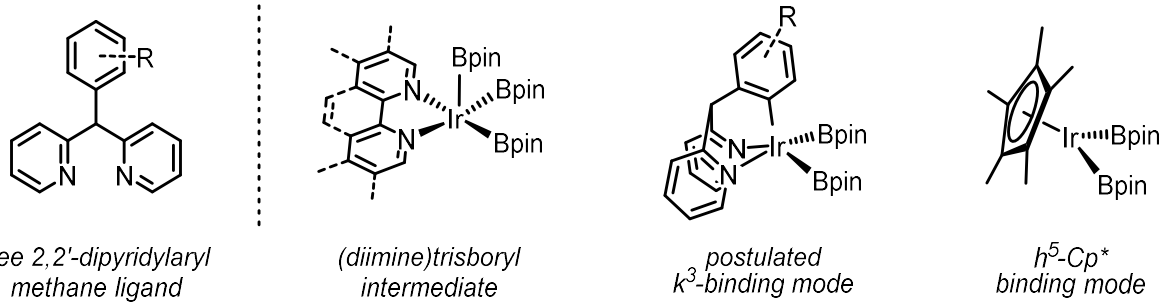

free 2,2'-dipyridylaryl methane ligand | *(diimine)trisboryl intermediate* | *postulated k^3-binding mode* | *h^5-Cp* binding mode*

Figure 2.1: *Structure of 2,2'-dipyridylarylmethane and postulated binding modes for diimine, 2,2'-dipyridylarylmethane, and Cp* ligands for iridium-catalyzed C-H borylation*

Facially coordinating ligands have previously proven effective in C-H borylation, particularly in the case of seminal Cp*Rh catalysts. [Cp*Rh(C_6Me_6)] is notably efficient for the challenging borylation of unactivated alkane substrates, with excellent turnover numbers and product incorporation of both boron equivalents of B_2pin_2.[11,12] Successful C-H borylation of both aromatic and alkane substrates has also been achieved using tris(pyrazolyl)borate (Tp) iridium catalysts.[13,14] Beyond Cp and Tp derivatives, alternative structures which engender facial monoanionic metal coordination are scarcely developed for purposes of catalysis. Specifically, 2,2'-dipyridylarylmethane scaffolds have been previously investigated as ancillary ligands in other applications, but not implemented in catalytic endeavors.[6,7,15,16] Meridional tridentate (pincer) monoanionic ligands have also been detailed in high turnover borylation of simple arene and alkane substrates, reinforcing the efficacy of the proposed electronic structure.[17–19] Unfortunately, pincer-type ligands require extensive preparations and suffer issues of usability due to required pre-complexation with metal catalyst. Additionally, facial alignment of boryl ligands has been indicated as the preferred inherent geometry of iridium borylation catalysts through the synthesis and study of *fac*-[$(PMe_3)_3Ir(Bpin)_3$] by Smith and coworkers.[8]

2,2'-dipyridylarylmethane structures provide an adaptable and effective ligand framework for iridium-catalyzed C-H borylation. Later chapters will describe fruitful investigations of these structures in the borylation of undirected alkyl and aryl substrates, as well as directed borylation of arenes through secondary coordination sphere interaction. Development of sustainable and practical catalysts is predicated upon not only reaction conditions and outcomes, but also on efficient processes for the

preparation of ligand and pre-catalyst materials. The remainder of this chapter will detail streamlined syntheses and alternative routes to access and derivatize 2,2'-dipyridylarylmethane compounds.

2.2 Ligand Syntheses

2,2'-dipyridylarylmethane compounds were originally pursued through derivatization of the commonly used 2,2'-dipyridylmethane (dpm) ligand (**Figure 2.2**). Dpm is readily prepared in yields exceeding 90% through lithiation of 2-picoline and treatment with 2-fluoropyridine. A suite of aryl-substituted derivatives was divergently synthesized by benzylic lithiation of dpm and subsequent nucleophilic aromatic substitution with the corresponding fluoroarene. When modestly electron-deficient 4-fluoroarenes were deployed in the reaction, such as in the case of **1**, a mixture of *meta*- and *para*- product regioisomers was obtained. This outcome is proposed to occur by the formation of a benzyne intermediate, mirroring findings by Cao and coworkers.[20] The unselective nature of this reaction enabled the simultaneous generation of isomeric derivatives **1a** and **1b** from a single reaction which are readily separable by column chromatography. Unfortunately, nucleophilicity of the dpm anion is tempered by resonance stabilization resulting in disfavored S_NAr and dismal yields of 15-34% across a variety of arene electrophiles. Additionally, preparation of 2,2'-dipyridylmethane compounds via this method disfavors production of *o*-substituted derivatives.

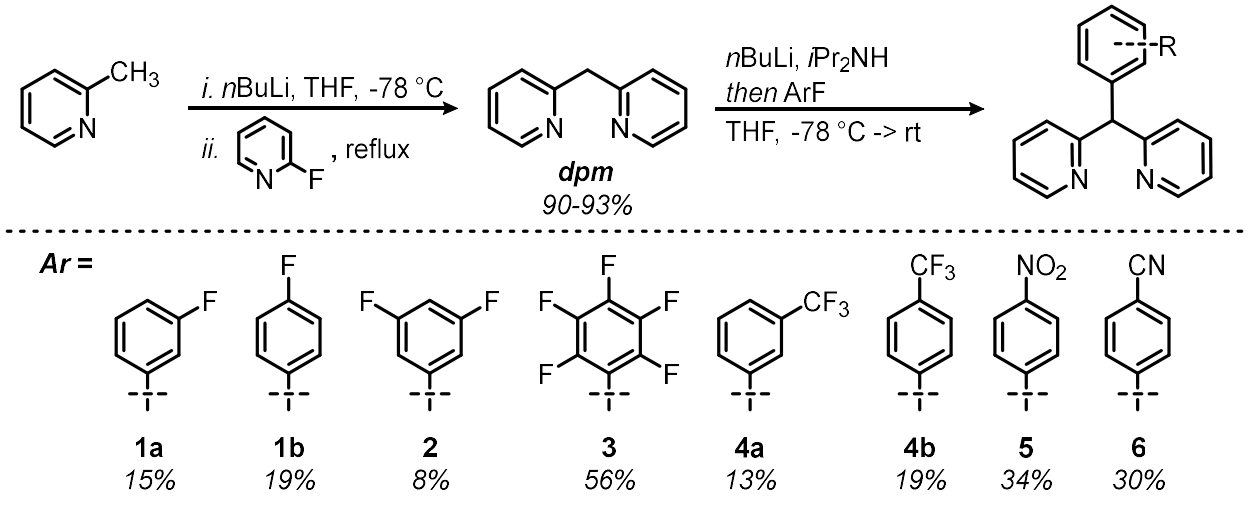

Figure 2.2: *General scheme for the synthesis of dpm and derivatization to 2,2'-dipyridyl arylmethanes by S_NAr. See general procedure A, section 2.4.*

We later determined that drastic improvements in yield could be achieved through the alternate bond disconnection between 2-benzylpyridine and pyridine. The analogous S_NAr strategy involving the strongly electrophilic 2-fluoropyridine and relatively destabilized 2-benzylpyridine anion proved fruitful in the preparation of **13**, with a yield of 83%. Additional 2,2'-dipyridylarylmethane derivatives were later pursued by this superior method; however, synthesis of aryl-functionalized analogs first requires the succinct preparation of substituted 2-benzylpyridines.

Initially these compounds were pursued via addition of aryl Grignard to 2-pyridinecarboxaldehyde, followed by benzylic deoxygenation with hydroiodic acid (**Figure 2.3**). While the Grignard was consistently executed in suitable yields, the product alcohol presented a challenging substrate for deoxygenation to the corresponding benzylpyridine. Particularly in cases of electron deficient aryl groups this method is notoriously low yielding[21], while the HI reagent also suffers complications of light and oxygen sensitivity. Grignard reactions were also used in the preparation of the methine functionalized derivatives (**22 & 23**), from the addition of aryl magnesium bromide to 2,2'-dipyridylketone and further substitution of the resulting alcohol with diethylaminosulfur trifuoride (DAST) (**Figure 2.4**).

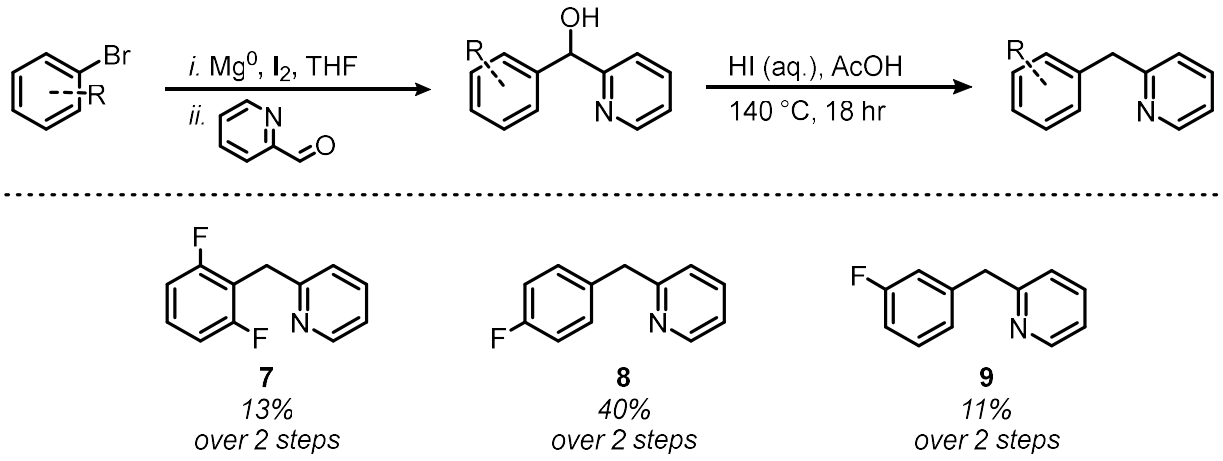

Figure 2.3: *Preparation of 2-benzylpyridines by Grignard and deoxygenation with HI. See general procedure B, section 2.4.*

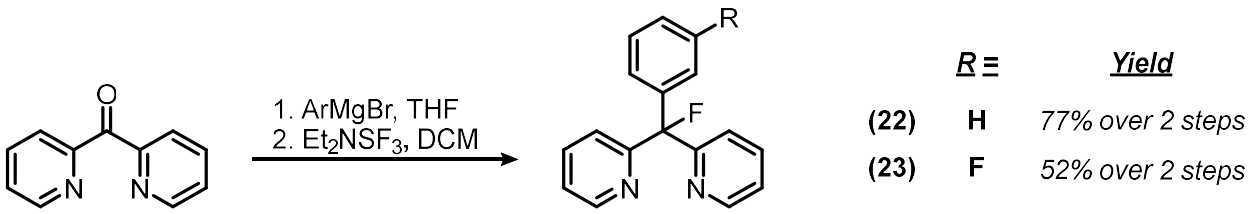

Figure 2.4: *Synthesis of fluorinated methine derivatives* ***22*** *and* ***23***

A surrogate route to the precursor 2-benzylpyridines **9-12** was established involving Pd-catalyzed oxidative coupling of aryl bromide and a 2-picoline derivative (**Figure 2.5**). First, addition of deprotonated 2-picoline to diisopropylketone near-quantitatively generates 2,4-dimethyl-3-(2-pyridylmethyl)pentan-3-ol. Coupling to aryl bromide via extrusion of diisopropylketone is then completed, producing 2-benzylpyridines in yields in the range of 60-90%. The resulting 3-step synthesis of 2,2'-dipyridylarylmethane derivatives offers a drastic increase in overall yield relative to previous routes, using accessible conditions and starting materials. In this manner, various aryl and pyridine substitution patterns were incorporated into the ligand structure to give ligands **1a** and **13-21** (**Figure 2.6**).

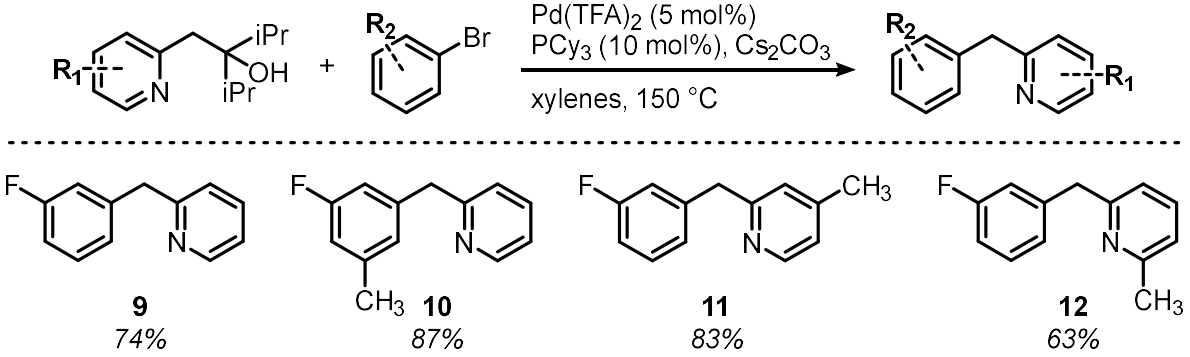

Figure 2.5: *Synthesis of 2-benzylpyridines by Pd-catalyzed cross-coupling. See general procedure C, section 2.4.*

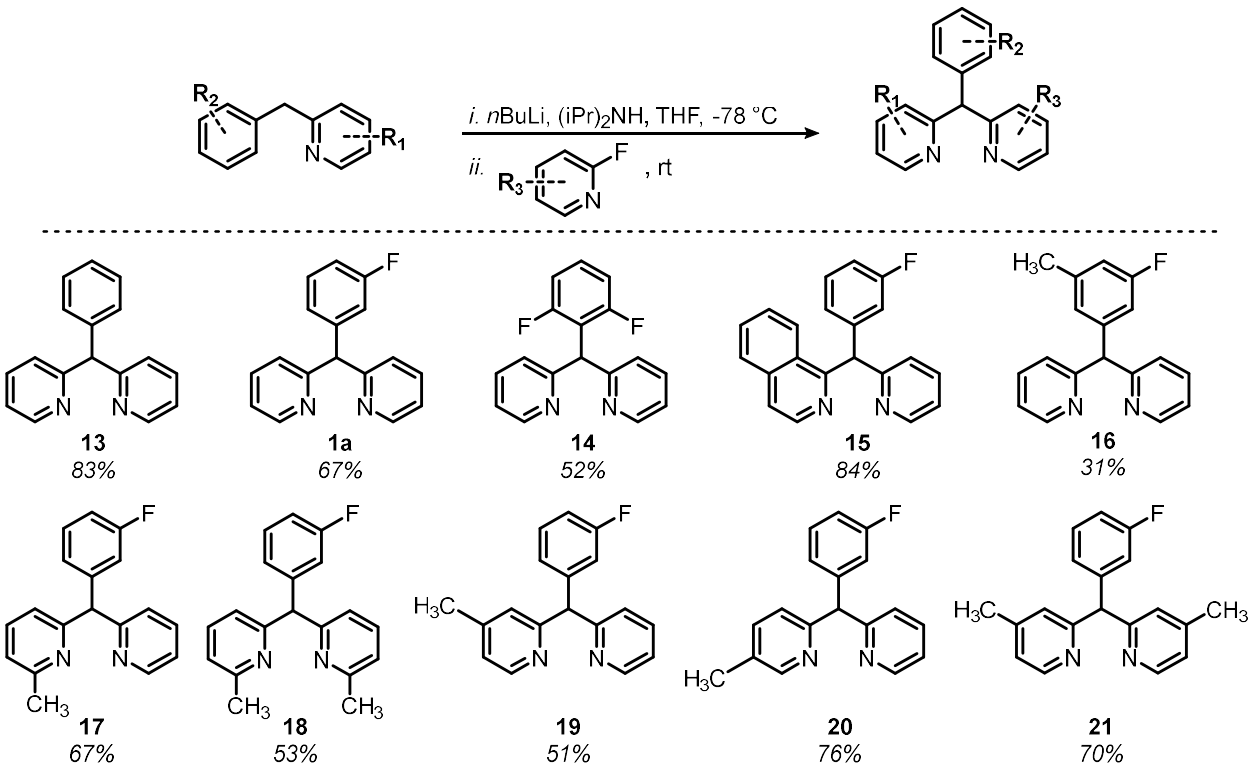

Figure 2.6: *Synthesis of 2,2'-dipyridylarylmethanes* ***13-21****. See general procedure D, section 2.4.*

A related series of compounds containing an additional methylene linkage in the backbone were also prepared for purposes of exploring alternate binding mode and geometry or secondary coordination sphere effects. These 2,2'-dipyridylbenzylmethane compounds were prepared according to **Figure 2.7**, wherein lithiation of dpm followed by nucleophilic substitution of a benzyl bromide affords the desired structure. Bromo (**24**), trifluoromethyl (**25**), nitro (**26**), and cyano (**27**) substituted products were obtained readily in good yield.

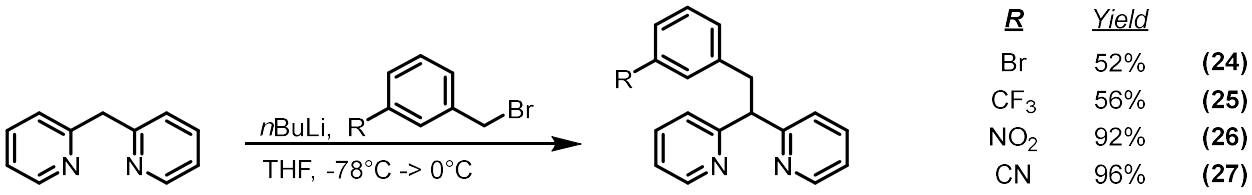

R	*Yield*	
Br	52%	**(24)**
CF_3	56%	**(25)**
NO_2	92%	**(26)**
CN	96%	**(27)**

Figure 2.7: *Preparation of 2,2'dipyridylbenzylmethanes* ***24-27****. See general procedure E, section 2.4.*

In cases of nitro and cyano functionalized derivatives **5**, **6**, **26** & **27** additional operations were performed to generate 2,2'-dipyridylarylmethane and 2,2'-dipyridylbenzylmethane ligands **28-35** (F**igure 2.8**)**.** Each ligand in this series contains a hydrogen bond donating substituent—the function for which is described in detail in Chapter 3. The nitro- derivatives **5** and **26** were advanced to the amines **30** and **31** via reduction with trichlorosilane, followed by treatment with isocyanate or acetic anhydride to give the corresponding urea (**33**, **34**) or acetamide (**32**), respectively. The cyano compounds, **6** and **27**, were manipulated further by oxygenation or Ritter reaction to generate amide **28** and N-*tert*-butyl amides **29** and **35**.

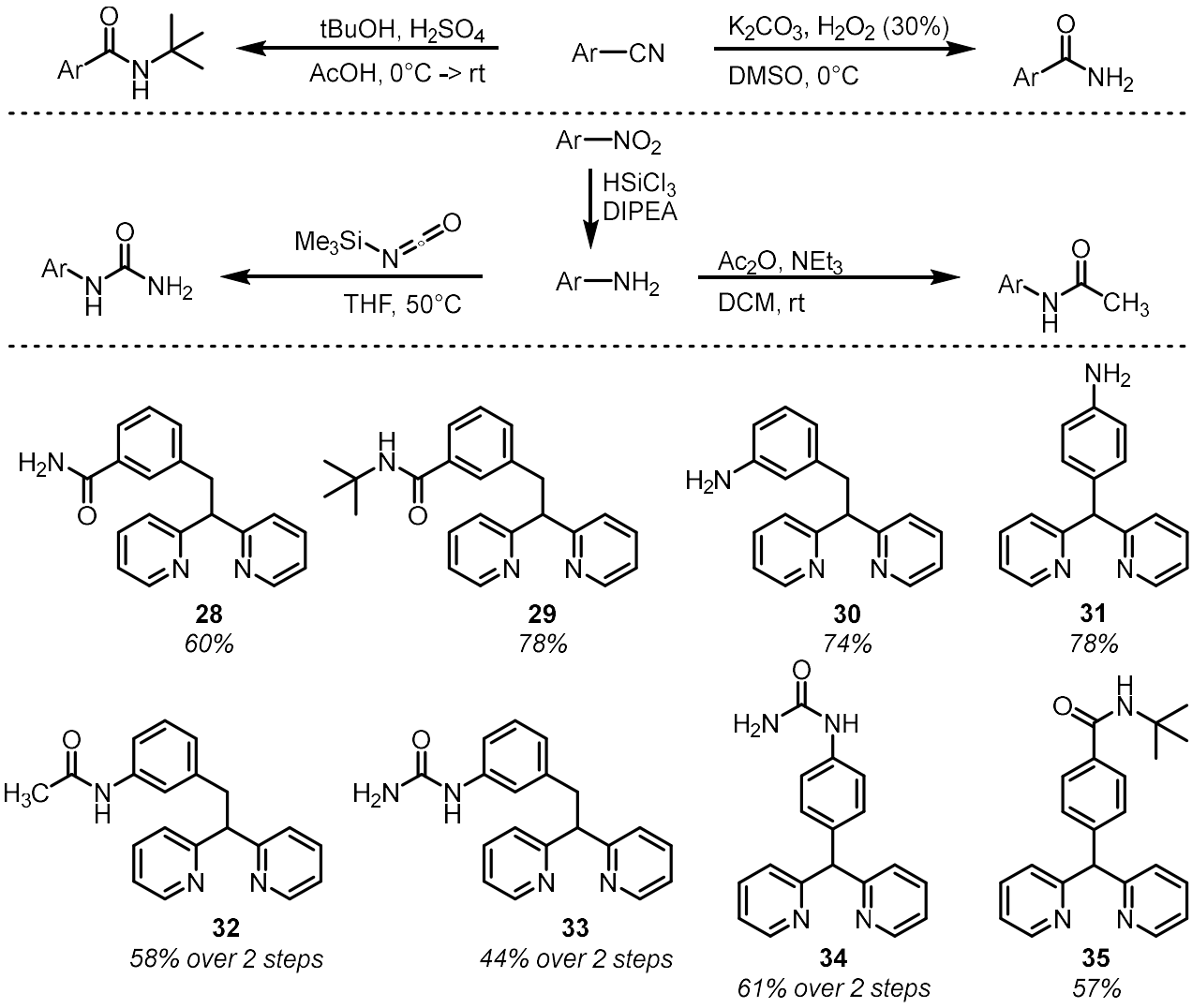

Figure 2.8: *Conversion of -NO_2 and -CN substituents to hydrogen bond donating groups in the preparation of ligands* ***28-35****. Yields reported based on CN or NO_2 precursor.*

2.3 Conclusions

2,2'-dipyridylarylmethanes constitute a promising ligand structure for study in the iridium-catalyzed C-H borylation of arene and alkane substrates due to their unique coordination mode and tunability. Synthesis of an extensive series of 2,2'-dipyridylarylmethane and 2,2'-dipyridylbenzylmethane ligands was pursued and various substituents about the aryl ring were achieved. Derivatives containing assorted patterns of methylation about the pyridine ring were also assembled for later screening in the borylation reaction. Structures containing hydrogen bond donors for the purpose of directed C-H borylation by noncovalent interaction between ligand and substrate were also successfully produced. Route optimization enabled drastic improvement in overall yield for the synthesis of 2,2'-dipyridylarylmethane compounds, resulting in ready access to derivatives for study in the C-H borylation reaction.

Portions of this chapter have been adapted with permission from Jones, M.R., Schley, N.D.; Ligand-Driven Advances in Iridium-Catalyzed sp3 C–H Borylation: 2,2'-Dipyridylarylmethan. Synlett 2021; 32(09): 845-850. DOI: 10.1055/a-1344-1904 Georg Thieme Verlag KG Copyright 2021

*Reprinted (adapted) with permission from Margaret R. Jones, Caleb D. Fast, and Nathan D. Schley. Journal of the American Chemical Society **2020** 142 (14), 6488-6492. DOI: 10.1021/jacs.0c00524. Copyright 2020 American Chemical Society.*

This material is based upon work supported by the National Science Foundation under grant no. CHE-1847813.

2.4 Experimental

General Considerations: Syntheses and manipulations with organometallic reagents were carried out using standard vacuum, Schlenk, cannula, or glovebox techniques under N_2 in oven- or flame-dried glassware unless otherwise specified. Tetrahydrofuran, dichloromethane, toluene, pentane, and diethyl ether were degassed with argon and dried over activated alumina using a solvent purification system.

Spectroscopy: ^{1}H, $^{13}C\{^{1}H\}$, and ^{19}F NMR spectra were recorded on Bruker NMR spectrometers at ambient temperatures unless otherwise noted. ^{1}H and $^{13}C\{1H\}$ chemical shifts are referenced to residual solvent signals, ^{19}F chemical shifts are referenced to an external C_6F_6 standard.

Ligand syntheses: Di(2-pyridyl)methane (**dpm**)[22], di(2-pyridyl)(phenyl)fluoromethane (**22**)[6] and di(2-pyridyl)(3-fluorophenyl)fluoromethane (**23**)[6] were prepared according to published procedures. 2-fluoropyridine, 2-benzylpyridine, 1,4-difluorobenzene, 2,2'-dipyridyl ketone, phenyl magnesium bromide, diethylaminosulfur trifluoride, 2,6-difluorobromobenzene, and pyridine-2-carboxaldehyde were purchased from chemical vendors and used as received.

General Procedures

General procedure A: *Preparation of 2,2'-dipyridylarylmethanes by LDA-mediated addition of dpm to fluoroarene*

A 3-necked round bottom flask was fitted with an addition funnel and placed under an atmosphere of nitrogen. THF and iPr_2NH (3 equiv., 1M) were added and the solution was cooled to -78 °C. *n*BuLi (3 equiv., 2.2 M in hexanes) was then added dropwise over 15 min. The resulting solution was allowed to warm to 0 °C while stirring for 1 hr. To the addition funnel was added 2,2'-dipyridylmethane (1 equiv.) in THF (0.5 M); the solution was added dropwise over 20 min and allowed to stir for 30 min upon completion of the addition while warming to room temperature. At this point a solution of fluoroarene (1.5 equiv.) in THF (0.5 M) was added and the resulting solution was allowed to stir at room temperature for 18 hr. The mixture was quenched by slow addition of deionized water and the organic layer extracted. The aqueous phase was washed with three portions of dichloromethane and the combined organic layers were washed with brine, dried over Na_2SO_4, and concentrated *in vacuo*. The resulting mixture was purified by column chromatography (75 → 100% EtOAc in hexanes and flushed with 10% MeOH in CH_2Cl_2) to give the product 2,2'-dipyridylarylmethane.

General procedure B: *Preparation of 2-benzylpyridine via Grignard followed by deoxygenation with concentrated HI*

A flame-dried 250 mL 3-neck round bottom flask fitted with an addition funnel was charged with magnesium turnings (1.4 equiv.) and 2-3 iodine crystals under an atmosphere of nitrogen. The flask was heated briefly until iodine vapor was observed. Upon cooling to room temperature, dry, degassed THF was added. A solution of bromoarene (1.3 equiv) in THF (2 M) was added dropwise over 20 min. After initiation,

the solution was stirred at ambient temperature for 1 hr. At this point the mixture was cooled to 0 °C, and a solution of pyridine-2-carboxaldehyde (1 equiv) in 0.5 M THF was added dropwise over 30 min. Upon completion of the addition, the reaction was allowed to warm to room temperature and was stirred for 2 hours. The mixture was quenched by slow addition of saturated aqueous NH_4Cl and the organic layer separated. The aqueous phase was washed with three portions of dichloromethane and the combined organic layers were washed with brine, dried over Na_2SO_4, and concentrated *in vacuo*. The resulting mixture was passed through a plug of silica with ethyl acetate, concentrated on a rotary evaporator, and dried under vacuum to give the product alcohol (**7a**-**9a**).

2-benzylpyridines were synthesized from the alcohol products by a variation of a reported procedure.[21] A round bottom flask fitted with a condenser was charged with (aryl)(2-pyridyl)methanol (1 equiv) under an atmosphere of N_2. To the flask was added acetic acid (12 mL), followed by careful addition of concentrated aqueous HI (5.3 equiv). The mixture was heated to 140 °C and stirred for 20 hr. The flask was then cooled to room temperature and diluted with deionized water. The mixture was neutralized by the addition of saturated aqueous $NaHCO_3$, made basic with Na_2CO_3, and extracted twice with portions of ethyl acetate. The combined organic fractions were dried over Na_2SO_4, concentrated under vacuum, and purified by column chromatography on silica gel (10% - 20% EtOAc in hexane).

General procedure C: *Preparation of 2-benzylpyridines by Pd-catalyzed coupling*

These compounds were synthesized according to a reported literature procedure[23] with the following modifications: In an inert atmosphere glove box, a round bottom flask was charged with $Pd(TFA)_2$ (5 mol %)[24], PCy_3 (10 mol%), and Cs_2CO_3 (1.5 equiv) and fitted with condenser. The apparatus was placed under an atmosphere of nitrogen (removed from box, sealed) and a solution of bromoarene (1 equiv) in 0.4 M xylenes was added. Finally, 2,4-dimethyl-3-(2-pyridylmethyl)pentan-3-ol (1.2 equiv) was added, and stirred under reflux for 16 hr. The resulting mixture was then cooled to ambient temperature and filtered through a pad of celite. Celite was rinsed through with an additional portion of ethyl acetate and then the solvent was removed under reduced pressure. The crude mixture was purified by column chromatography (20% ethyl acetate in hexanes) to give the pure product 2-benzylpyridine.

General procedure D: *Preparation of 2,2'-dipyridylarylmethanes by LDA-mediated addition of 2-benzylpyridine to 2-fluoropyridine*

These compounds were synthesized according to a reported literature procedure[20] with the following modifications: A Schlenk flask was charged with iPr_2NH (1.5 equiv.) in THF (1 M) under an atmosphere of nitrogen and was cooled to -78 °C. ^{n}BuLi (1.5 equiv., 2.2 M in hexanes) was added dropwise over 15 min to generate LDA. The resulting solution was allowed to warm to 0 °C while stirring for 1 hr. 2-benzylpyridine (1 equiv.) and THF (0.5 M) were added to a separate Schlenk flask, placed under an atmosphere of nitrogen, and cooled to 0 °C. The LDA solution was transferred dropwise via cannula to the 2-benzylpyridine solution, and the resulting mixture allowed to warm to ambient temperature while stirring for 30 min. 2-fluoropyridine (1.5 equiv.) in THF (0.5 M) was then added dropwise via syringe over 15 min, and the reaction allowed to stir at room temperature for 16 hr. The mixture was quenched by slow addition of deionized water and the organic layer extracted. The aqueous phase was washed with three portions of dichloromethane and the combined organic layers were washed with brine and dried over Na_2SO_4 followed by concentration *in vacuo*. The resulting mixture was purified by column chromatography (60% EtOAc in hexanes and flushed with 10% MeOH in CH_2Cl_2) to give the product 2,2'-dipyridylarylmethane.

General procedure E: *Synthesis of 2,2'-dipyridylbenzylmethanes*

A Schlenk flask was fitted with a magnetic stir bar, placed under an atmosphere of nitrogen, and cooled to -78 °C. To the flask was added THF and 2,2'-dipyridylarylmethane (1 equiv., 0.2 M), followed by dropwise addition of *n*BuLi (1.1 equiv., 2.2 M in hexanes) over 15 minutes. The resulting solution was allowed to warm to 0 °C while stirring for 1 hr. A solution of benzyl bromide (1.2 equiv.) in THF (1 M) was then added dropwise via syringe over 15 min, and the reaction allowed to stir at room temperature for 16 hr. The mixture was quenched by slow addition of deionized water and the organic layer extracted. The aqueous phase was washed with three portions of ethyl acetate and the combined organic layers were washed with brine and dried over Na_2SO_4 followed by concentration *in vacuo*. The resulting mixture was purified by column chromatography (40-60% EtOAc in hexanes) to give the product 2,2'-dipyridylbenzylmethane.

Synthesis and Characterization of Products:

Di(2-pyridyl)(3-fluorophenyl)methane (1a). This product was obtained through general procedure A from 1,4-difluorobenzene (3.6 mL, 35.2 mmol) as a mixture of isomers **1a** and **1b**. Separation by column chromatography affords the pure product **1a** as a red-brown solid. Yield: 0.71 g (15%); mp 90-92 °C.

Alternatively, **1a** can be prepared from 2-(3-fluorobenzyl)pyridine **(9)** (0.10 g, 0.53 mmol) by general procedure D. Yield: 0.094 g (67%).

^{1}H NMR ($CDCl_3$, 400 MHz): δ 8.60 (d, *J* = 4.8 Hz, 2H), 7.64 (td, *J* = 7.7, 1.9 Hz, 2H), 7.28 (dd, *J* = 8.0, 6.2 Hz, 1H), 7.25 (d, *J* = 7.1 Hz, 2H), 7.16 (dd, *J* = 7.6, 4.7 Hz, 2H), 7.06 (d, *J* = 7.9 Hz, 1H), 7.01 (dt, *J* = 10.1, 2.2 Hz, 1H), 6.93 (td, *J* = 8.4, 2.5 Hz, 1H), 5.81 (s, 1H) ^{13}C NMR ($CDCl_3$, 600 MHz): δ 161.6-164.0 (d, J_{CF} = 245 Hz), 161.4, 149.5, 144.2 (d, J_{CF} = 7.1 Hz), 136.6, 129.8 (d, J_{CF} = 8.4 Hz), 124.9 (d, J_{CF} = 2.5 Hz), 123.9, 121.7, 116.3 (d, J_{CF} = 21.6 Hz), 113.6 (d, J_{CF} = 21.1 Hz), 61.2. HRMS $[M+H]^+$ Calc. 265.1063, Found 265.1109

Di(2-pyridyl)(4-fluorophenyl)methane (1b). This product was obtained through general procedure A from 1,4-difluorobenzene (3.6 mL, 35.2 mmol) as a mixture of isomers **1a** and **1b**. Separation by column chromatography affords the pure product **1b** as a red-brown oil. Yield: 0.89 g (19%).

^{1}H NMR ($CDCl_3$, 400 MHz): δ 8.58 (d, *J* = 4.9 Hz, 2H), 7.62 (td, *J* = 7.7, 1.9 Hz 2H), 7.26 (td, *J* = 5.6, 2.6 Hz, 2H), 7.23 (d, *J* = 6.9 Hz, 2H), 7.14 (dd, *J* = 7.6, 4.9 Hz, 2H), 6.99 (t, *J* = 8.7 Hz, 2H), 5.79 (s, 1H). ^{13}C NMR ($CDCl_3$, 600 MHz): δ 160.4-162.9 (d, J_{CF} = 245 Hz), 161.8, 149.4, 137.3 (d, J_{CF} = 30.4 Hz), 136.5, 130.7 (d, J_{CF} = 7.7 Hz), 123.9, 121.6, 115.3 (d, J_{CF} = 21.5 Hz), 60.8. HRMS $[M+H]^+$ Calc. 265.1063, Found 265.1109

Di(2-pyridyl)(3,5-difluorophenyl)methane (2). This product was obtained through general procedure A from 1,3,5-trifluorobenzene (0.6 mL, 2.9 mmol) as a red-brown solid. Yield: 0.065 g (8%)

^{1}H NMR ($CDCl_3$, 400 MHz): δ 8.61 (d, *J* = 5.0 Hz, 2H), 7.66 (td, *J* = 7.7, 1.9 Hz, 2H), 7.28 (d, *J* = 7.9 Hz, 2H), 7.18 (ddd, *J* = 7.5, 4.9, 0.9 Hz, 2H), 6.83 (m, 2H), 6.68 (tt, *J* = 8.8, 2.2 Hz, 1H), 5.76 (s, 1H). ^{19}F{^{1}H} NMR ($CDCl_3$, 376 MHz): δ -109.9.

Di(2-pyridyl)(pentafluorophenyl)methane (3). This product was obtained through

general procedure A from perfluorobenzene (0.67 mL, 5.8 mmol) as a tan solid. Yield: 0.55 g (56%)

^{1}H NMR ($CDCl_3$, 400 MHz): δ 8.59 (d, *J* = 4.8 Hz, 2H), 7.65 (td, *J* = 7.7, 1.8 Hz, 2H), 7.21 (dd, *J* = 7.3, 5.1 Hz, 2H), 7.10 (d, *J* = 8.0 Hz, 2H), 6.13 (s, 1H). ^{19}F{^{1}H} NMR ($CDCl_3$, 376 MHz): δ -139.3 (dd, *J* = 6.9, 22.8 Hz, 2F), -156.2 (t, *J* = 20.9, 1F), -162.6 (td, *J* = 6.5, 20.9 Hz, 2F)

Di(2-pyridyl)(3-(trifluoromethyl)phenyl)methane (4a). This product was obtained through general procedure A from 1-fluoro-3-(trifluoromethyl)benzene (0.74 mL, 5.8 mmol) as a red-brown solid. Yield: 0.12 g (13%)

^{1}H NMR ($CDCl_3$, 400 MHz): δ 8.60 (d, *J* = 5.0 Hz, 2H), 7.66 (td, *J* = 7.7, 1.9 Hz, 2H), 7.58 (s, 1H), 7.50 (d, *J* = 7.3 Hz, 2H), 7.45 (t, *J* = 6.9 Hz, 1H), 7.25 (d, *J* = 8.4 Hz, 2H), 7.17 (ddd, *J* = 7.5, 4.9, 0.9 Hz, 2H), 5.85 (s, 1H).

Di(2-pyridyl)(4-(trifluoromethyl)phenyl)methane (4b). This product was obtained through general procedure A from 1-fluoro-4-(trifluoromethyl)benzene (0.74 mL, 5.8 mmol) as a red-brown solid. Yield: 0.18 g (19%)

^{1}H NMR ($CDCl_3$, 400 MHz): δ 8.60 (d, *J* = 5.0 Hz, 2H), 7.63 (td, *J* = 7.7, 1.9 Hz, 2H), 7.53 (m, 2H), 7.43 (m, 2H), 7.25 (d, *J* = 8.4 Hz, 2H), 7.17 (ddd, *J* = 7.5, 4.9, 0.9 Hz, 2H), 5.85 (s, 1H).

Di(2-pyridyl)(4-nitrophenyl)methane (5). This product was obtained through general procedure A from 1-fluoro-4-nitrobenzene (0.50 g, 3.5 mmol) as a brown viscous oil. Yield: 0.13 g (26%)

^{1}H NMR ($CDCl_3$, 400 MHz): δ 8.61 (d, *J* = 5.0 Hz, 2H), 8.17 (d, *J* = 8.9 Hz, 2H), 7.67 (td, *J* = 7.7, 1.9 Hz, 2H), 7.48 (d, *J* = 8.9 Hz, 2H), 7.27 (d, *J* = 7.7 Hz, 2H), 7.20 (ddd, *J* = 7.5, 4.9, 1.2 Hz, 2H), 5.87 (s, 1H).

Di(2-pyridyl)(4-cyanophenyl)methane (6). This product was obtained through general procedure A from 1-fluoro-4-cyanobenzene (0.42 g, 3.5 mmol) as a brown viscous oil. Yield: 0.24 g (30%)

^{1}H NMR ($CDCl_3$, 400 MHz): δ 8.39 (d, *J* = 5.2 Hz, 2H), 7.47 (td, *J* = 7.7, 1.9 Hz, 2H), 7.42 (d, *J* = 8.2 Hz, 2H), 7.25 (d, *J* = 8.4 Hz, 2H), 7.10 (d, *J* = 7.8 Hz, 2H), 7.00 (dd, *J* = 7.6, 4.9 Hz, 2H), 5.87 (s, 1H).

(2,6-difluorophenyl)(2-pyridyl)methanol (7a). This product was prepared from 2,6-difluorobromobenzene (1.20 g, 6.24 mmol) according to part one of general procedure B. **7a** was obtained as a pale yellow crystalline solid. Yield: 0.980 g (92%).
^{1}H NMR ($CDCl_3$, 600 MHz): δ 8.60 (d, *J* = 4.7 Hz, 1H), 7.65 (td, *J* = 7.7, 1.7 Hz, 1H), 7.28 – 7.21 (m, 2H), 7.15 (d, *J* = 7.9 Hz, 1H), 6.87 (t, *J* = 8.3, 2H), 6.20 (d, *J* = 5.1 Hz, 1H), 5.45 (d, *J* = 5.3 Hz, 1H) ^{13}C{^{1}H} NMR ($CDCl_3$, 151 MHz): δ 161.6 (dd, J_{CF} = 250.4, 8.0 Hz), 159.1, 147.9, 137.1, 130.0 (t, J_{CF} = 10.6 Hz), 122.7, 120.6, 119.1 (t, J_{CF} = 16.1 Hz), 111.9 (dd, J_{CF} = 4.7 Hz, 21.4 Hz), 65.7 (t, J_{CF} = 3.3 Hz) ^{19}F{^{1}H} NMR ($CDCl_3$, 376 MHz): δ -114.7 HRMS [M+H]+ Calc. 222.0725, Found 222.0727

2-(2,6-difluorobenzyl)pyridine (7) The product was prepared from **7a** (0.626 g, 2.83 mmol) according to general procedure B. The product was obtained as a pale yellow oil. Yield: 0.087 g (14%); Recovered (2,6-difluorophenyl)(2-pyridyl)methanol (**7a**): 0.520 g (83%).
^{1}H NMR ($CDCl_3$, 400 MHz): δ 8.54 (d, *J* = 4.6 Hz, 1H), 7.58 (dt, *J* = 1.8, 7.7 Hz, 1H), 7.21 (m, 1H), 7.11 (m, 2H), 6.90 (t, *J* = 7.7 Hz, 2H), 4.23 (s, 2H). ^{13}C{^{1}H} NMR ($CDCl_3$, 151 MHz): δ 161.85 (dd, *J* = 247.8, 8.4 Hz), 159.0, 149.6, 136.8, 128.5 (t, *J* = 10.2 Hz), 122.6, 121.7, 115.3, (t, *J* = 20.2), 111.5 (dd, *J* = 20.9, 5.3 Hz), 31.3 (t, *J* = 2.5 Hz). ^{19}F{^{1}H} NMR ($CDCl_3$, 376 MHz): δ -114.3 HRMS [M+H]+ Calc. 206.0776, Found 206.0771

(4-fluorophenyl)(2-pyridyl)methanol (8a). This product was prepared from 4-fluorobromobenzene (0.53 g, 3 mmol) according to part one of general procedure B. **8a** was obtained as a pale yellow crystalline solid. Yield: 0.51 g (89%).
Product was characterized according to previously published values.[25]

2-(4-fluorobenzyl)pyridine (8) The product was prepared from **8a** (0.5 g, 2.5 mmol) according to general procedure B. The product was obtained as a pale yellow oil. Yield: 0.21 g (46%)
Product was characterized according to previously published values.[23]

(3-fluorophenyl)(2-pyridyl)methanol (9a). This product was prepared from 3-fluorobromobenzene (0.53 g, 3 mmol) according to part one of general procedure B. **9a**

was obtained as a pale yellow crystalline solid. Yield: 0.46 g (75%).
Product was characterized according to previously published values.[25]

2-(3-fluorobenzyl)pyridine (9) The product was prepared from **9a** (0.5 g, 2.5 mmol) according to general procedure B. The product was obtained as a pale yellow oil. Yield: 0.065 g (14%);
Alternatively, **9** can be prepared by general procedure C from 3-fluorobromobenzene (0.88 g, 5 mmol) and 2,4-dimethyl-3-(2-pyridylmethyl)pentan-3-ol (1.25 g, 6 mmol) . Yield: 0.68 g (74%).
Product was characterized according to previously published values.[23]

2-(3-fluoro-5-methylbenzyl)pyridine (10) The product was prepared from 3-bromo-5-fluorotoluene (0.71 g, 3.8 mmol) and 2,4-dimethyl-3-(2-pyridylmethyl)pentan-3-ol (0.94 g, 4.5 mmol) according to general procedure B. The product was obtained as a pale yellow oil. Yield: 0.67 g (87%)
^{1}H NMR ($CDCl_3$, 400 MHz): δ 8.56 (d, *J* = 4.6 Hz, 1H), 7.60 (td, *J* = 1.8, 7.7 Hz, 1H), 7.13 (m, 2H), 6.87 (s, 1H), 6.75 (t, *J* = Hz, 2H), 4.10 (s, 2H), 2.31 (s, 3H).

2-(3-fluorobenzyl)-4-picoline (11) The product was prepared from 3-fluorobromobenzene (0.34 g, 3.8 mmol) and 2,4-dimethyl-3-((4-methylpyridin-2-yl)methyl)pentan-3-ol (1.0 g, 4.5 mmol) according to general procedure B. The product was obtained as a pale yellow oil. Yield: 0.64 g (83%)
^{1}H NMR ($CDCl_3$, 400 MHz): δ 8.41 (d, *J* = 4.6 Hz, 1H), 7.25 (td, *J* = 6.1, 7.8 Hz, 1H), 7.04 (d, *J* = 7.6 Hz, 1H), 6.92-6.98 (m, 3H), 6.90 (td, *J* = 2.8, 8.7 Hz, 1H), 4.10 (s, 2H), 2.29 (s, 3H).

2-(3-fluorobenzyl)-6-picoline (12) The product was prepared from 3-fluorobromobenzene (0.44 g, 2.5 mmol) and 2,4-dimethyl-3-((2-methylpyridin-2-yl)methyl)pentan-3-ol (0.66 g, 3.0 mmol) according to general procedure B. The product was obtained as a pale yellow oil. Yield: 0.32 g (63%)
^{1}H NMR ($CDCl_3$, 400 MHz): δ 7.46 (t, *J* = 7.7 Hz, 1H), 7.24 (td, *J* = 6.1, 7.9 Hz, 1H), 7.03 (d, *J* = 7.8 Hz, 1H), 6.98 (d, *J* = 7.8 Hz, 1H), 6.95 (dt, *J* = 2.3, 10.2 Hz, 1H), 6.90 (dd, *J* = 2.6, 8.7 Hz, 1H), 6.86 (d, *J* = 7.8 Hz, 1H), 4.12 (s, 2H), 2.55 (s, 3H). ^{19}F{^{1}H}

NMR ($CDCl_3$, 376 MHz): δ -113.5.

Di(2-pyridyl)(phenyl)methane (13). The product was synthesized according to general procedure D from 2-benzylpyridine (1.0 g, 5.9 mmol) and 2-fluoropyridine (0.76 mL, 8.86 mmol). 1.2 g, 83% of **13** was obtained as an off-white crystalline solid.
Product was characterized according to previously published values.[20]

Di(2-pyridyl)(2,6-difluorophenyl)methane (14). This product was prepared and purified according to general procedure D from **7** (0.050 g, 0.244 mmol). The product was obtained as a red-brown solid. Yield: 0.036 g (52%); mp 98-100 °C.
^{1}H NMR ($CDCl_3$, 600 MHz): δ 8.59 (d, *J* = 4.2 Hz, 2H), 7.62 (td, *J* = 7.7, 1.8 Hz, 2H), 7.26 – 7.21 (m, 1H), 7.16 (dd, *J* = 7.2, 5.0 Hz, 2H), 7.11 (d, *J* = 7.9 Hz, 2H) 6.90 (t, *J* = 8.2, 2H), 6.20 (s, 1H) ^{13}C{^{1}H} NMR ($CDCl_3$, 151 MHz): δ 161.6 (dd, J_{CF} = 248.9, 8.0 Hz), 160.3, 149.6, 136.6, 129.1 (t, J_{CF} = 10.5 Hz), 123.4, 121.9, 118.2 (t, J_{CF} = 17.3 Hz), 111.9 (dd, J_{CF} = 4.3 Hz, J_{CF} = 21.3 Hz), 51.4. ^{19}F{^{1}H} NMR ($CDCl_3$, 376 MHz): δ -111.6
HRMS [M+H]+ Calc. 283.1041, Found 283.1049

1-((3-fluorophenyl)(pyridin-2-yl)methyl)isoquinoline (15). The product was synthesized according to general procedure D from **9** (0.10 g, 0.54 mmol) and 1-chloroisoquinoline (0.13 g, 0.80 mmol). 0.21 g, 84% of **16** was obtained as an off-white solid. ^{1}H NMR ($CDCl_3$, 400 MHz): δ 8.58 (d, *J* = 5.0 Hz, 1H), 8.50 (d, *J* = 5.6 Hz, 1H), 8.24 (d, *J* = 8.5 Hz, 1H), 7.83 (d, *J* = 8.4 Hz, 1H), 7.77 (td, *J* = 7.9, 1.3 Hz, 1H), 7.65 (m, 1H), 7.62 (d, *J* = 5.8 Hz, 1H), 7.52 – 7.58 (m, 2H), 7.28 (td, *J* = 7.9, 6.1 Hz, 1H), 7.19 (t, *J* = 5.9 Hz, 1H), 7.08 (d, *J* = 7.5 Hz, 1H), 7.00 (dt, *J* = 2.0, 10.4 Hz, 1H), 6.93 (td, *J* = 2.7, 8.6 Hz, 1H), 6.71 (s, 1H).

Di(2-pyridyl)(3-fluoro-5-methylphenyl)methane (16). The product was synthesized according to general procedure D from **10** (0.25 g, 1.25 mmol) and 2-fluoropyridine (0.17 mL, 1.9 mmol). 0.11 g, 31% of **16** was obtained as an off-white solid.
^{1}H NMR ($CDCl_3$, 400 MHz): δ 8.51 (d, *J* = 5.0 Hz, 2H), 7.56 (td, *J* = 7.7, 1.9 Hz, 2H), 7.18 (d, *J* = 8.1 Hz, 2H), 7.08 (ddd, *J* = 7.5, 4.8, 1.2 Hz, 2H), 6.79 (s, 1H), 6.72 (d, *J* = 9.9 Hz, 1H), 6.67 (d, *J* = 9.9 Hz, 1H), 5.70 (s, 1H), 2.22 (s, 3H). ^{19}F{^{1}H} NMR ($CDCl_3$, 376 MHz): δ -114.2

(pyridine-2-yl)(6-methylpyridin-2-yl)(3-fluorophenyl)methane (17). The product was synthesized according to general procedure D from **9** (0.18 g, 1.0 mmol) and 2-fluoro-6-methylpyridine (0.17 mL, 1.5 mmol). 0.19 g, 67% of **17** was obtained as a tan solid.
^{1}H NMR ($CDCl_3$, 400 MHz): δ 8.59 (d, *J* = 5.0 Hz, 1H), 7.62 (td, *J* = 7.7, 1.9 Hz, 1H), 7.51 (td, *J* = 7.8 Hz, 1H), 7.25 (m, 2H), 7.15 (dd, *J* = 4.9, 7.5 Hz, 1H), 7.05 (m, 2H), 7.01 (d, *J* = 8.3 Hz, 1H), 6.98 (dt, *J* = 2.1, 10.3 Hz, 1H), 6.91 (td, *J* = 2.5, 8.5 Hz, 1H), 5.78 (s, 1H), 2.53 (s, 3H).

Di(6-methylpyridin-2-yl)(3-fluorophenyl)methane (18). The product was synthesized according to general procedure D from **12** (0.20 g, 1.0 mmol) and 2-fluoro-6-methylpyridine (0.17 g, 1.5 mmol). 0.15 g, 53% of **18** was obtained as a tan solid.
^{1}H NMR ($CDCl_3$, 400 MHz): δ 7.50 (td, *J* = 7.8 Hz, 2H), 7.23 (td, *J* = 7.9, 6.1 Hz, 1H), 7.06 (d, *J* = 7.6 Hz, 2H), 7.03 (d, *J* = 7.7 Hz, 1H), 7.00 (d, *J* = 7.5 Hz, 2H), 6.98 (dt, *J* = 2.1, 10.3 Hz, 1H), 6.90 (td, *J* = 2.5, 8.5 Hz, 1H), 5.75 (s, 1H), 2.55 (s, 6H).

(pyridine-2-yl)(4-methylpyridin-2-yl)(3-fluorophenyl)methane (19). The product was synthesized according to general procedure D from **9** (0.10 g, 0.54 mmol) and 2-fluoro-4-methylpyridine (0.08 mL, 0.8 mmol). 0.076 g, 51% of **19** was obtained as a pale orange solid.
^{1}H NMR ($CDCl_3$, 400 MHz): δ 8.59 (d, *J* = 4.8 Hz, 1H), 8.45 (d, *J* = 4.8 Hz, 1H), 7.63 (td, *J* = 7.7, 1.9 Hz, 1H), 7.27 (m, 1H), 7.24 (s, 1H), 7.16 (ddd, *J* = 7.7, 5.0, 1.0 Hz, 1H), 7.07 (s, 1H), 7.05 (d, *J* = 8.1 Hz, 1H), 6.96 – 7.03 (m, 2H), 6.93 (td, *J* = 8.9, 2.8 Hz, 1H), 5.76 (s, 1H), 2.31 (s, 3H).

(pyridine-2-yl)(5-methylpyridin-2-yl)(3-fluorophenyl)methane (20). The product was synthesized according to general procedure D from **9** (0.10 g, 0.54 mmol) and 2-fluoro-5-methylpyridine (0.08 mL, 0.8 mmol). 0.114 g, 76% of **20** was obtained as a pale orange solid.
^{1}H NMR ($CDCl_3$, 400 MHz): δ 8.59 (d, *J* = 5.1 Hz, 1H), 8.42 (s, 1H), 7.63 (td, *J* = 7.9, 1.8 Hz, 1H), 7.44 (dd, *J* = 7.9, 2.1 Hz, 1H), 7.23 - 7.29 (m, 2H), 7.12 – 7.17 (m, 2H), 7.04 (d, *J* = 7.7 Hz, 1H), 6.99 (dt, *J* = 10.2, 2.2 Hz, 1H), 6.92 (td, *J* = 2.7, 8.4 Hz, 1H), 5.77 (s, 1H), 2.31 (s, 3H).

Di(4-methylpyridin-2-yl)(3-fluorophenyl)methane (21). The product was synthesized according to general procedure D from **11** (0.25 g, 1.25 mmol) and 2-fluoro-4-methylpyridine (0.16 mL, 1.9 mmol). 0.26 g, 70% of **18** was obtained as a beige solid.
^{1}H NMR ($CDCl_3$, 400 MHz): δ 8.44 (d, *J* = 5.0 Hz, 2H), 7.27 (td, *J* = 7.9, 6.3 Hz, 1H), 7.09 (s, 2H), 7.06 (d, *J* = 7.9 Hz, 1H), 7.00 (dt, *J* = 1.7, 9.6 Hz, 1H), 6.98 (d, *J* = 5.1 Hz, 2H), 6.90 (td, *J* = 2.5, 8.5 Hz, 1H), 5.75 (s, 1H), 2.31 (s, 6H). ^{19}F{^{1}H} NMR ($CDCl_3$, 376 MHz): δ -114.1

Di(2-pyridyl)(3-bromobenzyl)methane (24). The product was synthesized according to general procedure E from 1-bromo-3-(bromomethyl)benzene (0.86 g, 3.4 mmol) and 2,2'-dipyridylmethane (0.5 g, 2.9 mmol). 0.51 g, 52% of the product was obtained as a red viscous oil.
^{1}H NMR ($CDCl_3$, 400 MHz): δ 8.58 (d, *J* = 4.9 Hz, 2H), 7.55 (td, *J* = 1.8, 7.7 Hz, 2H), 7.27 (d, *J* = 8.0 Hz, 2H), 7.25 (s, 1H), 7.22 (m, 1H), 7.10 (ddd, *J* = 1.1, 4.8, 7.7 Hz, 2H), 6.99 (m, 2H), 4.53 (t, *J* = 8.1 Hz, 1H), 3.56 (d, *J* = 7.6 Hz, 2H).

Di(2-pyridyl)(3-(trifluoromethyl)benzyl)methane (25). The product was synthesized according to general procedure E from 1-(bromomethyl)-3-(trifluoromethyl)benzene (0.83 g, 3.4 mmol) and 2,2'-dipyridylmethane (0.5 g, 2.9 mmol). 0.54 g, 56% of the product was obtained as a red-brown viscous oil.
^{1}H NMR ($CDCl_3$, 400 MHz): δ 8.58 (d, *J* = 5.0 Hz, 2H), 7.55 (td, *J* = 1.8, 7.7 Hz, 2H), 7.35 (m, 1H), 7.32 (s, 1H), 7.27 (d, *J* = 7.9 Hz, 2H), 7.24 (m, 2H), 7.22 (m, 1H), 7.10 (ddd, *J* = 1.1, 4.8, 7.7 Hz, 2H), 4.54 (t, *J* = 8.1 Hz, 1H), 3.65 (d, *J* = 7.6 Hz, 2H).

Di(2-pyridyl)(3-nitrobenzyl)methane (26). The product was synthesized according to general procedure E from 1-(bromomethyl)-3-nitrobenzene (0.73 g, 3.4 mmol) and 2,2'-dipyridylmethane (0.5 g, 2.9 mmol). 0.88 g, 92% of the product was obtained as a red-brown viscous oil.
^{1}H NMR ($CDCl_3$, 400 MHz): δ 8.58 (d, *J* = 5.0 Hz, 2H), 7.95 (m, 2H), 7.55 (td, *J* = 1.8, 7.7 Hz, 2H), 7.42 (d, *J* = 7.7 Hz, 1H), 7.31 (t, *J* = 7.8 Hz, 1H), 7.26 (d, *J* = 7.8 Hz, 2H), 7.11 (ddd, *J* = 1.1, 4.8, 7.7 Hz, 2H), 4.57 (t, *J* = 7.9 Hz, 1H), 3.71 (d, *J* = 8.1 Hz, 2H).

Di(2-pyridyl)(3-cyanobenzyl)methane (27). The product was synthesized according

to general procedure E from 1-(bromomethyl)-3-cyanobenzene (0.67 g, 3.4 mmol) and 2,2'-dipyridylmethane (0.5 g, 2.9 mmol). 0.83 g, 96% of the product was obtained as a red-brown viscous oil.

^{1}H NMR ($CDCl_3$, 400 MHz): δ 8.57 (d, *J* = 5.0 Hz, 2H), 7.55 (td, *J* = 1.8, 7.7 Hz, 2H), 7.36 (m, 3H), 7.24 (m, 3H), 7.10 (ddd, *J* = 1.1, 4.8, 7.7 Hz, 2H), 4.52 (t, *J* = 7.9 Hz, 1H), 3.63 (d, *J* = 7.8 Hz, 2H).

2.5 *References*

(1) Vasko, P.; Kinnunen, V.; Moilanen, J. O.; Roemmele, T. L.; Boeré, R. T.; Konu, J.; Tuononen, H. M. Group 13 Complexes of Dipyridylmethane, a Forgotten Ligand in Coordination Chemistry. *Dalton Trans.* **2015**, *44* (41), 18247–18259.

(2) Sberegaeva, A. V.; Zavalij, P. Y.; Vedernikov, A. N. Oxidation of a Monomethylpalladium(II) Complex with O2 in Water: Tuning Reaction Selectivity to Form Ethane, Methanol, or Methylhydroperoxide. *J. Am. Chem. Soc.* **2016**, *138* (4),

(3) Boller, T. M.; Murphy, J. M.; Hapke, M.; Ishiyama, T.; Miyaura, N.; Hartwig, J. F. Mechanism of the Mild Functionalization of Arenes by Diboron Reagents Catalyzed by Iridium Complexes. Intermediacy and Chemistry of Bipyridine-Ligated Iridium Trisboryl Complexes. *J. Am. Chem. Soc.* **2005**, *127* (41), 14263–14278.

(4) Li, Q.; Liskey, C. W.; Hartwig, J. F. Regioselective Borylation of the C–H Bonds in Alkylamines and Alkyl Ethers. Observation and Origin of High Reactivity of Primary C–H Bonds Beta to Nitrogen and Oxygen. *J. Am. Chem. Soc.* **2014**, *136* (24), 8755–8765.

(5) Oeschger, R. J.; Larsen, M. A.; Bismuto, A.; Hartwig, J. F. Origin of the Difference in Reactivity between Ir Catalysts for the Borylation of C–H Bonds. *J. Am. Chem. Soc.* **2019**, *141* (41), 16479–16485.

(6) Chong, E.; Kampf, J. W.; Ariafard, A.; Canty, A. J.; Sanford, M. S. Oxidatively Induced C–H Activation at High Valent Nickel. *J. Am. Chem. Soc.* **2017**, *139* (17), 6058–6061.

(7) Maleckis, A.; Sanford, M. S. Facial Tridentate Ligands for Stabilizing Palladium(IV) Complexes. *Organometallics* **2011**, *30* (24), 6617–6627.

(8) Cho, J.-Y.; Tse, M. K.; Holmes, D.; Maleczka, R. E.; Smith, M. R. Remarkably Selective Iridium Catalysts for the Elaboration of Aromatic C-H Bonds. *Science* **2002**, *295* (5553), 305–308.

(9) Ishiyama, T.; Takagi, J.; Hartwig, J. F.; Miyaura, N. A Stoichiometric Aromatic C□H Borylation Catalyzed by Iridium(I)/2,2′-Bipyridine Complexes at Room Temperature. *Angew. Chem. Int. Ed.* **2002**, *41* (16), 3056–3058.

(10) Preshlock, S. M.; Ghaffari, B.; Maligres, P. E.; Krska, S. W.; Maleczka, R. E.; Smith, M. R. High-Throughput Optimization of Ir-Catalyzed C–H Borylation: A Tutorial for Practical Applications. *J. Am. Chem. Soc.* **2013**, *135* (20), 7572–7582.

(11) Chen, H.; Schlecht, S.; Semple, T. C.; Hartwig, J. F. Thermal, Catalytic, Regiospecific Functionalization of Alkanes. *Science* **2000**, *287* (5460), 1995–1997.

(12) Lawrence, J. D.; Takahashi, M.; Bae, C.; Hartwig, J. F. Regiospecific Functionalization of Methyl C−H Bonds of Alkyl Groups in Reagents with Heteroatom Functionality. *J. Am. Chem. Soc.* **2004**, *126* (47), 15334–15335.

(13) Murata, M.; Odajima, H.; Watanabe, S.; Masuda, Y. Aromatic C–H Borylation Catalyzed by Hydrotris(Pyrazolyl)Borate Complexes of Rhodium and Iridium. *Bull. Chem. Soc. Jpn.* **2006**, *79* (12), 1980–1982.

(14) Murphy, J. M. The Synthesis of Organoboron Compounds by Metal-Catalyzed Carbon-Hydrogen Borylation of Alkanes and Arenes. Ph.D., Yale University, United States -- Connecticut, **2009**.

(15) Hierlinger, C.; Cordes, D. B.; Slawin, A. M. Z.; Jacquemin, D.; Guerchais, V.; Zysman-Colman, E. Phosphorescent Cationic Iridium(III) Complexes Bearing a Nonconjugated Six-Membered Chelating Ancillary Ligand: A Strategy for Tuning the Emission towards the Blue. *Dalton Trans.* **2018**, *47* (31), 10569–10577.

(16) Naredla, R. R.; Zheng, C.; Nilsson Lill, S. O.; Klumpp, D. A. Charge Delocalization and Enhanced Acidity in Tricationic Superelectrophiles. *J. Am. Chem. Soc.* **2011**, *133* (33), 13169–13175.

(17) Ito, J.; Kaneda, T.; Nishiyama, H. Intermolecular C–H Bond Activation of Alkanes and Arenes by NCN Pincer Iridium(III) Acetate Complexes Containing Bis(Oxazolinyl)Phenyl Ligands. *Organometallics* **2012**, *31* (12), 4442–4449.

(18) Press, L. P.; Kosanovich, A. J.; McCulloch, B. J.; Ozerov, O. V. High-Turnover Aromatic C–H Borylation Catalyzed by POCOP-Type Pincer Complexes of Iridium. *J. Am. Chem. Soc.* **2016**, *138* (30), 9487–9497.

(19) Kuleshova, O.; Asako, S.; Ilies, L. Ligand-Enabled, Iridium-Catalyzed Ortho-Borylation of Fluoroarenes. *ACS Catal.* **2021**, 5968–5973.

(20) Ji, X.; Huang, T.; Wu, W.; Liang, F.; Cao, S. LDA-Mediated Synthesis of Triarylmethanes by Arylation of Diarylmethanes with Fluoroarenes at Room Temperature. *Org. Lett.* **2015**, *17* (20), 5096–5099..

(21) Chandrasekar, S.; Karthikeyan, I.; Sekar, G. An Efficient and Metal Free Synthesis of Benzylpyridines Using HI through the Deoxygenation Reaction. *RSC Adv.* **2015**, *5* (72), 58790–58797.

(22) Tan, P. W.; Mak, A. M.; Sullivan, M. B.; Dixon, D. J.; Seayad, J. Thioamide-Directed Cobalt(III)-Catalyzed Selective Amidation of C(Sp^3)−H Bonds. *Angew. Chem. Int. Ed.* **2017**, *56* (52), 16550–16554.

(23) Ren, L.; Wang, L.; Lv, Y.; Li, G.; Gao, S. Synergistic H4NI–AcOH Catalyzed Oxidation of the Csp3–H Bonds of Benzylpyridines with Molecular Oxygen. *Org. Lett.* **2015**, *17* (9), 2078–2081.

(24) Efimenko, I. A.; Podobedov, R. E.; Churakov, A. V.; Kuz'mina, L. G.; Garbuzova, I. A.; Lokshin, B. V.; Maksimov, A. L.; Flid, V. R. Binary Palladium Carboxylates with Electron-Donating and Electron-Withdrawing Substituents in the Carboxylate Ligand: Synthesis and Structural Studies. *Russ. J. Coord. Chem.* **2011**, *37* (8), 625.

(25) Nian, S.; Ling, F.; Chen, J.; Wang, Z.; Shen, H.; Yi, X.; Yang, Y.-F.; She, Y.; Zhong, W. Highly Enantioselective Hydrogenation of Non-Ortho-Substituted 2-Pyridyl Aryl Ketones via Iridium-f-Diaphos Catalysis. *Org. Lett.* **2019**, *21* (14), 5392–5396.

CHAPTER 3

Iridium/2,2'-Dipyridylarylmethane Catalysts in the Regioselective Borylation of sp^2 C-H Bonds

3.1 Background: Catalyst-Controlled Selectivity in C-H Borylation of Arenes

The selectivity of arene C-H borylation can be categorized into multiple subtypes, dependent upon presence of directing groups, substrate-intrinsic activation, or catalyst control in the case of unactivated, undirected substrates (**Figure 3.1**). A number of research endeavors over the past two decades have focused on the directed borylation of C-H bonds, particularly in arene substrates, allowing access to site-selectivity via chelation assistance. Most commonly this is achieved through *ortho*-cyclometallation, though systems which facilitate activation of *meta*- and *para*- positions have also been developed.[1–4] In contrast, C-H borylation of undirected substrates has proven more challenging, especially in the case of alkane substrates, and seen slower progress as a result. Non-directed borylation can be further divided into activated and unactivated substrate classes, owing to C-H bonds which are intrinsically activated through bond polarization, acidity, dissociation energy, or electron density.

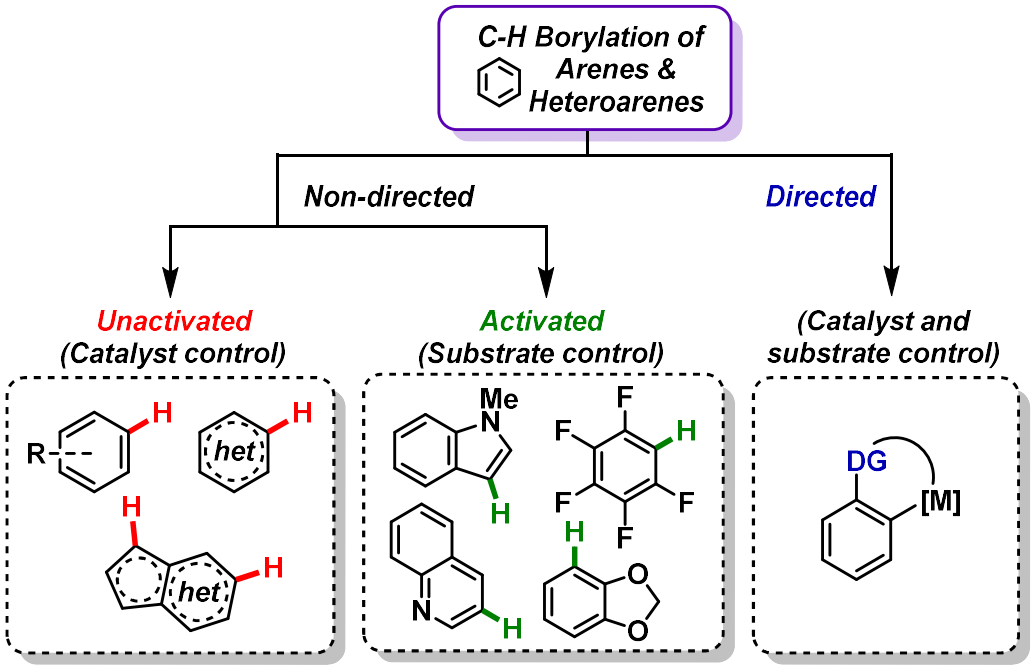

Figure 3.1: *Classification of selectivity types in the borylation of aromatic C-H bonds*

3.1.1 Selectivity Trends in Non-directed C-H Borylation of Arenes

Non-directed C-H functionalization presents a far greater challenge than directed functionalization, in terms of both selectivity and reactivity. While directing groups are often used to furnish a template for site selectivity, they can also increase reaction rate and provide favorable interactions which lower the activation energy of C-H cleavage.[5] Absent these kinetic, thermodynamic, and selectivity benefits of chelation-assistance, non-directed C-H borylation often requires harsher conditions or excess substrate. Despite these disadvantages, strict patterns of selectivity have been observed in non-directed borylation of arenes and heteroarene substrates. While many substrates lack directing groups, they may be otherwise activated through C-H bond strength, acidity, or polarity relative to other C-H bonds. Favorable reactivity of activated C-H bonds has allowed for milder conditions and predictable site-selectivity when certain substrate classes are employed, such as polyfluoroarenes[6–8], indoles[9,10], and quinolines[10–13].

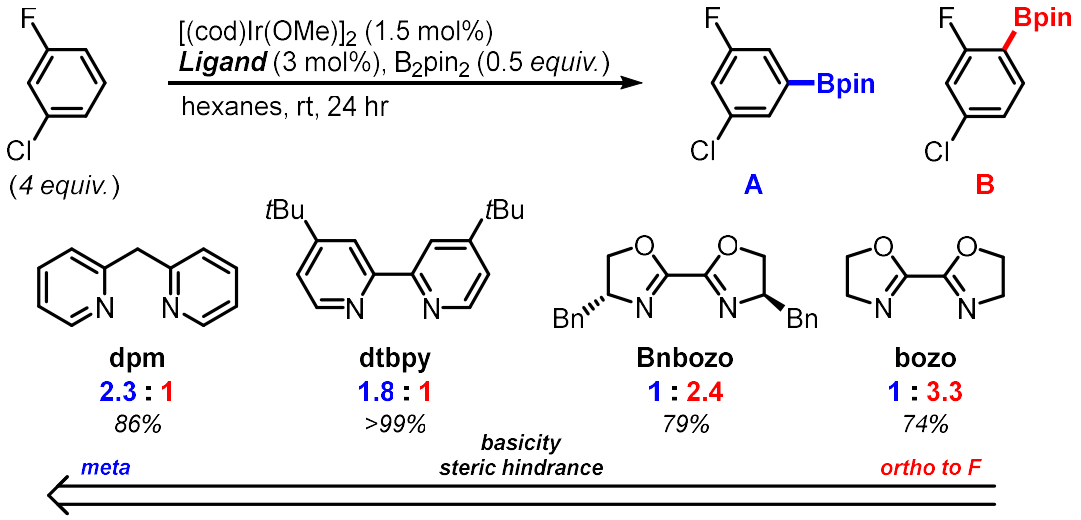

Figure 3.2: *Ligand-dependent variability of regioselectivity in the C-H borylation of fluoroarenes*[7]

Steric and electronic trends in non-directed arene and heteroarene borylation have been well established for Cp*Rh and diimine/Ir catalysts. Notable steric control over selectivity has been observed in C-H borylation, with a high degree of regiospecificity for unhindered C-H bonds. Hartwig, Smith, and others have capitalized upon this property for selective functionalization of 1,3-disubstituted arenes at the 5-position.[14–19]

Tethered, small-sized, or linear substituents which impart minimal steric hindrance have been demonstrated to override this effect, favoring ortho borylation in the cases of benzodioxoles[20], fluoroarenes[6,7], or cyano-substituted arenes[21], respectively. Smith and coworkers observed that the use of unhindered electron-poor diimine ligands, such as 2,2'-bis-2-oxazoline (bozo), afford enhanced selectivity for borylation ortho to fluorine substituents, while more hindered, electron rich ligands, such as 2,2'-dipyridylmethane (dpm), favor the meta borylation product (**Figure 3.2**).[7]

Significant enhancement in the rate of monosubstituted arene borylation can be attributed to the presence of electron withdrawing groups, as electron poor arenes undergo faster rates of oxidative addition.[6,14,15] However, while electron density of the arene is key to reaction kinetics, it exerts minimal control over positional selectivity with monosubstituted arenes, often yielding a statistical mixture of meta- and para- products of borylation.[5,6,15] This distribution of products can be perturbed slightly by the electronic nature of the R group, with electron-donating groups favoring meta functionalized products and electron-withdrawing groups yielding improved ratios of the para borylation product (**Figure 3.3**).[15] Alternatively, heteroarenes can afford predictable inherent site selectivity due to unsymmetric distribution of electron density about the ring, such has been demonstrated with indoles, pyridines, benzoxazoles, thiophenes, and more. [10–13] One could envision control over site selectivity in the borylation of elaborate polyaromatic substrates dependent upon established trends in reaction rate of the various aromatic moieties.

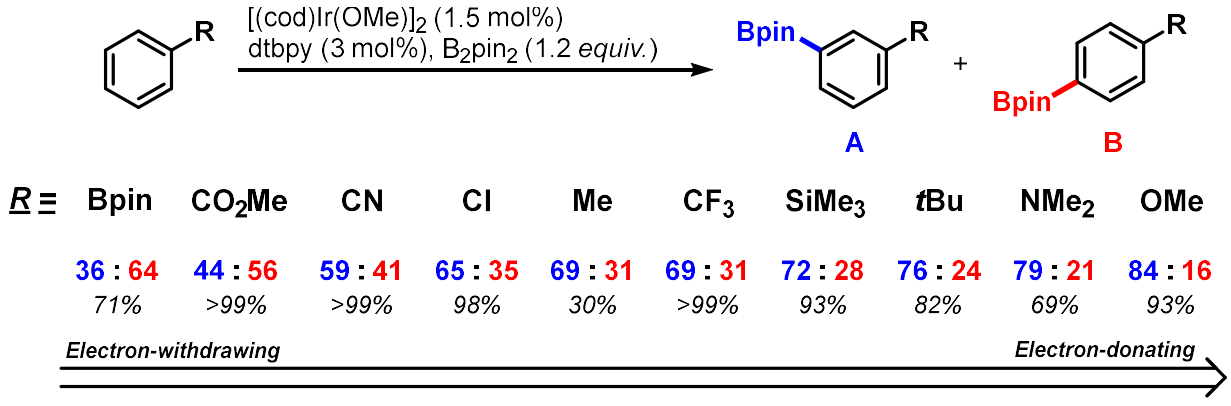

Figure 3.3: *Trends in reactivity and regioselectivity in the C-H borylation of monosubstituted arenes by the dtbpy/Ir catalyst.*[15]

3.1.2 Overview of Catalysts for Directed C-H Borylation

The benchmark catalysts for C-H borylation derived from iridium precursor and di-imine ligand generate a 16-electron active species which is not typically conducive to directed borylation. A change in catalyst structure is necessary for chelate-assisted C-H activation to occur, enabled either by opening of an additional vacant site at the metal center or by secondary interaction at the ligand. Directed C-H borylation has been achieved predominantly through the use of novel ligand structures, which can be broadly categorized into three types (**Figure 3.4**). The first involves the use of ligands which produce a lower valent 14-electron resting state metal boryl species capable of additional chelation to Lewis basic directing groups.[1,3,4,22] A second type, relay directed activation, entails functionalization of the substrate with a directing group which binds covalently to the metal center in place of a boryl ligand, and therefore does not require adjustment of the diimine ligand.[4] The final type maintains the core diimine coordination structure but the ligand backbone is furnished with distal groups which facilitate secondary coordination with substrate, through Lewis acid-base, electrostatic, or hydrogen bonding interactions.[2] Catalysts of the third variant have been developed for arene and heteroarene borylation, yet remain inaccessible in the alkane borylation reaction due to limitations of condition set.

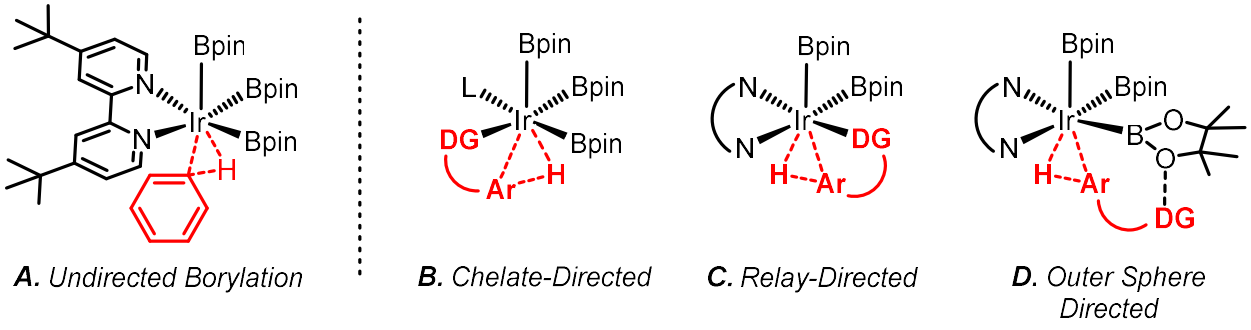

Figure 3.4: *Strategies for iridium-catalyzed directed C-H borylation*

Numerous catalysts have now been published which facilitate chelate-directed ortho borylation through the adjustment of coordination number about the catalyst. Simplistic chelate-directed systems were derived first from monodentate phosphine ligated catalysts, which display enhanced propensity towards C-H borylation ortho to amide and ester substituents.[6,23,24] In cases of rigid, strongly coordinating aryl

substrates, such as 2-arylpyridines[12,25], 2-benzylpyridines[26], benzylic phosphines[27], and benzoquinolines[25], chelate-directed borylation can be achieved without the use of a ligand. Similarly, the use of hemilabile N,N'-coordinating pyridine hydrazone ligands was found to encourage high degrees of chelate-directed borylation through opening of a coordination site at the metal center.[28] Many elegant monoanionic bidentante, or LX-type, ligands have also been developed which mitigate issues of speciation inherent to monophosphine-bound iridium systems[29] and offer enhanced control over steric and electronic properties of the catalyst.[1,4] This concept was exemplified in the design of phosphinosilyl iridium catalysts by Smith and coworkers, which enable ortho selectivity in the borylation of N- and O-substituted aromatics.[30] Another prime example of this catalyst variant is illustrated by the Li group and others in the use of B,N-bidentate ligands to access highly active and selective catalysts for both sp^2 and special cases of sp^3 C-H borylation.[1,31–34]

Selective C-H borylation catalysts involving the use of relay directing groups have predominantly been spearheaded by Hartwig and coworkers, utilizing substrates which contain silyl directing groups. Relay directed borylation has been achieved for both the ortho-borylation of silylarenes[35] and borylation at the γ-position of alkylsilanes[36]. Selectivity is achieved through replacement of one anionic boryl ligand of the traditional [(N^N)Ir(Bpin)$_3$] resting state structure by σ-metathesis with silane substrate. More recently, this strategy has been used in conjunction with chiral 2-pyridyloxazole ligands for the enantioselective sp^2 borylation of benzylic silanes.[37]

The final category of directing interaction involves outer-sphere noncovalent coordination between catalyst and substrate, allowing for directed functionalization of more distal positions. Archetypal instances of this type of directing interaction were proposed to occur by interaction of a Lewis acidic metal-boryl with substrates containing Lewis basic groups[38,39], or by hydrogen bond between aniline and boryl oxygen atom[40,41] (**Figure 3.5A**). Reimagined bipy ligand derivatives, furnished with remote recognition elements, were later prepared with the purpose of achieving catalysts which enable similar noncovalent interactions and provide site-selectivity (**Figure 3.5B**).[2] In contrast to traditional directed ortho-metalation catalysts, these systems afford either meta- or para- products of C-H borylation with a high degree of regioselectivity. Approaches have included the use of Lewis acid-base pairs[42,42], electrostatic

interaction[39,43,44], hydrogen bonding[40,45,46], and ion pairs[47–49] as directing groups in the secondary coordination sphere. While these elegant catalyst systems provide excellent site selectivity, they are constrained to arene substrates containing specific recognition groups.

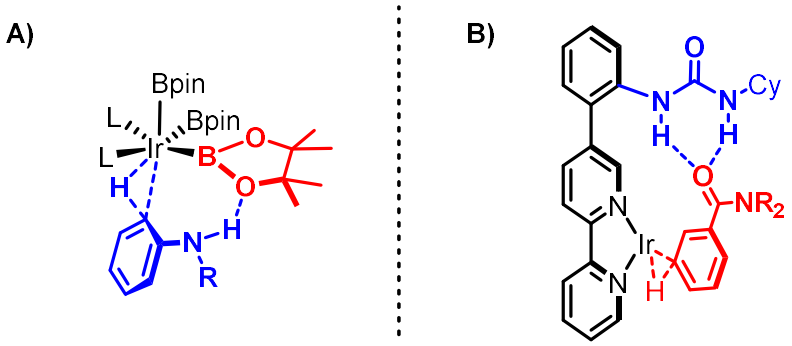

Figure 3.5: *Proposed transition state hydrogen bonding interaction of* ***A)*** *aniline with metal-boryl*[40,41] *and* ***B)*** *between L-Shaped diimine ligand and benzamide substrate.*[45]

3.2 Introduction: Iridium/2,2'-dipyridylarylmethane catalysts in the selective C-H borylation of arenes

We applied principles from the wealth of prior directed arene borylation examples and from intrinsic trends in undirected arene borylation in our design of 2,2'-dipyridylarylmethane ligand platforms for regioselective transformations. The following chapter describes work inspired by the use of L-shaped diimine ligands for C-H borylation directed by secondary coordination sphere interaction.[2] We envisioned that partnering advantages of 2,2'-dipyridylarylmethane ligands with the incorporation of a molecular recognition unit, in this case a hydrogen-bond donor, could provide efficient and selective borylation of arenes. Using ligand derivatives constructed in Ch. 2, we imagined that pairing with substrates containing hydrogen bond accepting groups would facilitate stabilizing interactions in the transition state, favoring site-selective borylation (**Figure 3.6**). Similarly, we also considered 2,2'-dipyridylbenzylmethane derivatives which may provide a more distal interaction and varied geometry about the metal center for selective arene borylation. Herein we report the survey of various 2,2'-dipyridylarylmethane and HBD-substituted ligands, **L1-L15**, in the selective borylation of monosubstituted or unsymmetrical 1,2-disubstituted arenes.

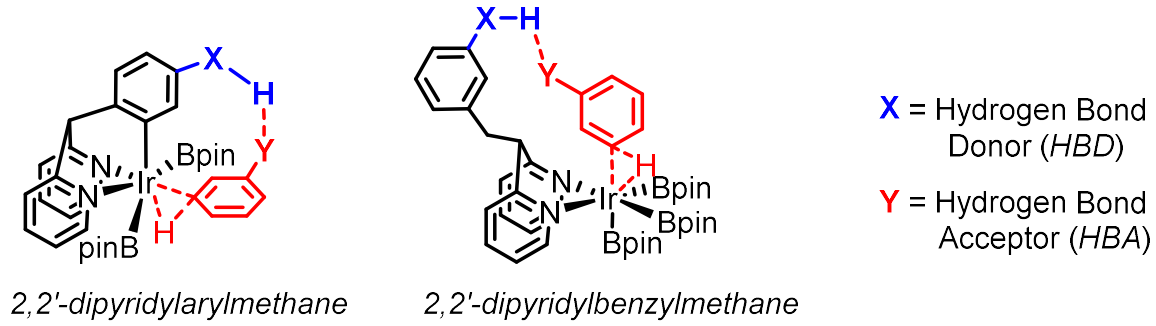

Figure 3.6: *Proposed interaction of HBD incorporated 2,2'-dipyridylarylmethane (left) or 2,2'-dipyridylbenzylmethane (right) ligated iridium with HBA-containing arene substrate.*

3.3 Results and Discussion

3.3.1 Substrate-controlled Regioselectivity in the Borylation of Arenes by Iridium/2,2'-dipyridylarylmethane catalysts

We initially set out to benchmark the inherent activity and selectivity of dpm, 2,2'-dipyridylarylmethane, and 2,2'-dipyridylbenzylmethane ligands which do not contain directing functionality (**L1-L7**, **Figure 3.7**) against the standard dtbpy ligand for arene borylation. We identified methyl benzoate and fluorobenzene as particularly high yielding substrates for the typical arene borylation reaction, offering unique intrinsic selectivity profiles. Ligands **L1-L7** were screened along with $[(cod)Ir(OMe)]_2$ pre-catalyst for the C-H borylation of each of these monosubstituted arene substrates.

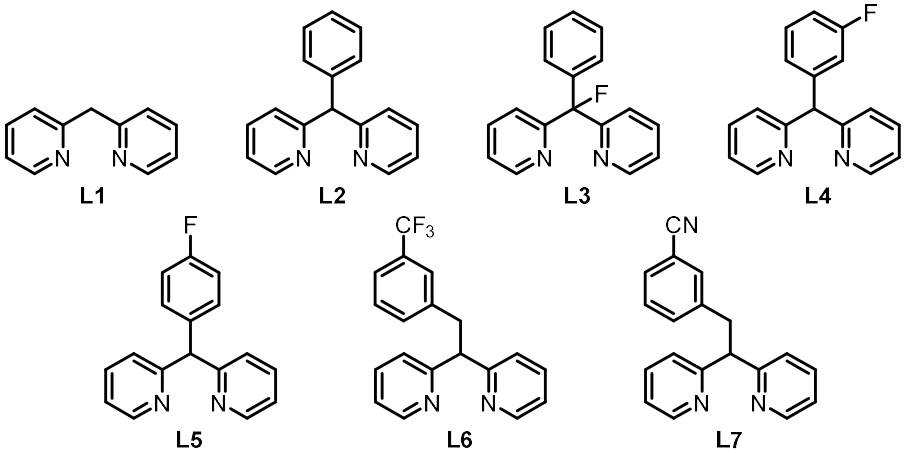

Figure 3.7: *2,2'-dipyridylarylmethane and 2,2'dipyridylbenzylmethane ligands* ***L1-L7***

Interestingly, derivatives **L2-L7** offer a marked increase in yield of organoborane relative to the parent structure dpm (**L1**) under these conditions for both substrates. In the borylation of methylbenzoate (**Table 3.1**), *meta* and *para* products are obtained in a nearly 1:1 mixture when the standard dtbpy ligand is used. A similar 1:1 product distribution is also observed for dpm (**L1**), phenyl (**L2**), and methine-fluorinated (**L3**), however, a notable shift in product ratio to favor formation of the meta isomer is found with aryl-substituted derivatives **L4**-**L7**. This outcome is indicative of the importance of ligand aryl group substitution on properties of the resultant catalyst, supporting a role for more proximal interaction of ligand aryl substituent with the metal center.

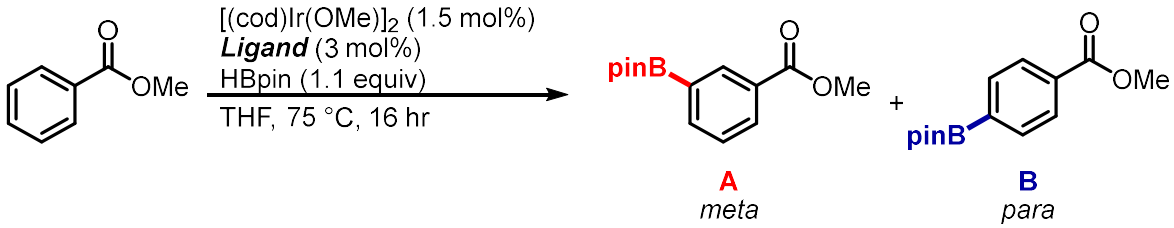

Ligand	Yield[a]	Product Ratio (A:B)
dtbpy	92%	51 : 49
L1	24%	43 : 57
L2	88%	56 : 44
L3	61%	54 : 46
L4	59%	72 : 28
L5	53%	77 : 23
L6	79%	67 : 33
L7	27%	62 : 38

Table 3.1: *Survey of ligands **L1-L6** in the borylation of methylbenzoate. Yields and product ratios determined by ^{1}H NMR with TCE internal standard. a) yield calculated based on 1 equiv. methylbenzoate*

In contrast to most substrates where C-H borylation of the ortho position is sterically prohibited, fluorobenzene affords the opportunity to explore trends which include ortho-borylation due to the small size of the fluorine atom. In the borylation of fluorobenzene, only subtle differences in the ratio of meta to (ortho + para) are observed across the series indicating minimal difference in the electronic nature of the catalysts, however, stark differences in ortho:para ratios were found (**Table 3.2**). Borylation ortho

to fluorine has previously been demonstrated to trend with reduced steric crowding of the metal center by spectator ligands,[7] comparison of relative ortho:para borylation may provide insight into catalyst geometry and relative bite angle across the ligand series. The standard dtbpy/Ir catalyst electronically favors the meta position when compared to a purely statistical distribution of products, and relative to **L1-L6**. Adjusting for the 2:1 distribution of ortho to para positions, product ratios were found to be nearly 1:1 for dtbpy, heavily favor ortho-borylation for **L1** and **L3**, and slightly favor para-borylation for **L2** and **L4-L6**. In cases where the para product (**B**) is favored relative to ortho (**C**), it is expected that the aryl group of the ligand is not distal from the metal center, resulting in enhanced steric preference.

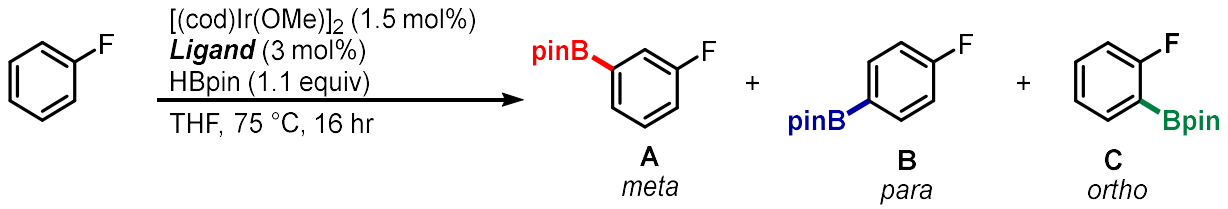

Ligand	Yield[a]	Product Ratio (A : B : C)	Product Ratio (A : B+C)	Product Ratio (B : C/2)
dtbpy	67%	58 : 15 : 27	58 : 42	1 : 0.9
L1	42%	47 : 8 : 45	47 : 53	1 : 2.8
L2	66%	48 : 22 : 30	48 : 52	1 : 0.7
L3	60%	48 : 10 : 42	48 : 52	1 : 2.1
L4	53%	55 : 18 : 27	55 : 45	1 : 0.8
L5	72%	54 : 21 : 25	54 : 46	1 : 0.6
L6	62%	46 : 26 : 28	46 : 54	1 : 0.5

Table 3.2: *Survey of ligands **L1-L6** in the borylation of fluorobenzene. Yields and product ratios determined by ^{1}H NMR with TCE internal standard. a) yield calculated based on 1 equiv. fluorobenzene*

3.3.2 Catalyst-controlled Regioselectivity by Secondary Coordination Interaction in the Borylation of Arenes by Iridium/2,2'-dipyridylarylmethane Catalysts

Additional 2,2'-dipyridylmethane ligands were designed for the purpose of imparting selectivity in a catalyst-controlled manner for the C-H borylation of arenes with multiple potential sites of functionalization. We sought to accomplish this through incorporation of a pendant hydrogen bond donor to the 2,2'dipyridylarylmethane or 2,2'-

dipyridylbenzylmethane ligand frameworks, which may provide favorable transition state interaction with substrates containing a corresponding Lewis basic substituent. Ligands **L8-L15** (**Figure 3.8**) were prepared with this goal in mind, and screened alongside $[(cod)Ir(OMe)]_2$ for the C-H borylation of various monosubstituted arenes.

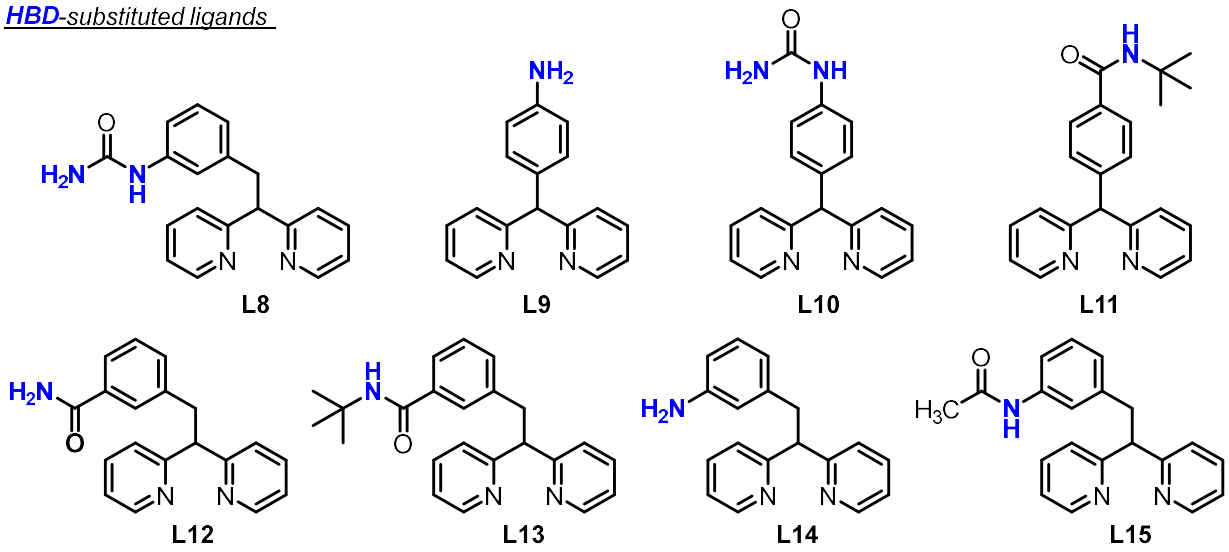

Figure 3.8: *2,2'-dipyridylarylmethane and 2,2'dipyridylbenzylmethane ligands derivatives containing hydrogen bond donor substituents,* ***L8-L15****.*

Methyl benzoate, benzonitrile, and anisole were selected as suitable substrates containing appropriate Lewis basic recognition elements. The monosubstituted arenes were used for initial survey of ligands **L8-L15** (**Tables 3.3-3.5**). Unfortunately, the entirety of the HBD ligand set produced much lower yields for arene C-H borylation reaction relative to the standard dtbpy or unsubstituted ligand variants **L5** and **L6**. Subtle selectivity differences were observed for each substrate across the HBD-ligand set, however, none induced notable positional specificity. This is again suggestive of a profound effect of ligand aryl substitution on speciation or function of the resulting catalyst, rather than involvement of the desired hydrogen bonding interaction with substrate. It is possible that alternate coordination structures of the hydrogen bond donating substituent, or drastic change in electronic structure relative to the parent 2,2'-dipyridylarylmethane or 2,2'-dipyridylbenzylmethane contribute to both yield and selectivity.

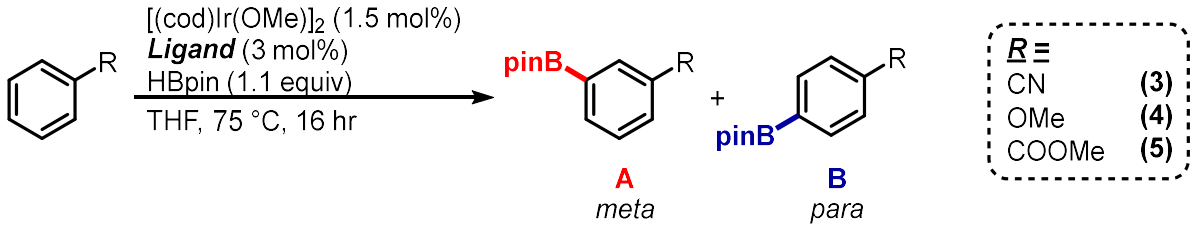

3)

Ligand	Yield	Product Ratio (A:B)
dtbpy	31%	78 : 22
L5	60%	82 : 18
L6	52%	68 : 32
L10	26%	82 : 20
L11	19%	79 : 21
L8	14%	69 : 31
L12	16%	63 : 37
L13	20%	61 : 39
L14	12%	67 : 33

4)

Ligand	Yield	Product Ratio (A:B)
dtbpy	84%	56 : 44
L5	32%	64 : 36
L6	68%	64 :36
L10	*trace*	-
L11	8%	-
L12	44%	68 : 32
L13	62%	67 : 33
L14	17%	62 : 38
L15	21%	61 : 39

5)

Ligand	Yield	Product Ratio (A:B)
dtbpy	92%	51 : 49
L8	34%	57 : 43
L10	31%	47 : 53
L11	63%	45 : 54
L12	38%	64 : 36

Tables 3.3-3.5: *Survey of ligands* ***L8-L15*** *in the borylation of anisole (3), benzonitrile (4) and methylbenzoate (5). Yields and product ratios determined by GC-FID using dodecane as an internal standard.*

As in established systems for C-H borylation direct by non-covalent interaction, the desirable hydrogen bond donor-acceptor relationship is likely to be highly specific to certain functional groups. Despite modest yields and minimal differences in selectivity observed in the C-H borylation of methyl benzoate, benzonitrile, and anisole for the ligand series, **L13** was selected as a representative derivative for exploration of additional HBA-containing arene and heteroarene substrates (**Figure 3.9**). In most cases, conversion to borylated product was considerably lower than established values, with the exception of indene and furan substrates. This is particularly true in the case of

more coordinating nitrogen-containing functional groups or N-heterocycles, possibly indicating greater sensitivity of the catalyst to poisoning by coordinating groups during activation. Substrates containing acetyl groups were susceptible to formation byproducts of reduction, likely through competing hydroboration side reaction. In some instances, proper protecting group strategies may provide more suitable substrates. However, the poor yields preclude further study of regioselectivity and suggest that re-optimization of the reaction or redesign of ligand derivatives is necessary to achieve the desired goal.

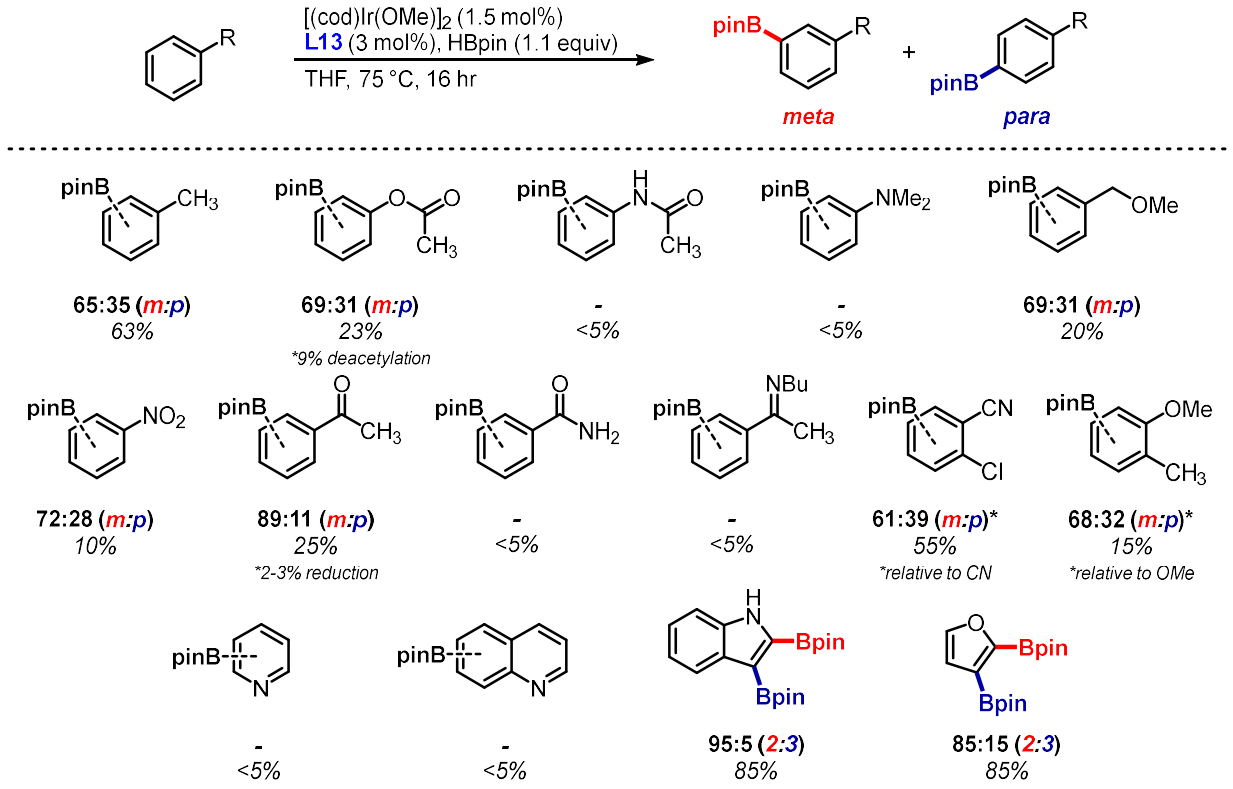

Figure 3.9: *C-H borylation of HBA-containing substrates catalyzed by* ***L13****/[(cod)Ir(OMe)]*$_2$

3.4 Conclusions

The borylation of arene C-H bonds in acceptable yield has been achieved using 2,2'-dipyridylarylmethane supported iridium catalysts, however, this platform currently offers no advantage over the established dtbpy/Ir system. While the ligands **L2-L7** produced acceptable yields and altered selectivity patterns compared to dtbpy, the HBD-

substituted ligand series **L8-L15** resulted in the formation of significantly less active catalysts. Variance in selectivity appears to result from the electronic and geometric nature of the ligand rather than hydrogen bonding interaction. Ligand selection affords modest control over site-selectivity even when absent any directing group interaction. Continued tuning of ligand structure through substitution of the 2,2'-dipyridylarylmethane framework offers a route to more efficient catalyst platforms and exaggerated site-selectivity for arene C-H borylation.

This material is based upon work supported by the National Science Foundation under grant no. CHE-1847813.

3.5 Experimental

General Considerations: Syntheses and manipulations with organometallic reagents were carried out using standard vacuum, Schlenk, cannula, or glovebox techniques under N_2 in oven- or flame-dried glassware unless otherwise specified. Tetrahydrofuran, dichloromethane, toluene, pentane, and diethyl ether were degassed with argon and dried over activated alumina using a solvent purification system.

Spectroscopy: ^{1}H NMR spectra were recorded on Bruker NMR spectrometers at ambient temperatures unless otherwise noted. ^{1}H chemical shifts are referenced to residual solvent signals.

Organometallic starting materials: Bis(1,5-cyclooctadiene)diiridium(I) dichloride $[(cod)IrCl]_2$[50] and Bis(1,5-cyclooctadiene)diiridium(I) dimethoxide $[(cod)IrOMe]_2$[51] were prepared according to published procedures. $IrCl_3 \cdot 3H_2O$, pinacolborane were purchased from chemical vendors and used as received.

Substrates: Methyl benzoate, fluorobenzene, anisole, benzonitrile, *N,N'*-dimethyl aniline, nitrobenzene, acetophenone, benzamide, 2-methoxytoluene, quinoline, pyridine, indene, and furan were purchased from chemical vendors and used as received. Phenyl acetate, *N*-phenylacetamide, benzyl methyl ether, and *N*-butyl-1-phenylethan-1-imine were prepared and characterized by reported literature

procedures.

General procedure for arene borylation

In an inert-atmosphere glove box, a 4 mL vial was charged with $[Ir(COD)OMe]_2$ (0.002 g, 0.006 mmol (Ir basis), 3 mol % Ir). HBpin (0.032 mL, 0.22 mmol) and THF (1.2 mL, 167 mM) were added and the solution stirred for 3 min. The resulting solution was transferred to a separate 4 mL vial charged with ligand (0.006 mmol, 3 mol %), then arene substrate (0.20 mmol) was added. The vial was sealed with a PTFE-lined cap, removed from the glove box, and heated to 75 °C in an oil bath with stirring for 16 hr. At this point the reaction was cooled to room temperature, and the crude mixture analyzed by GC-FID calibrated to a dodecane internal standard. The crude mixture was concentrated *in vacuo* and analyzed by ^{1}H NMR with a tetrachloroethane standard to obtain NMR yields and product isomer ratios.

4,4,5,5-tetramethyl-2-aryl-1,3,2-dioxaborolane products:

Products of the borylation of toluene[52], methyl benzoate[53], fluorobenzene[54], anisole[6], benzonitrile[21], *N,N'*-dimethyl aniline[52], acetophenone[55], 2-methoxytoluene[15], 1-chloro-2-cyanobenzene[15], pyridine[12], indene[41,56], furan[10], phenyl acetate[47], benzyl methyl ether[57] were characterized by comparison to reported ^{1}H NMR literature values.

3.6 References

(1) Xu, L.; Wang, G.; Zhang, S.; Wang, H.; Wang, L.; Liu, L.; Jiao, J.; Li, P. Recent Advances in Catalytic C−H Borylation Reactions. *Tetrahedron* **2017**, *73* (51), 7123–7157.

(2) Haldar, C.; Emdadul Hoque, M.; Bisht, R.; Chattopadhyay, B. Concept of Ir-Catalyzed CH Bond Activation/Borylation by Noncovalent Interaction. *Tetrahedron Lett.* **2018**, *59* (14), 1269–1277.

(3) F. Hartwig, J. Regioselectivity of the Borylation of Alkanes and Arenes. *Chem. Soc. Rev.* **2011**, *40* (4), 1992–2002.

(4) Ros, A.; Fernández, R.; Lassaletta, J. M. Functional Group Directed C–H Borylation. *Chem. Soc. Rev.* **2014**, *43* (10), 3229–3243.

(5) Hartwig, J. F.; Larsen, M. A. Undirected, Homogeneous C–H Bond Functionalization: Challenges and Opportunities. *ACS Cent. Sci.* **2016**, *2* (5), 281–292.

(6) Cho, J.-Y.; Iverson, C. N.; Smith, M. R. Steric and Chelate Directing Effects in Aromatic Borylation. *J. Am. Chem. Soc.* **2000**, *122* (51), 12868–12869.

(7) Miller, S. L.; Chotana, G. A.; Fritz, J. A.; Chattopadhyay, B.; Maleczka, R. E.; Smith, M. R. C–H Borylation Catalysts That Distinguish Between Similarly Sized Substituents Like Fluorine and Hydrogen. *Org. Lett.* **2019**, *21* (16), 6388–6392.

(8) Lafrance, M.; Rowley, C. N.; Woo, T. K.; Fagnou, K. Catalytic Intermolecular Direct Arylation of Perfluorobenzenes. *J. Am. Chem. Soc.* **2006**, *128* (27), 8754–8756.

(9) Feng, Y.; Holte, D.; Zoller, J.; Umemiya, S.; Simke, L. R.; Baran, P. S. Total Synthesis of Verruculogen and Fumitremorgin A Enabled by Ligand-Controlled C–H Borylation. *J. Am. Chem. Soc.* **2015**, *137* (32), 10160–10163.

(10) Seechurn, C. C. C. J.; Sivakumar, V.; Satoskar, D.; Colacot, T. J. Iridium-Catalyzed C–H Borylation of Heterocycles Using an Overlooked 1,10-Phenanthroline Ligand: Reinventing the Catalytic Activity by Understanding the Solvent-Assisted Neutral to Cationic Switch. *Organometallics* **2014**, *33* (13),

(11) Wright, J. S.; Scott, P. J. H.; Steel, P. G. Iridium-Catalysed C−H Borylation of Heteroarenes: Balancing Steric and Electronic Regiocontrol. *Angew. Chem. Int. Ed.* **2021**, *60* (6), 2796–2821.

(12) Sadler, S. A.; Tajuddin, H.; Mkhalid, I. A. I.; Batsanov, A. S.; Albesa-Jove, D.; Cheung, M. S.; Maxwell, A. C.; Shukla, L.; Roberts, B.; Blakemore, D. C.; Lin, Z.; Marder, T. B.; Steel, P. G. Iridium-Catalyzed C–H Borylation of Pyridines. *Org. Biomol. Chem.* **2014**, *12* (37), 7318–7327.

(13) Larsen, M. A.; Hartwig, J. F. Iridium-Catalyzed C–H Borylation of Heteroarenes: Scope, Regioselectivity, Application to Late-Stage Functionalization, and Mechanism. *J. Am. Chem. Soc.* **2014**, *136* (11), 4287–4299.

(14) Mkhalid, I. A. I.; Barnard, J. H.; Marder, T. B.; Murphy, J. M.; Hartwig, J. F. C−H Activation for the Construction of C−B Bonds. *Chem. Rev.* **2010**, *110* (2), 890–931.

(15) Tajuddin, H.; Harrisson, P.; Bitterlich, B.; Collings, J. C.; Sim, N.; Batsanov, A. S.; Cheung, M. S.; Kawamorita, S.; Maxwell, A. C.; Shukla, L.; Morris, J.; Lin, Z.; Marder, T. B.; Steel, P. G. Iridium-Catalyzed C–H Borylation of Quinolines and Unsymmetrical 1,2-Disubstituted Benzenes: Insights into Steric and Electronic Effects on Selectivity. *Chem. Sci.* **2012**, *3* (12), 3505–3515.

(16) Cho, J.-Y.; Tse, M. K.; Holmes, D.; Maleczka, R. E.; Smith, M. R. Remarkably Selective Iridium Catalysts for the Elaboration of Aromatic C-H Bonds. *Science* **2002**, *295* (5553), 305–308.

(17) Ishiyama, T.; Takagi, J.; Ishida, K.; Miyaura, N.; Anastasi, N. R.; Hartwig, J. F. Mild Iridium-Catalyzed Borylation of Arenes. High Turnover Numbers, Room Temperature Reactions, and Isolation of a Potential Intermediate. *J. Am. Chem. Soc.* **2002**, *124* (3), 390–391.

(18) Maleczka, Robert E.; Shi, F.; Holmes, D.; Smith, M. R. C−H Activation/Borylation/Oxidation: A One-Pot Unified Route To Meta-Substituted Phenols Bearing Ortho-/Para-Directing Groups. *J. Am. Chem. Soc.* **2003**, *125* (26), 7792–7793.

(19) Murphy, J. M.; Liao, X.; Hartwig, J. F. Meta Halogenation of 1,3-Disubstituted Arenes via Iridium-Catalyzed Arene Borylation. *J. Am. Chem. Soc.* **2007**, *129* (50), 15434–15435.

(20) Britt A. Vanchura, I. I.; Preshlock, S. M.; Roosen, P. C.; Kallepalli, V. A.; Staples, R. J.; Robert E. Maleczka, J.; Singleton, D. A.; Milton R. Smith, I. I. I. Electronic Effects in Iridium C–H Borylations: Insights from Unencumbered Substrates and Variation of Boryl Ligand Substituents. *Chem. Commun.* **1389**, *46* (41), 7724–7726.

(21) Chotana, G. A.; Rak, M. A.; Smith, M. R. Sterically Directed Functionalization of Aromatic C−H Bonds: Selective Borylation Ortho to Cyano Groups in Arenes and Heterocycles. *J. Am. Chem. Soc.* **2005**, *127* (30), 10539–10544.

(22) Kuroda, Y.; Nakao, Y. Catalyst-Enabled Site-Selectivity in the Iridium-Catalyzed C–H Borylation of Arenes. *Chem. Lett.* **2019**, *48* (9), 1092–1100.

(23) Ishiyama, T.; Isou, H.; Kikuchi, T.; Miyaura, N. Ortho-C–H Borylation of Benzoate Esters with Bis(Pinacolato)Diboron Catalyzed by Iridium–Phosphine Complexes. *Chem. Commun.* **2010**, *46* (1), 159–161.

(24) Kawamorita, S.; Ohmiya, H.; Hara, K.; Fukuoka, A.; Sawamura, M. Directed Ortho Borylation of Functionalized Arenes Catalyzed by a Silica-Supported Compact Phosphine−Iridium System. *J. Am. Chem. Soc.* **2009**, *131* (14), 5058–5059.

(25) Fernández-Salas, J. A.; Manzini, S.; Piola, L.; Slawin, A. M. Z.; Nolan, S. P. Ruthenium Catalysed C–H Bond Borylation. *Chem. Commun.* **2014**, *50* (51), 6782–6784.

(26) Yang, Y.; Gao, Q.; Xu, S. Ligand-Free Iridium-Catalyzed Dehydrogenative Ortho C−H Borylation of Benzyl-2-Pyridines at Room Temperature. *Adv. Synth. Catal.* **2019**, *361* (4), 858–862.

(27) Crawford, K. M.; Ramseyer, T. R.; Daley, C. J. A.; Clark, T. B. Phosphine-Directed C□H Borylation Reactions: Facile and Selective Access to Ambiphilic Phosphine Boronate Esters. *Angew. Chem. Int. Ed.* **2014**, *53* (29), 7589–7593.

(28) Ros, A.; Estepa, B.; López-Rodríguez, R.; Álvarez, E.; Fernández, R.; Lassaletta, J. M. Use of Hemilabile N,N Ligands in Nitrogen-Directed Iridium-Catalyzed Borylations of Arenes. *Angew. Chem. Int. Ed.* **2011**, *50* (49), 11724–11728.

(29) Chotana, G. A.; Britt A. Vanchura, I. I.; Tse, M. K.; Staples, R. J.; Robert E. Maleczka, J.; Milton R. Smith, I. I. I. Getting the Sterics Just Right: A Five-Coordinate Iridium Trisboryl Complex That Reacts with C–H Bonds at Room Temperature. *Chem. Commun.* **2009**, No. 38, 5731–5733.

(30) Ghaffari, B.; Preshlock, S. M.; Plattner, D. L.; Staples, R. J.; Maligres, P. E.; Krska, S. W.; Maleczka, R. E.; Smith, M. R. Silyl Phosphorus and Nitrogen Donor Chelates for Homogeneous Ortho Borylation Catalysis. *J. Am. Chem. Soc.* **2014**, *136* (41), 14345–14348.

(31) Wang, G.; Liu, L.; Wang, H.; Ding, Y.-S.; Zhou, J.; Mao, S.; Li, P. N,B-Bidentate Boryl Ligand-Supported Iridium Catalyst for Efficient Functional-Group-Directed C–H Borylation. *J. Am. Chem. Soc.* **2017**, *139* (1), 91–94.

(32) Wang, G.; Xu, L.; Li, P. Double N,B-Type Bidentate Boryl Ligands Enabling a Highly Active Iridium Catalyst for C–H Borylation. *J. Am. Chem. Soc.* **2015**, *137* (25), 8058–8061.

(33) Zou, X.; Zhao, H.; Li, Y.; Gao, Q.; Ke, Z.; Senmiao Xu. Chiral Bidentate Boryl Ligand Enabled Iridium-Catalyzed Asymmetric C(Sp^2)–H Borylation of Diarylmethylamines. *J. Am. Chem. Soc.* **2019**, *141* (13), 5334–5342.

(34) Shi, Y.; Gao, Q.; Xu, S. Chiral Bidentate Boryl Ligand Enabled Iridium-Catalyzed Enantioselective C(Sp3)–H Borylation of Cyclopropanes. *J. Am. Chem. Soc.* **2019**, *141* (27), 10599–10604.

(35) Boebel, T. A.; Hartwig, John. F. Silyl-Directed, Iridium-Catalyzed Ortho-Borylation of Arenes. A One-Pot Ortho-Borylation of Phenols, Arylamines, and Alkylarenes. *J. Am. Chem. Soc.* **2008**, *130* (24), 7534–7535.

(36) Larsen, M. A.; Cho, S. H.; Hartwig, J. Iridium-Catalyzed, Hydrosilyl-Directed Borylation of Unactivated Alkyl C–H Bonds. *J. Am. Chem. Soc.* **2016**, *138* (3), 762–765.

(37) Wang, Y.-X.; Zhang, P.-F.; Ye, M. Well-Designed Chiral Ligands for Enantioselective Ir-Catalyzed C(Sp^2)–H Borylation. *Chin. J. Chem.* **2020**, *38* (12), 1762–1766.

(38) Liskey, C. W.; Hartwig, J. F. Iridium-Catalyzed Borylation of Secondary C–H Bonds in Cyclic Ethers. *J. Am. Chem. Soc.* **2012**, *134* (30), 12422–12425.

(39) Bisht, R.; Chattopadhyay, B. Formal Ir-Catalyzed Ligand-Enabled Ortho and Meta Borylation of Aromatic Aldehydes via in Situ-Generated Imines. *J. Am. Chem. Soc.* **2016**, *138* (1), 84–87.

(40) Roosen, P. C.; Kallepalli, V. A.; Chattopadhyay, B.; Singleton, D. A.; Maleczka, R. E.; Smith, M. R. Outer-Sphere Direction in Iridium C–H Borylation. *J. Am. Chem. Soc.* **2012**, *134* (28), 11350–11353.

(41) Preshlock, S. M.; Plattner, D. L.; Maligres, P. E.; Krska, S. W.; Maleczka, R. E.; Smith, M. R. A Traceless Directing Group for C□H Borylation. *Angew. Chem. Int. Ed.* **2013**, *52* (49), 12915–12919.

(42) Li, H. L.; Kuninobu, Y.; Kanai, M. Lewis Acid–Base Interaction-Controlled Ortho-Selective C−H Borylation of Aryl Sulfides. *Angew. Chem.* **2017**, *129* (6), 1517–1521.

(43) Chattopadhyay, B.; Dannatt, J. E.; Andujar-De Sanctis, I. L.; Gore, K. A.; Maleczka, R. E.; Singleton, D. A.; Smith, M. R. Ir-Catalyzed Ortho-Borylation of Phenols Directed by Substrate–Ligand Electrostatic Interactions: A Combined Experimental/in Silico Strategy for Optimizing Weak Interactions. *J. Am. Chem. Soc.* **2017**, *139* (23), 7864–7871.

(44) Chaturvedi, J.; Haldar, C.; Bisht, R.; Pandey, G.; Chattopadhyay, B. Meta Selective C–H Borylation of Sterically Biased and Unbiased Substrates Directed by Electrostatic Interaction. *J. Am. Chem. Soc.* **2021**, *143* (20), 7604–7611.

(45) Kuninobu, Y.; Ida, H.; Nishi, M.; Kanai, M. A Meta-Selective C–H Borylation Directed by a Secondary Interaction between Ligand and Substrate. *Nat. Chem.* **2015**, *7* (9), 712–717.

(46) Davis, H. J.; Genov, G. R.; Phipps, R. J. Meta-Selective C−H Borylation of Benzylamine-, Phenethylamine-, and Phenylpropylamine-Derived Amides Enabled by a Single Anionic Ligand. *Angew. Chem. Int. Ed.* **2017**, *56* (43), 13351–13355.

(47) Mihai, M. T.; Williams, B. D.; Phipps, R. J. Para-Selective C–H Borylation of Common Arene Building Blocks Enabled by Ion-Pairing with a Bulky Countercation. *J. Am. Chem. Soc.* **2019**, *141* (39), 15477–15482.

(48) Hoque, M. E.; Bisht, R.; Haldar, C.; Chattopadhyay, B. Noncovalent Interactions in Ir-Catalyzed C–H Activation: L-Shaped Ligand for Para-Selective Borylation of Aromatic Esters. *J. Am. Chem. Soc.* **2017**, *139* (23), 7745–7748.

(49) Davis, H. J.; Mihai, M. T.; Phipps, R. J. Ion Pair-Directed Regiocontrol in Transition-Metal Catalysis: A Meta-Selective C–H Borylation of Aromatic Quaternary Ammonium Salts. *J. Am. Chem. Soc.* **2016**, *138* (39), 12759–12762.

(50) Herde, J. L.; Lambert, J. C.; Senoff, C. V.; Cushing, M. A., Cyclooctene and 1,5-Cyclooctadiene Complexes of Iridium(I). *Inorg. Synth*. **1974**, 18-20

(51) Uson, R.; Oro, L. A.; Cabeza, J. A.; Bryndza, H. E.; Stepro, M. P. Dinuclear Methoxy, Cyclooctadiene, and Barrelene Complexes of Rhodium(I) and Iridium(I). *Inorg. Synth.* **1985**, 126–130.

(52) Cho, J.-Y.; Iverson, C. N.; Smith, M. R. Steric and Chelate Directing Effects in Aromatic Borylation. *J. Am. Chem. Soc.* **2000**, *122* (51), 12868–12869.

(53) Jover, J.; Maseras, F. Mechanistic Investigation of Iridium-Catalyzed C–H Borylation of Methyl Benzoate: Ligand Effects in Regioselectivity and Activity. *Organometallics* **2016**, *35* (18), 3221–3226.

(54) Esteruelas, M. A.; Martínez, A.; Oliván, M.; Oñate, E. Direct C−H Borylation of Arenes Catalyzed by Saturated Hydride-Boryl-Iridium-POP Complexes: Kinetic Analysis of the Elemental Steps. *Chem. – Eur. J.* **2020**, *26* (55), 12632–12644.

(55) Maeda, K.; Uemura, Y.; Chun, W.-J.; Satter, S. S.; Nakajima, K.; Manaka, Y.; Motokura, K. Controllable Factors of Supported Ir Complex Catalysis for Aromatic C–H Borylation. *ACS Catal.* **2020**, *10* (24), 14552–14559.

(56) Ishiyama, T.; Takagi, J.; Nobuta, Y.; Miyaura, N. Iridium-Catalyzed C-H Borylation of Arenes and Heteroarenes: 1-Chloro-3-iodo-5-(4,4,5,5-tetramethyl-1,3,2-dioxaborolan-2-yl)benzene and 2-(4,4,5,5,-Tetramethyl-1,3,2-dioxaborolan-2-yl)indole. *Org. Synth.* **2005**, 82, 126.

(57) Dai, R.; Guo, X.; Liu, C.; Liu, K.; Liu, L. N.; Liu, X.; Qing, H. Magnolol Derivative with Benzyl Alcohol or Benzyl Methyl Ether Substituent. CN104892374A, September 9, **2015**.

CHAPTER 4

Iridium-Catalyzed sp^3 C–H Borylation Enabled by 2,2′-Dipyridylarylmethane Ligands

4.1 Introduction

The functionalization of inert C-H bonds has garnered considerable attention as a means of rapidly elaborating abundant chemical feedstocks to higher-value materials.[1-2] C-H borylation is a versatile functionalization reaction that yields organoborane products which are widely applicable intermediates in organic synthesis. Arene borylation in particular has been developed and studied extensively since its inception,[3-4] yielding accessible and broadly applicable methods with wide scope. Unfortunately, the analogous iridium-catalyzed sp^3 borylation of aliphatic substrates remains limited by harsh reaction conditions, a requirement for catalysis in neat substrate, and incomplete conversion of the diboron reagent. [5-9]

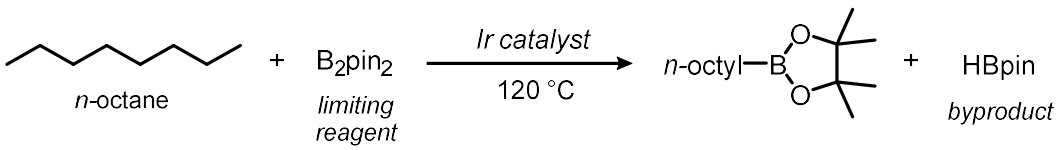

		turnovers
[Ir]/Me$_4$Phen	*neat octane: 88%*	*9*
	5 equiv. octane: 9%	*3*
This work	*neat octane: 199%*	*200*
	5 equiv. octane: 103%	*34*

***Figure 4.1**: Previously reported conditions for iridium-catalyzed alkane borylation using Me$_4$phen with yields reported on a diboron basis.*[8, 10]

Of the limitations of existing systems for alkane borylation, the requirement for catalysis in neat substrate is among the most constraining from the standpoint of usability. There are several reported iridium-catalyzed sp^3 borylation systems that

operate on either smaller excesses of alkane (*ca.* 5 equiv.) or limiting alkane, but each of these cases relies on the increased reactivity of a subset of activated alkane substrates including benzylic[11-12] or cyclopropane derivatives,[13-14] alkyl silanes,[10, 15] or substrates bearing directing groups.[12, 14, 16-19] Unactivated substrates undergo borylation in reduced yields when smaller excesses are used in solvent. For instance, the tetramethylphenanthroline (Me_4phen)/Ir borylation system gives roughly 1 equivalent of product per equivalent of B_2pin_2 when neat *n*-octane is used as the substrate, but this yield drops to 17% when conducted using 4 equivalents of *n*-octane relative to B_2pin_2 in cyclooctane solvent (**Figure 4.1**).[8, 10]

The former example illustrates a second weakness of most iridium catalysts for sp^3 borylation. The diboron source B_2pin_2 contains two equivalents of the pinacolboryl moiety, however, most iridium-catalyzed examples only incorporate one boron equivalent per diboron unit into product. This observation has led to an accepted convention where yields are reported relative to B_2pin_2, occasionally leading to reported yields exceeding 100% when quantities of the HBpin byproduct are also consumed in alkane borylation.[8] This limitation does not extend to rhodium systems for alkane borylation, some of which can utilize HBpin as the boron source.[6] The reduced reactivity of HBpin relative to B_2pin_2 has been attributed to differences in enthalpic driving force provided by the two reagents,[20] but the success of rhodium catalysts indicates that the primary limitation for iridium systems is kinetic in nature, indicating that a suitable iridium catalyst should be capable of fully consuming the borylating agent.

With the limitations of existing systems in mind, we undertook a study of alkane borylation using dipyridylarylmethane ligands **L2**-**6**. The dipyridylarylmethane moiety conserves the chelating bis-pyridine backbone of conventionally used dtbpy or Me_4Phen ligands, while also allowing for incorporation of substituents that project out of the N-M-N plane.[24-25] Our intention was that this ligand framework might bind in a facial κ^3 mode analogous to the Cp* ligand upon cyclometalation of the aryl group, as described in Chapter 2. Facial coordination would expand opportunities for modulation of ligand steric and electronic parameters through incorporation of functionality on the cyclometalated ring. We report that exploration of dipyridylarylmethane ligands resulted in a highly active catalyst for alkane borylation which demonstrates both enhanced catalytic performance and improved conversion efficiency of the boron reagent. These

improvements allow for catalysis under non-neat conditions and improved functional group compatibility.

4.2 Results and Discussion

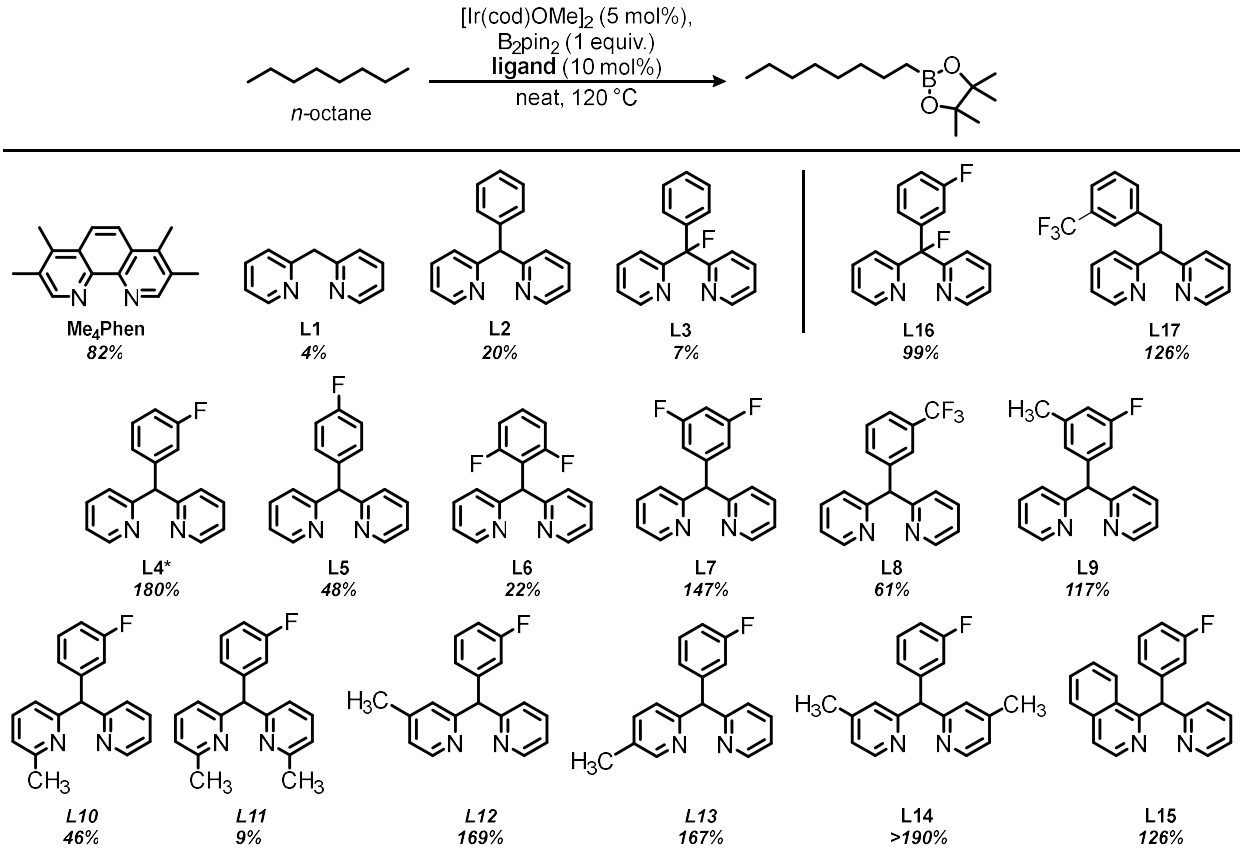

Figure 4.2: *Comparison of ligands for n-octane borylation. [a]NMR yields reported relative to molar equivalents of B_2pin_2.*

Ligands **L1**-**L17** were surveyed for the borylation of *n*-octane in combination with the precatalyst [Ir(cod)OMe]$_2$ (Table 1). **L1** produced only trace quantities of octyl-Bpin. **L2** gave improved results relative to the parent scaffold **L1**, but still underperformed Me$_4$phen. **L3**, which differs by fluorination of the methine position, is similarly low-yielding to **L1**. Given the poor performance of **L2** and **L3**, we were delighted to find that the fluorinated arene derivatives **L4** and **L5** produce substantial improvements in yield relative to **L1**. The obstructed *o*-difluoro derivative, **L6**, cannot achieve the κ^3 binding mode illustrated in Figure 3, and provides poor yields by comparison. Meta fluoro-

substituted **L4** displayed remarkable efficacy – providing near-quantitative consumption of both borane equivalents of B_2pin_2. Following the convention wherein yields of product are calculated based on one equivalent of B_2pin_2, **L4** facilitates a yield of 180%, reflecting significant consumption of the byproduct HBpin. **L4** demonstrates a substantial increase in yield relative to the established ligand Me_4phen when compared both under analogous conditions and under reported optimized conditions for Me_4phen. Thus **L4** represents a dramatic improvement relative to established ligands for alkane C-H borylation.

4.2.1 Reaction Optimization and Scope

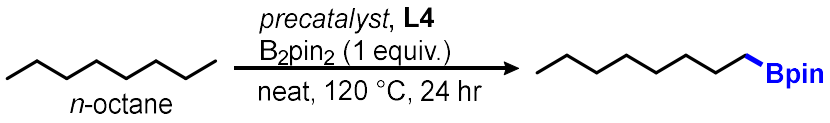

Entry	Precatalyst	(mol%)	Variation	Yield[a]
1	$[Ir(cod)OMe]_2$	(5%)	None	180%
2	$[Rh(cod)OMe]_2$	(5%)	None	6%
3	$[Ru(cod)(methallyl)_2]$	(5%)	None	24%
4	$[Ir(cod)Cl]_2$	(5%)	None	*nd*
5	-	-	Catalyst omitted	*nd*
6	$[Ir(cod)OMe]_2$	(1%)	None	143%
7	$[Ir(cod)OMe]_2$	(5%)	Me_4phen instead of **L4**	82%
8	$[Ir(cod)OMe]_2$	(5%)	**L4** omitted	<1%
9	$[(Mes)Ir(Bpin)_3]$	(1%)	None	>199%
10	$[(Mes)Ir(Bpin)_3]$	(1%)	Me_4phen instead of **L4**	52%
11	$[(Mes)Ir(Bpin)_3]$	(1%)	**L4** omitted	trace
12	$[(Mes)Ir(Bpin)_3]$	(1%)	HBpin instead of B_2pin_2	37%[b]
13	$[(Mes)Ir(Bpin)_3]$	(1%)	0.10 equiv. B_2Pin_2 + 0.80 equiv. HBpin[c]	37%[b]
14	$[(Mes)Ir(Bpin)_3]$	(1%)	0.10 equiv. B_2Pin_2 ***then*** 0.80 equiv. HBpin[d]	71%[b]

***Table 4.1**: Optimization of catalytic C−H borylation under neat conditions. [a]Yield determined by GC-FID with dodecane internal standard; based on 1 equiv. B_2pin_2. [b]Percentage of total boron consumption. [c]HBpin both added prior to heating. [d]HBpin added after 30 min of heating at 120 °C*

Optimization of the alkane borylation reaction was performed using **L4** and n-octane. In control experiments which omit either pre-catalyst or ligand, no product is formed. Although Cp*Rh and Cp*Ru complexes are excellent alkane borylation catalysts,[4] neither [Rh(cod)OMe]$_2$/**L4** nor [(cod)Ru(methallyl)$_2$]/**L4** give active catalyst systems (Table 1, Entry 2 & 3). The use of [(Mes)Ir(Bpin)$_3$] as the precatalyst produces a quantitative yield at a catalyst loading of only 1 mol% (Table 1, Entry 9). Using [(Mes)Ir(Bpin)$_3$], we found that maximal yields were obtained at a reaction temperature of 120 °C for 24 hours.

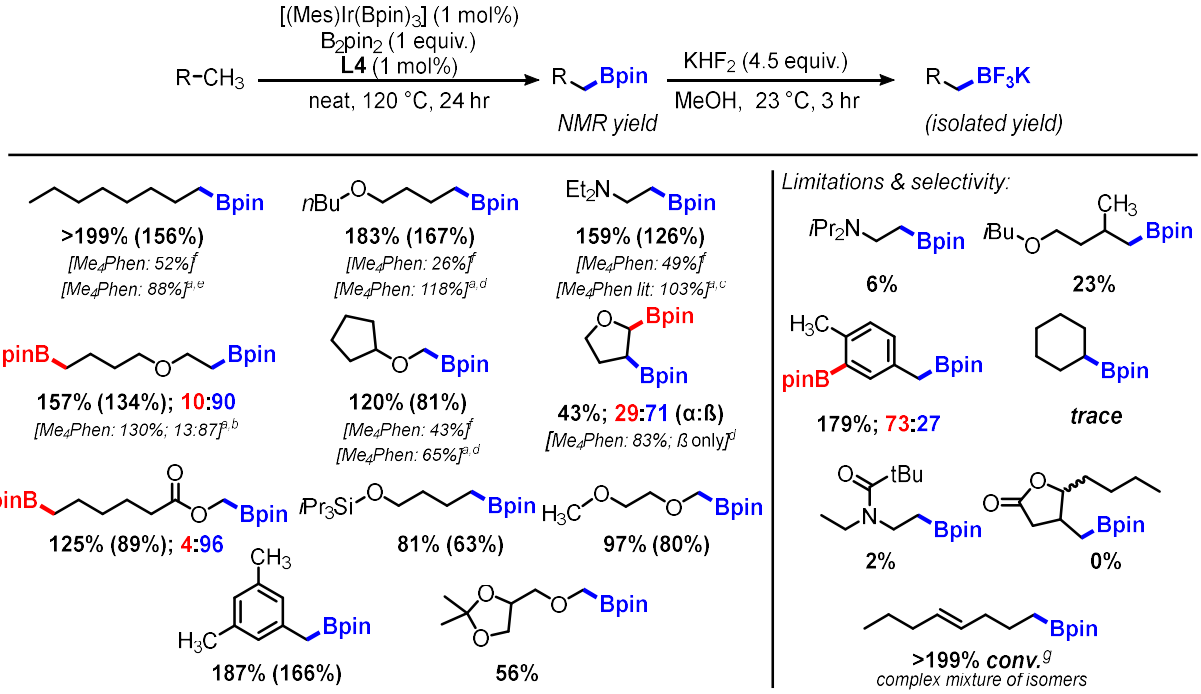

Figure 4.3: *Substrate scope for catalytic borylation under neat conditions. [a]Reported GC yield with 1[b], 2[c] or 4%[d] [(Mes)Ir(Bpin)$_3$].[5] [e]Reported GC yield with [(cod)Ir(OMe)]$_2$ (10% Ir), 120 °C.[8] [f]GC yields using Me$_4$Phen under our conditions. [g]Full conversion of B$_2$pin$_2$ reagent to a complex mixture of isomerization, borylation, and hydrogenation products of 4-octene.*

Following the optimized conditions in **Table 4.1**, the reaction scope was explored using the substrates shown in **Figure 4.3**. For several substrates, results with the [(Mes)Ir(Bpin)$_3$]/**L4** system are compared with results using [(Mes)Ir(Bpin)$_3$]/Me$_4$phen under our optimized conditions. Where available, yields for [(Mes)Ir(Bpin)$_3$]/Me$_4$phen using alternate reaction conditions are noted. In all cases we find a substantial increase

in product formation using **L4** versus Me_4phen. This catalytic system is compatible with ethers, tertiary amines, and esters. Butyl ethyl ether shows good β-selectivity,[5] while cyclopentyl methyl ether and methyl butyrate undergo selective borylation at the methyl group. Selectivity for C-H bonds β to Lewis bases has been attributed to a directing effect in a previous iridium system.[5] Both secondary[28] and α-branched primary C-H bonds are found to be poor substrates. Importantly, a variety of substrates are found to undergo catalytic sp^3 borylation in yields in excess of 100% on a B_2Pin_2 basis, demonstrating the remarkable effectiveness of the [(Mes)Ir(Bpin)$_3$]/**L4** system over previously-reported iridium catalysts.

The high yields obtained with this catalyst under neat substrate conditions suggested it might be competent for catalysis in solvent at reduced substrate concentrations. Borylation in solvent is common for arene borylation but remains rare in sp^3 borylation examples. Nearly all previous examples of sp^3 borylation of simple alkane and ether substrates are performed in neat substrate to obtain reasonable yields of the organoborane.[5-9, 29] Previous attempts at performing this reaction on un-activated substrates in solvent typically give either poor yield of the desired organoborane or extensive borylation of the reaction solvent.[8, 10] Capitalizing on the superior efficacy of the [(Mes)Ir(Bpin)$_3$]/**L4** system, C-H borylation without the use of neat, excess substrate was explored.

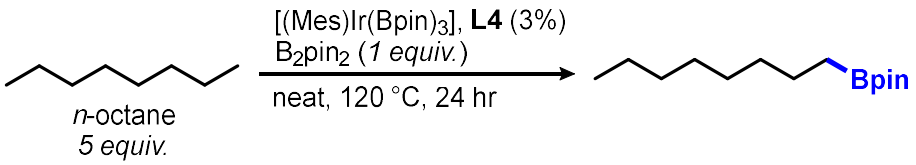

Entry	Solvent	Octyl-Bpin Yield[a]	Solvent-Bpin Yield[a]
1	Cyclooctane	57%	< 5%
2	THF	8%	24%
3	1,4-dioxane	< 5%	21%
4	Isooctane	63%	< 1%
5	Cyclohexane	79%	< 5%
6[b]	Cyclohexane	103%	< 5%

Table 4.2. *Survey of solvents for catalytic C-H borylation. [a]Yields determined by GC-FID with a dodecane standard; based on 1 equiv. B_2pin_2. [b]48 hr.*

With the poor catalytic performance of [(Mes)Ir(Bpin)$_3$]/**L4** towards secondary or branched alkanes (**Figure 4.3**) in mind, we examined a selection of potential solvents (**Table 4.2**), arriving at the optimized conditions used in **Figure 4.4**. We find that the [(Mes)Ir(Bpin)$_3$]/**L4** system is capable of productive alkane borylation in cyclohexane with negligible competitive solvent borylation. While the reaction proceeds to 22% yield with a single equivalent of substrate, five molar equivalents of substrate are required for high yields, representing a substantial improvement over the typical requirement for neat substrate.

A survey of substrates for sp^3 borylation in cyclohexane solvent reveals several interesting features. All substrates which were successful under neat conditions translate well into our conditions in solvent, despite this representing a *ca.* 15-fold decrease in substrate concentration. Additionally, the lactone and amide substrates, which do not undergo catalytic borylation under our neat conditions, can be borylated effectively in cyclohexane. The lactone substrate is borylated at the α-branched methyl group rather than on the less hindered *n*-butyl group, which we suspect results from a directing effect analogous to that observed previously for other Lewis-basic substrates.[5] The success of these relatively polar substrates highlights the importance of pursuing catalysts which are capable of alkane borylation in solvent, as such systems can enable the practical application of C-H borylation to substrates not suitable for neat conditions.

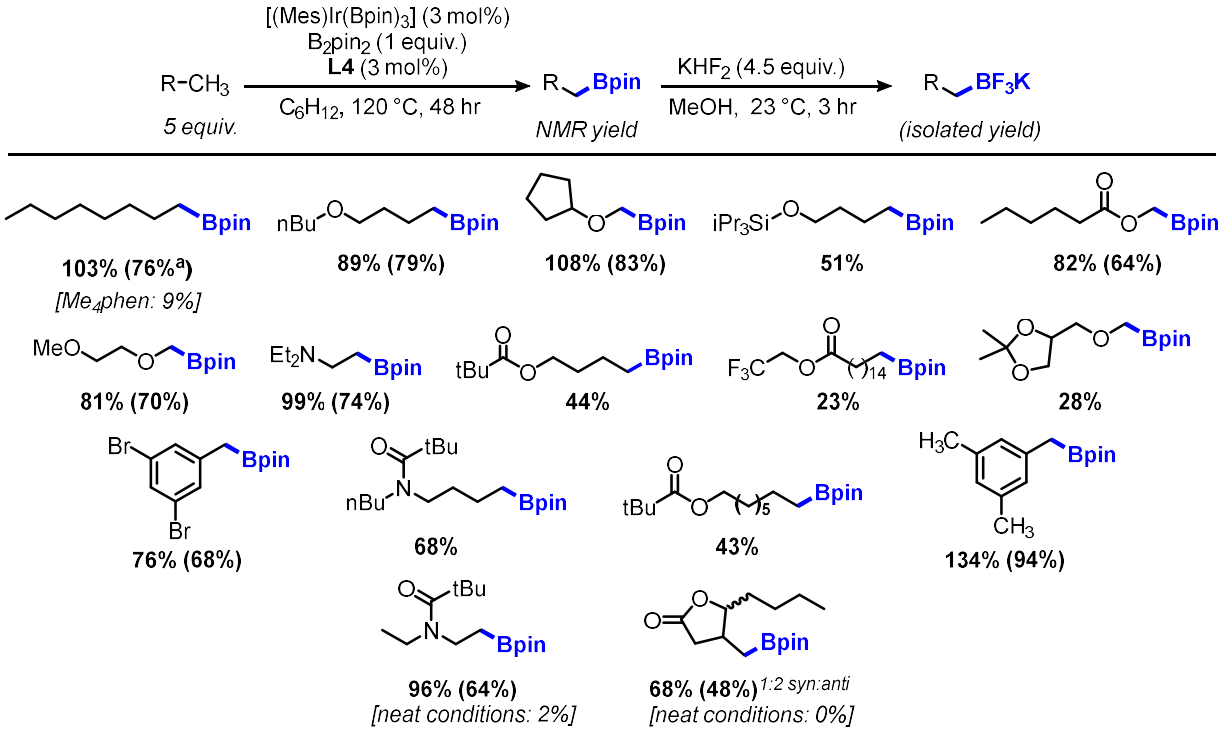

Figure 4.4: *Substrate scope for catalytic C-H borylation conducted in cyclohexane solvent.* [a]*Isolated as octylBpin*.

Under optimized conditions in solvent, yields in excess of 100% are observed for fewer substrates than under neat conditions. At present it is not clear what feature of the [(Mes)Ir(Bpin)$_3$]/**L4** catalyst system is responsible for the enhanced consumption of HBpin relative to (Me$_4$phen)/Ir systems. When HBpin alone is used as the boron source under neat conditions, modest yields of organoborane are observed (Table 4.1, entry 12). This outcome is lower than expected based on HBpin consumption when B_2pin_2 is used as the boron source. However, when HBPin is added after an initial 1 hour incubation time with B_2pin_2, substantial HBpin conversion is observed, suggesting differing roles for B_2pin_2 and HBpin in catalyst activation (**Table 4.1**, entries 13 & 14). Results from a ^{11}B NMR study on a neat borylation reaction (**Figure 4.5**) are consistent with substantial buildup of HBpin during the initial phase of catalysis. At longer reaction times, HBpin incorporation into product becomes evident, confirming that HBpin is still a competent boron source for alkane borylation. A similar difference in reaction rate between B_2pin_2 and HBpin has been observed in a Cp*Rh system.[6]

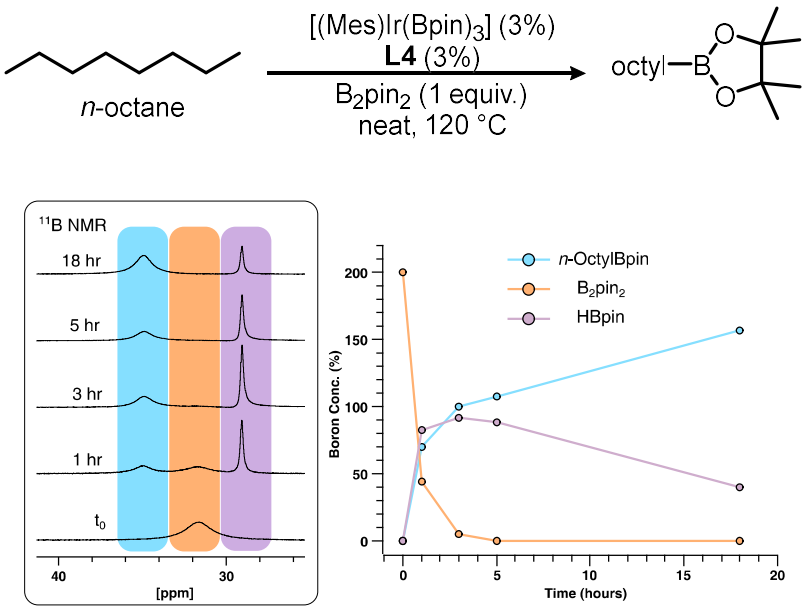

Figure 4.5: *B_2pin_2 and HBpin consumption by ^{11}B NMR spectroscopy, see the Experimental (section 4.4).*

The enhanced performance of the [(Mes)Ir(Bpin)$_3$]/**L4** system versus previous iridium catalysts for alkane borylation presumably stems from the structure of the iridium species generated *in situ*. A single major ^{19}F NMR species is observed from the reaction of [(Mes)Ir(Bpin)$_3$] with **L4** at 23 °C, which evolves to several species under catalytic conditions. Although we have not been successful in obtaining structural data elucidating the binding mode of **L4** under catalytic conditions, the significant change in reactivity as a function of substitution on the phenyl substituent argues that the aryl group does not remain distal from the metal center during key steps in the catalytic cycle. κ^3 coordination in the active species is also supported by the poor activity of hindered **L6**/Ir system. It is tempting to speculate a role for a κ^3 binding mode resulting from phenyl group cyclometalation, but it is also possible that sp^2 borylation of the ligand[30] would situate a pinacolborane group proximal to the metal center. The Hartwig group has previously proposed a role for secondary coordination sphere interactions between metal-boryls and substrate in alkane borylation.[5]

4.3 Conclusions

Regardless of the mode by which **L4** enables enhanced alkane borylation catalysis, it is evident that the resulting [(Mes)Ir(Bpin)$_3$]/**L4** catalyst system possesses

major advantages over previously reported iridium catalysts. For many examples under neat conditions, both the B_2pin_2 reagent and its byproduct HBpin are consumed to give borylated product. As B_2pin_2 is typically the limiting reagent under such conditions, the [(Mes)Ir(Bpin)$_3$]/**L4** system presents an advantage in terms of product yield and efficient utilization of the costly boron source. Additionally, this catalyst allows for the borylation of smaller excesses of substrate in hydrocarbon solvents without need for directing-group strategies. The key enabling advance here is the application of a dipyridylarylmethane ligand. Substitution of the parent ligand is found to impart profound changes to catalyst efficiency, which suggests that dipyridylarylmethane ligands are likely to offer a new and highly tunable ligand scaffold for alkane borylation catalysis. Our ongoing efforts are directed at understanding the binding mode and substituent effects of dipyridylarylmethane ligands in borylation catalysis in hopes of developing increasingly active catalysts.

*Reprinted (adapted) with permission from Margaret R. Jones, Caleb D. Fast, and Nathan D. Schley. Journal of the American Chemical Society **2020** 142 (14), 6488-6492. DOI: 10.1021/jacs.0c00524. Copyright 2020 American Chemical Society.*

This material is based upon work supported by the National Science Foundation under grant no. CHE-1847813.

4.4 Experimental

General Considerations. Syntheses and manipulations with organometallic reagents were carried out using standard vacuum, Schlenk, cannula, or glovebox techniques under N_2 in oven- or flame-dried glassware unless otherwise specified. Tetrahydrofuran, dichloromethane, toluene, pentane, and diethyl ether were degassed with argon and dried over activated alumina using a solvent purification system.

Spectroscopy. ^{1}H, $^{13}C\{^{1}H\}$, ^{11}B, and ^{19}F NMR spectra were recorded on Bruker NMR spectrometers at ambient temperatures unless otherwise noted. ^{1}H and $^{13}C\{^{1}H\}$

chemical shifts are referenced to residual solvent signals, ^{19}F chemical shifts are referenced to an external C_6F_6 standard. $^{13}C\{^1H\}$ resonances for boron-attached carbon atoms are not observed and are not included in the listings of spectral data.

Synthesis and Characterization

Organometallic starting materials. Bis(1,5-cyclooctadiene)diiridium(I) dichloride $[(cod)IrCl]_2$,[31] Bis(1,5-cyclooctadiene)diiridium(I) dimethoxide $[(cod)IrOMe]_2$,[32] $[(cod)RhOMe]_2$,[32] (η^5-indenyl)(1,5-cyclooctadiene)iridium [(Ind)Ir(cod)],[33] and (η^6-mesitylene)(tris-pinacolboryl)iridium $[(Mes)Ir(Bpin)_3]$,[34] were prepared according to published procedures. $IrCl_3 \cdot 3H_2O$, pinacolborane and bispinacolatodiboron were purchased from chemical vendors and used as received.

Substrate syntheses. *n*-octane, cyclohexane, cyclooctane, isooctane, di-*n*-butyl ether, triethylamine, cyclopentyl methyl ether, mesitylene, ethyl *n*-butyl ether, methyl butanoate, 3,5-dibromotoluene, dimethoxy ethane, and 5-butyl-4-methyldihydro-2(3*H*)-furanone (1.3:1 *cis*:*trans*) were purchased from chemical vendors and used as received. Diethylpivalamide,[35] n-butyl pivalate,[36] and butoxytriisopropylsilane[37-38] were prepared and characterized by reported literature procedures.

Ligand syntheses. Di(2-pyridyl)methane (**L1**)[39] and di(2-pyridyl)(phenyl)fluoromethane (**L3**)[40] were prepared according to published procedures. Tetramethylphenanthroline, 2-fluoropyridine, 2-benzylpyridine, 1,4-difluorobenzene, 2,2-dipyridyl ketone, phenyl magnesium bromide, diethylaminosulfur trifluoride, 2,6-difluorobromobenzene, and pyridine-2-carboxaldehyde were purchased from chemical vendors and used as received. Syntheses and characterization of **L4**-**L17** are described in chapter 2 of this document.

General procedures

Procedure for ligand comparisons (Figure 4.2). In an inert-atmosphere glove box, a 4 mL vial was charged with $[Ir(COD)OMe]_2$ (0.0030 g, 0.010 mmol (Ir basis), 10 mol %

Ir) and B_2pin_2 (0.026 g, 0.10 mmol). *n*-octane (1.0 mL, 200 mM) was added and the solution stirred for 3 min. The resulting solution was transferred to a separate 4 mL vial charged with ligand (0.010 mmol, 10 mol %). The vial was sealed with a PTFE-lined cap, removed from the glove box, and heated to 120 °C in an oil bath with stirring for 24 hr. At this point the reaction was cooled to room temperature and the crude mixture analyzed by GC-FID. Yields were obtained using a calibrated dodecane internal standard.

Procedure for catalytic borylation of neat substrate (Figure 4.3). In an inert-atmosphere glove box, a 4 mL vial equipped with magnetic stirbar was charged with [(Mes)Ir(Bpin)$_3$] (0.0021 g, 3.0 μmol, 1 mol %), **L4** (0.0008 g, 3.0 μmol, 1 mol %), and B_2pin_2 (0.076 g, 300 μmol). Substrate (3 mL) was then added to give a pale yellow-orange solution. The vial was sealed with a PTFE-lined cap, removed from the glove box and was heated in a 120 °C oil bath with stirring for 24 hr, giving a deep red solution. The crude mixture was cooled to room temperature, concentrated *in vacuo*, and analyzed by ^{1}H NMR with a tetrachloroethane standard to obtain NMR yields. Isolated yields were obtained by conversion to the trifluoroborate salt according to the general procedure given below.

Procedure for catalytic borylation of substrate in cyclohexane solvent (Figure 4.4). In an inert-atmosphere glove box, a 15 mL Schlenk bomb flask equipped with a magnetic stirbar was charged with [(Mes)Ir(Bpin)$_3$] (0.0062 g, 9 μmol, 3 mol %), **L4** (0.0024 g, 9 μmol, 3 mol %), and B_2pin_2 (0.076 g, 300 μmol). The mixture was taken up in 2.7 mL cyclohexane and allowed to stir for 2-3 min at room temperature to give a pale yellow-orange solution, followed by the addition of substrate (1.5 mmol, 5.0 equiv.). The reaction flask was sealed with a PTFE plug, was removed from the glove box and was heated in a 120 °C oil bath for 48 hours to give a deep red solution. The crude mixture was cooled to room temperature, concentrated *in vacuo*, and analyzed by ^{1}H NMR with a tetrachloroethane standard to obtain NMR yields. Isolated yields were obtained by conversion to the trifluoroborate salt according to the general procedure given below.

Procedure for conversion of boronate esters to potassium trifluoroborates for isolation. In air, the crude boronate ester was taken up in 2 mL MeOH and transferred to a 20 mL glass vial equipped with a magnetic stirbar. To this solution was added

aqueous KHF_2 (0.287 mL of a 4.7 M solution, 1.35 mmol, 4.5 equiv.), and the mixture was allowed to stir at ambient temperature for 3 hr. The resulting mixture was concentrated on a rotary evaporator. A 5 mL portion of methanol was added followed by evaporation again. This process was repeated two additional times to remove free pinacol. The mixture was then triturated with three, 3 mL portions of acetone and the extracts were filtered and evaporated to dryness. The crude residue was washed with 2 mL diethyl ether and dried *in vauco* to give the pure alkyl trifluoroborate.

Procedure for ^{11}B NMR monitoring of the borylation of neat *n*-octane (Figure 4.5). In an inert-atmosphere glove box, a 4 mL vial was charged with [(Mes)Ir(Bpin)$_3$] (0.0021 g, 3.0 μmol, 3 mol %), **L4** (0.0008 g, 3.0 μmol, 3 mol %), and B_2pin_2 (0.026 g, 100 μmol). The mixture was then taken up in 1 mL of *n*-octane, stirred briefly, and 0.5 mL of the resulting solution was added to a J. Young NMR tube equipped with a sealed C_6D_6 capillary. The sealed tube was then removed from the glove box and an initial ^{11}B NMR spectrum was collected at room temperature. The J. Young tube was then heated in a 120 °C oil bath. The tube was removed from heat after 1, 3, 5, and 18 hours for analysis by ^{11}B NMR. NMR spectra were collected at 23 °C after which the tube was returned to the oil bath. ^{11}B integrations were calculated by fitting to Lorentzian functions using Fityk[41] and normalized to give the data presented in Figure 4.5. The *y*-axis is presented as 2*(normalized peak area).

Synthesis and Characterization of Borylated Products

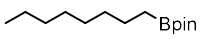

4,4,5,5-tetramethyl-2-octyl-1,3,2-dioxaborolane. This product was synthesized according to the general procedure for borylation under neat conditions. The crude boronate ester was isolated by column chromatography (5% EtOAc in hexane) to give the product as a pale yellow oil. Yield: 0.113 g (156%).

This product was also synthesized according to the general procedure for borylation in cyclohexane solvent using 0.244 mL *n*-octane. The crude boronate ester was isolated by column chromatography (5% EtOAc in hexane) to give the product as a pale yellow oil. Yield: 0.055 g (76%).

This product has been previously characterized.[42]

^{1}H NMR ($CDCl_3$, 400 MHz): δ 1.43-1.18 (m, 12H), 1.23 (s, 12H), 0.86 (t, J = 6.8 Hz, 3H), 0.75 (t, *J* = 7.7 Hz, 2H).

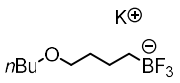

Potassium 4-(*n*-butoxy)*n*-butyltrifluoroborate. This product was synthesized according to the general procedure for borylation under neat conditions using 3 mL di-*n*-butyl ether. The crude boronate ester was then converted to the trifluoroborate according to the general procedure. The product was isolated as a white solid. Yield: 0.118 g (167%).

This product was also synthesized according to the general procedure for borylation in cyclohexane solvent using 0.254 mL di-*n*-butyl ether. The crude boronate ester was then converted to the trifluoroborate according to the general procedure. The product was isolated as a white solid. Yield: 0.056 g (79%).

This product has been previously characterized.[43]

^{1}H NMR (acetone-d_6, 400 MHz): δ 3.34 (t, *J* = 6.35 Hz, 2H), 3.32 (t, *J* = 7.28 Hz, 2H), 1.23-1.54 (m, 8H), 0.89 (t, *J* = 7.3 Hz, 3H), 0.12 (m, 2H)

^{13}C{^{1}H} NMR (acetone-d_6, 151 MHz): δ 72.4, 71.0, 34.6, 32.9, 23.2 (q, *J* = 2.6 Hz), 20.2, 14.3

HRMS $[M-K]^-$ Calc. 197.1330 , Found 197.1317

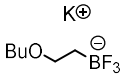

Potassium 2-butoxyethyltrifluoroborate. This product was synthesized according to the general procedure for borylation under neat conditions using 3 mL butyl methyl ether. The crude boronate ester was then converted to the trifluoroborate according to the general procedure. The product was isolated as a white solid. Yield: 0.084 g (134%).

This product has been previously characterized. [43]

^{1}H NMR (acetone-d_6, 400 MHz): δ 3.40 (q, *J* = 6.9 Hz, 2H), 3.09 (m, 2H), 1.32 – 1.26 (m, 2H), 1.15 – 1.07 (m, 2H), 0.87 (t, J = 7.4 Hz, 3H), 0.44 (br m, 2H)

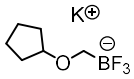

Potassium (cyclopentyloxy)methyltrifluoroborate. This product was synthesized according to the general procedure for borylation under neat conditions using 3 mL cyclopentyl methyl ether. The crude boronate ester was then converted to the trifluoroborate according to the general procedure. The product was isolated as a white solid. Yield: 0.048 g (81%).

This product was also synthesized according to the general procedure for borylation in cyclohexane solvent using 0.175 mL cyclopentyl methyl ether. The crude boronate ester was then converted to the trifluoroborate according to the general procedure. The product was isolated as a white solid. Yield: 0.051 g (83%).

This product has been previously characterized.[44]

^{1}H NMR (acetone-d_6, 400 MHz): δ 3.56 (m, 1H), 2.50 (q, J = 5.4 Hz, 2H) 1.42-1.58 (m, 6H), 1.28-1.36 (m, 2H)

^{13}C{^{1}H} NMR (acetone-d_6, 151 MHz): δ 84.5, 32.6, 24.2

HRMS [M-K]$^{-}$ Calc. 167.0861, Found 167.0853

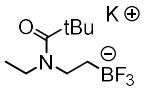

Potassium (2-(N-ethylpivalamido)ethyl)trifluoroborate. This product was synthesized according to the general procedure for borylation in cyclohexane solvent using 0.236 g N,N-diethylpivalamide. The crude boronate ester was then converted to the trifluoroborate according to the general procedure. The product was isolated as a white solid. Yield: 0.051 g (64%).

N,N-diethylpivalamide does not undergo efficient borylation following the general procedure for borylation under neat conditions. Analysis of the crude reaction mixture by ^{1}H NMR with a tetrachloroethane internal standard shows the formation of the corresponding boronate ester in low yield. Yield: 2%.

^{1}H NMR (acetone-d_6, 400 MHz): δ 3.19-3.45 (m, 4H), 1.20 (s, 9H), 1.02 (t, J = 6.7 Hz, 3H), 0.45 (m, 2H)

^{13}C{^{1}H} NMR (acetone-d_6, 151 MHz): δ 175.8, 41.2 (br), 39.2, 29.0, 13.3 (br)

HRMS [M-K]$^{-}$ Calc. 224.1439, Found 224.1431

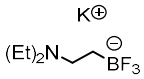

Potassium 2-(diethylamino)ethyltrifluoroborate. This product was synthesized according to the general procedure for borylation under neat conditions using 3 mL triethylamine. The crude boronate ester was then converted to the trifluoroborate according to the general procedure. The product was isolated as a white solid. Yield: 0.078 g (126%).

This product was also synthesized according to the general procedure for borylation in cyclohexane solvent using 0.208 mL triethylamine. The crude boronate ester was then converted to the trifluoroborate according to the general procedure. The product was isolated as a white solid. Yield: 0.046 g (74%).

This compound has been previously characterized.[43]

^{1}H NMR (acetone-d_6, 400 MHz): δ 3.21 (q, J = 7.3, 4H), 3.13 (m, 2H), 1.31 (t, J = 7.3 Hz, 6H), 0.47 (m, 2H)

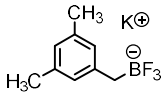

Potassium (3,5-dimethylbenzyl)trifluoroborate. This product was synthesized according to the general procedure for borylation under neat conditions using 3 mL mesitylene. The crude boronate ester was then converted to the trifluoroborate according to the general procedure. The product was isolated as a white solid. Yield: 0.106 g (166%).

This product was also synthesized according to the general procedure for borylation in cyclohexane solvent using 0.209 mL mesitylene. The crude boronate ester was then converted to the trifluoroborate according to the general procedure. The product was isolated as a white solid. Yield: 0.059 g (94%).

^{1}H NMR (acetone-d_6, 400 MHz): δ 6.59 (s, 2H), 6.37 (s, 1H), 2.02 (s, 6H), 1.43 (br, 2H)

^{13}C{^{1}H} NMR (acetone-d_6, 151 MHz): δ 147.9, 136.5, 127.8, 124.7, 21.6

HRMS $[M\text{-}K]^-$ Calc. 187.0911, Found 187.0905

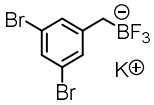

Potassium (3,5-dibromobenzyl)trifluoroborate. This product was synthesized according to the general procedure for borylation in cyclohexane solvent using 0.372 g 3,5-dibromotoluene. The crude boronate ester was purified by column chromatography (5→15% EtOAc in hexanes) and concentrated *in vacuo*. The boronate ester was then converted to the trifluoroborate according to the general procedure. The product was isolated as a white solid. Yield: 0.073 g (68%).

^{1}H NMR (acetone-d_6, 400 MHz): δ 7.09-7.13 (m, 3H), 1.49 (br, 2H)

^{13}C{^{1}H} NMR (acetone-d_6, 151 MHz): δ 154.1, 131.4, 127.9, 122.1

HRMS [M-K]$^{-}$ Calc. 314.8809, Found 314.8798

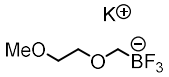

Potassium (2-methoxyethoxy)methyltrifluoroborate. This product was synthesized according to the general procedure for borylation under neat conditions using 3 mL dimethoxyethane. The crude boronate ester was then converted to the trifluoroborate according to the general procedure. The product was isolated as a white solid. Yield: 0.047 g (80%).

This product was also synthesized according to the general procedure for borylation in cyclohexane solvent using 0.156 mL dimethoxyethane. The crude boronate ester was then converted to the trifluoroborate according to the general procedure. The product was isolated as a white solid. Yield: 0.041 g (70%).

^{1}H NMR (acetone-d_6, 400 MHz): δ 3.46 (m, 4H), 3.33 (s, 3H), 2.71 (q, J = 5.3 Hz, 2H)

^{13}C{^{1}H} NMR (acetone-d_6, 151 MHz): δ 73.2, 72.6, 58.7

HRMS [M-K]$^{-}$ Calc. 157.0653, Found 157.0647

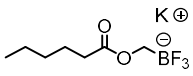

Potassium Methyltrifluoroborate hexanoate. This product was synthesized according to the general procedure for borylation under neat conditions using 3 mL methyl hexanoate. The crude boronate ester was then converted to the trifluoroborate

according to the general procedure with the following modifications to the workup: After conversion to the trifluoroborate, the crude reaction mixture was reduced to a volume of 1 mL. To prevent hydrolysis, 2 mL toluene was added to the mixture and the solution reduced in volume, this was repeated three times. After evaporation to dryness, the residue was extracted with acetone and the extracts were filtered and evaporated to dryness. The product was isolated as a white solid. Yield: 0.063 g (89%).

This product was also synthesized according to the general procedure for borylation in cyclohexane solvent using 0.220 mL methyl hexanoate. The crude boronate ester was then converted to the trifluoroborate according to the general procedure with the same modifications as above. The product was isolated as a white solid. Yield: 0.044 g (62%).
^{1}H NMR (acetone-d_6, 400 MHz): δ 3.16 (q, J = 5.3 Hz, 2H), 2.06 (t, J = 7.3 Hz, 2H), 1.42 (quintet, 7.4 Hz, 2H), 1.11-1.21 (m, 4H), 0.74 (t, 7.1 Hz, 3H)
^{13}C{^{1}H} NMR (acetone-d_6, 151 MHz): δ 175.2, 35.1, 32.2, 25.8, 23.2, 14.3
HRMS [M-K]$^-$ Calc. 197.0966, Found 197.0957

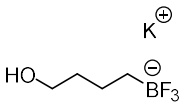

Potassium (4-hydroxybutyl)trifluoroborate. This product was synthesized according to the general procedure for borylation under neat conditions using 3 mL butoxytriisopropylsilane. The crude boronate ester was then converted to the trifluoroborate according to the general procedure with the following modifications: 10 equiv. KHF_2 was used and the reaction was carried out at 65 °C for 18 hr. The crude reaction mixture was evaporated to dryness *in vacuo.* The residue was washed with ice cold acetone, and the solid extracted with five, 3 mL portions of acetone. The combined acetone extracts were concentrated to 3 mL and precipitated with Et_2O to yield the product as a colorless solid. Yield: 0.034 g (63%).

This product was also synthesized according to the general procedure for borylation in cyclohexane solvent using 0.346 g butoxytriisopropylsilane. The crude mixture was cooled to room temperature, concentrated *in vacuo*, and analyzed by ^{1}H NMR with a tetrachloroethane standard to obtain an NMR yield of 4-(triisopropylsiloxy)butyl-

pinacolborane. (51%)

^{1}H NMR (D_2O, 400 MHz): δ 3.36 (t, *J* = 6.7 Hz, 2H), 1.30 (quintet, *J* = 7.3 Hz, 2H), 0.96-1.07 (m, 2H), 0.01 (q, *J* = 8.1 Hz, 2H)

^{13}C{^{1}H} NMR (D_2O, 101 MHz): δ 61.8, 34.4, 20.2

HRMS [M-K]$^-$ Calc. 141.0704, Found 141.0704

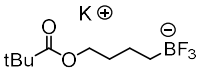

Potassium ((4-pivaloyloxy)butyl)trifluoroborate. This product was synthesized according to the general procedure for borylation in cyclohexane solvent using 0.277 mL butyl pivalate. The crude boronate ester was concentrated *in vacuo*, and analyzed by ^{1}H NMR with a tetrachloroethane standard to obtain an NMR yield. (44%).

The crude boronate ester was then converted to the known trifluoroborate according to the general procedure. The identity of the product was confirmed by comparison of ^{1}H NMR spectra to reported data.[45]

^{1}H NMR (acetone-d_6, 400 MHz): δ 3.98 (t, *J* = 6.9 Hz, 2H), 1.55 (p, J = 6.8 Hz, 2H), 1.31 (m, 2H), 1.14 (s, 9H), 0.10-0.15 (br m, 2H),

HRMS [M-K]$^-$ Calc. 225.1279, Found 225.1272

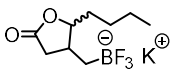

Potassium 4-methyl-5-(4-(trifluoroboranyl)butyl)dihydrofuran-2-one. This product was synthesized according to the general procedure for borylation in cyclohexane solvent using 0.246 mL 5-butyl-4-methyldihydrofuran-2(3*H*)-one (1:1.3 *syn*:*anti*). The crude boronate ester was then converted to the trifluoroborate according to the general procedure. The product was isolated as a white solid (1:2 *syn*:*anti*). Yield: 0.038 g (48%).

5-butyl-4-methyldihydrofuran-2(3*H*)-one does not undergo borylation following the general procedure for borylation under neat conditions. Analysis of the crude reaction mixture by ^{1}H NMR or GC-FID shows no evidence for formation of the corresponding boronate ester.

Assignment of the site of borylation was made on the basis of 1D and 2D NMR spectra and the observation of a major mass fragment at *m/z* = 282 (M-Bu) in the GC-MS (EI)

spectrum of the boronate ester prior to fluorination.

^{1}H NMR (acetone-d_6, 400 MHz): *syn* isomer: δ 4.33 (ddd, *J* = 9.6 Hz, 6.3 Hz, 4.2 Hz, 1H), 2.51 (m, 1H), 2.40 (dd, *J* = 7.7 Hz, 17.0 Hz, 1H), 2.31 (dd, *J* = 7.5 Hz, 17.1 Hz, 1H), 1.60 (m, 1H), 1.48-1.53 (m, 1H), 1.41-1.48 (m, 1H) 1.30-1.38 (m, 3H), 0.90 (t, *J* = 7.1 Hz, 3H), 0.28 (m, 1H), 0.07 (m, 1H) *anti* isomer: δ 3.96 (dt, *J* = 3.4 Hz, 8.0 Hz, 1H), 2.51 (dd, *J* = 7.9 Hz, 17.4 Hz, 1H), 2.16 (dd, *J* = 10.0 Hz, 17.3 Hz, 1H), 2.08, (m, 1H) 1.72 (m, 1H), 1.41-1.48 (m, 2H) 1.30-1.38 (m, 3H), 0.90 (t, *J* = 7.1 Hz, 3H), 0.43 (m, 1H), 0.15 (m, 1H)

^{13}C{^{1}H} NMR (acetone-d_6, 151 MHz): *syn* isomer: δ 178.7, 85.9, 37.2, 36.9, 30.3, 29.0, 23.4, 14.3, *anti* isomer: δ 178.4, 89.5, 40.1, 38.1, 34.3, 29.1, 23.3, 14.3.

HRMS $[M\text{-}K]^-$ Calc. 223.1123, Found 223.1110

4.5 References

(1) Wencel-Delord, J.; Glorius, F., C–H bond activation enables the rapid construction and late-stage diversification of functional molecules. *Nature Chemistry* **2013**, 5 (5), 369-375.

(2) Goldberg, K. I.; Goldman, A. S., Large-Scale Selective Functionalization of Alkanes. *Acc. Chem. Res*. **2017**, 50 (3), 620-626.

(3) Xu, L.; Wang, G.; Zhang, S.; Wang, H.; Wang, L.; Liu, L.; Jiao, J.; Li, P., Recent advances in catalytic C−H borylation reactions. *Tetrahedron* **2017**, 73 (51), 7123-7157.

(4) Hartwig, J. F., Borylation and Silylation of C–H Bonds: A Platform for Diverse C–H Bond Functionalizations. *Acc. Chem. Res*. **2012**, 45 (6), 864-873.

(5) Li, Q.; Liskey, C. W.; Hartwig, J. F., Regioselective Borylation of the C–H Bonds in Alkylamines and Alkyl Ethers. Observation and Origin of High Reactivity of Primary C–H Bonds Beta to Nitrogen and Oxygen. *J. Am. Chem. Soc*. **2014**, 136 (24), 8755-8765.

(6) Chen, H.; Schlecht, S.; Semple, T. C.; Hartwig, J. F., Thermal, Catalytic, Regiospecific Functionalization of Alkanes. *Science* **2000**, 287 (5460), 1995-1997.

(7) Lawrence, J. D.; Takahashi, M.; Bae, C.; Hartwig, J. F., Regiospecific

Functionalization of Methyl C−H Bonds of Alkyl Groups in Reagents with Heteroatom Functionality. *J. Am. Chem. Soc.* **2004**, 126 (47), 15334-15335.

(8) Liskey, C. W.; Hartwig, J. F., Iridium-Catalyzed Borylation of Secondary C–H Bonds in Cyclic Ethers. J. Am. Chem. Soc. **2012**, 134 (30), 12422-12425.

(9) Ohmura, T.; Torigoe, T.; Suginome, M., "Iridium-catalysed borylation of sterically hindered C(sp3)–H bonds: remarkable rate acceleration by a catalytic amount of potassium tert-butoxide." Chem. Commun. 2014, 50 (48), 6333-6336.

(10) Ohmura, T.; Torigoe, T.; Suginome, M., Functionalization of Tetraorganosilanes and Permethyloligosilanes at a Methyl Group on Silicon via Iridium-Catalyzed C(sp3)–H Borylation. *Organometallics* **2013**, 32 (21), 6170-6173.

(11) Larsen, M. A.; Wilson, C. V.; Hartwig, J. F., Iridium-Catalyzed Borylation of Primary Benzylic C–H Bonds without a Directing Group: Scope, Mechanism, and Origins of Selectivity. *J. Am. Chem. Soc.* **2015**, 137 (26), 8633-8643.

(12) Cho, S. H.; Hartwig, J. F., Iridium-Catalyzed Borylation of Secondary Benzylic C–H Bonds Directed by a Hydrosilane. *J. Am. Chem. Soc.* **2013**, 135 (22), 8157-8160.

(13) Liskey, C. W.; Hartwig, J. F., Iridium-Catalyzed C–H Borylation of Cyclopropanes. *J. Am. Chem. Soc.* **2013**, 135 (9), 3375-3378.

(14) Shi, Y.; Gao, Q.; Xu, S., Chiral Bidentate Boryl Ligand Enabled Iridium-Catalyzed Enantioselective C(sp3)–H Borylation of Cyclopropanes. *J. Am. Chem. Soc.* **2019**, 141 (27), 10599-10604.

(15) Ohmura, T.; Torigoe, T.; Suginome, M., Catalytic Functionalization of Methyl Group on Silicon: Iridium-Catalyzed C(sp^3)–H Borylation of Methylchlorosilanes. *J. Am. Chem. Soc.* **2012**, 134 (42), 17416-17419.

(16) Yamamoto, T.; Ishibashi, A.; Suginome, M., Boryl-Directed, Ir-Catalyzed C(sp3)–H Borylation of Alkylboronic Acids Leading to Site-Selective Synthesis of Polyborylalkanes. *Org. Lett.* **2019**, 21 (16), 6235-6240.

(17) Kawamorita, S.; Murakami, R.; Iwai, T.; Sawamura, M., Synthesis of Primary and Secondary Alkylboronates through Site-Selective C(sp^3)–H Activation with Silica-Supported Monophosphine–Ir Catalysts. *J. Am. Chem. Soc*. **2013**, 135 (8), 2947-2950.

(18) Mita, T.; Ikeda, Y.; Michigami, K.; Sato, Y., Iridium-catalyzed triple C(sp^3)–H borylations: construction of triborylated sp^3-carbon centers." *Chem*. *Commun*. **2013**, 49 (49), 5601-5603.

(19) Reyes, R. L.; Iwai, T.; Maeda, S.; Sawamura, M., Iridium-Catalyzed Asymmetric Borylation of Unactivated Methylene C(sp^3)–H Bonds. *J. Am. Chem. Soc.* **2019**, 141 (17), 6817-6821.

(20) Mkhalid, I. A. I.; Barnard, J. H.; Marder, T. B.; Murphy, J. M.; Hartwig, J. F., C−H Activation for the Construction of C−B Bonds. *Chem. Rev.* **2010**, 110 (2), 890-931.

(21) Hierlinger, C.; Cordes, D. B.; Slawin, A. M. Z.; Jacquemin, D.; Guerchais, V.; Zysman-Colman, E., Phosphorescent cationic iridium(III) complexes bearing a nonconjugated six-membered chelating ancillary ligand: a strategy for tuning the emission towards the blue. *Dalton Transactions* **2018**, 47 (31), 10569-10577.

(22) Maleckis, A.; Sanford, M. S., Facial tridentate ligands for stabilizing palladium(IV) complexes. *Organometallics* **2011**, 30 (24), 6617-6627.

(23) Chong, E.; Kampf, J. W.; Ariafard, A.; Canty, A. J.; Sanford, M. S., Oxidatively Induced C–H Activation at High Valent Nickel. *J. Am. Chem. Soc*. **2017**, 139 (17), 6058-6061.

(24) Sberegaeva, A. V.; Zavalij, P. Y.; Vedernikov, A. N., Oxidation of a Monomethylpalladium(II) Complex with O2 in Water: Tuning Reaction Selectivity to Form Ethane, Methanol, or Methylhydroperoxide. *J. Am. Chem. Soc*. **2016**, 138 (4), 1446-1455.

(25) Vasko, P.; Kinnunen, V.; Moilanen, J. O.; Roemmele, T. L.; Boere, R. T.; Konu, J.; Tuononen, H. M., "Group 13 complexes of dipyridylmethane, a forgotten ligand in coordination chemistry." Dalton Transactions 2015, 44 (41), 18247-18259.

(26) Chen, H.; Hartwig, J. F., Catalytic, Regiospecific End-Functionalization of Alkanes: Rhenium-Catalyzed Borylation under Photochemical Conditions. *Angew. Chem. Int. Ed.* **1999**, 38 (22), 3391-3393.

(27) Iverson, C. N.; Smith, M. R., Stoichiometric and Catalytic B−C Bond Formation from Unactivated Hydrocarbons and Boranes. *J. Am. Chem. Soc.* **1999**, 121 (33), 7696-7697.

(28) Wei, C. S.; Jiménez-Hoyos, C. A.; Videa, M. F.; Hartwig, J. F.; Hall, M. B., Origins of the Selectivity for Borylation of Primary over Secondary C−H Bonds Catalyzed by Cp*-Rhodium Complexes. *J. Am. Chem. Soc.* **2010**, 132 (9), 3078-3091.

(29) Murphy, J. M.; Lawrence, J. D.; Kawamura, K.; Incarvito, C.; Hartwig, J. F., Ruthenium-Catalyzed Regiospecific Borylation of Methyl C−H Bonds. *J. Am. Chem. Soc.* **2006**, 128 (42), 13684-13685.

(30) Yang, Y.; Gao, Q.; Xu, S., Ligand-Free Iridium-Catalyzed Dehydrogenative ortho C−H Borylation of Benzyl-2-Pyridines at Room Temperature. *Adv. Synth. Catal.* **2019**, 361 (4), 858-862.

(31) Herde, J. L.; Lambert, J. C.; Senoff, C. V.; Cushing, M. A., Cyclooctene and 1,5-Cyclooctadiene Complexes of Iridium(I). *Inorg. Synth*. **1974**, 18-20.

(32) Uson, R.; Oro, L. A.; Cabeza, J. A.; Bryndza, H. E.; Stepro, M. P., Dinuclear Methoxy, Cyclooctadiene, and Barrelene Complexes of Rhodium(I) and Iridium(I). *Inorg. Synth*. **1985**, 126-130.

(33) Merola, J. S.; Kacmarcik, R. T., Synthesis and reaction chemistry of (η5-indenyl)(cyclooctadiene)iridium: migration of indenyl from iridium to cyclooctadiene. *Organometallics* **1989**, 8 (3), 778-784.

(34) Chotana, G. A.; Vanchura, I. I. B. A.; Tse, M. K.; Staples, R. J.; Maleczka, J. R. E.; Smith, I. I. I. M. R., Getting the sterics just right: a five-coordinate iridium trisboryl complex that reacts with C–H bonds at room temperature. *Chem. Commun.* **2009**, (38), 5731-5733.

(35) Tan, P. W.; Mak, A. M.; Sullivan, M. B.; Dixon, D. J.; Seayad, J., Thioamide-Directed Cobalt(III)-Catalyzed Selective Amidation of C(sp^3)−H Bonds. *Angew. Chem. Int. Ed.* **2017**, 56 (52), 16550-16554.

(36) Miranda, M. O.; Pietrangelo, A.; Hillmyer, M. A.; Tolman, W. B., Catalytic decarbonylation of biomass-derived carboxylic acids as efficient route to commodity monomers. *Green Chemistry* **2012**, 14 (2), 490-494.

(37) Cunico, R. F.; Bedell, L., The triisopropylsilyl group as a hydroxyl-protecting function. *J. Org. Chem.* **1980**, 45 (23), 4797-4798.

(38) Horner, L.; Mathias, J., Chemoselektive mono- und disilyletherbildung aus tertiären und sekundären silanen. *Journal of Organometallic Chemistry* **1985**, 282 (2), 155-174.

(39) Dyker, G.; Muth, O., Synthesis of Methylene- and Methine-Bridged Oligopyridines. *Eur. J. Org. Chem*. **2004**, 2004 (21), 4319-4322.

(40) Chong, E.; Kampf, J. W.; Ariafard, A.; Canty, A. J.; Sanford, M. S., Oxidatively Induced C–H Activation at High Valent Nickel. *J. Am. Chem. Soc.* **2017**, 139 (17), 6058-6061.

(41) Wojdyr, M., Fityk: a general-purpose peak fitting program. *J. Appl. Crystallogr.* **2010**, 43 (5 Part 1), 1126-1128.

(42) Murphy, J. M.; Lawrence, J. D.; Kawamura, K.; Incarvito, C.; Hartwig, J. F., "Ruthenium-Catalyzed Regiospecific Borylation of Methyl C−H Bonds." *J. Am. Chem. Soc*. **2006**, 128 (42), 13684-13685.

(43) Li, Q.; Liskey, C. W.; Hartwig, J. F., Regioselective Borylation of the C–H Bonds in Alkylamines and Alkyl Ethers. Observation and Origin of High Reactivity of Primary C–H Bonds Beta to Nitrogen and Oxygen. *J. Am. Chem. Soc.* **2014**, 136 (24), 8755-8765.

(44) Molander, G. A.; Canturk, B., Preparation of Potassium Alkoxymethyltrifluoroborates and Their Cross-Coupling with Aryl Chlorides. *Org. Lett.* **2008**, 10 (11), 2135-2138.

(45) Molander, G. A.; Yokoyama, Y., One-Pot Synthesis of Trisubstituted Conjugated Dienes via Sequential Suzuki−Miyaura Cross-Coupling with Alkenyl- and Alkyltrifluoroborates. *J. Org. Chem.* **2006**, 71 (6), 2493-2498.

CHAPTER 5

Structural and Mechanistic Features of the Iridium/2,2'-Dipyridylarylmethane Catalyst

5.1 Introduction

The study of catalyst structure and mechanism is crucial to development of increasingly active ligand platforms for transition metal-catalyzed activation and functionalization of particularly inert C-H bonds. Previous reports have demonstrated the significance of subtle ligand modifications to the function of traditional diimine/Ir C-H borylation catalysts, through either enhanced catalyst performance[1–4] or, alternatively, off-cycle or deactivation processes[5,6]. Similarly, tenuous structural manipulations of the 2,2'-dipyridylarylmethane framework have been shown to give substantially different outcomes in the C-H borylation of alkanes. The survey of 2,2'-dipyridylarylmethane derivatives for alkane C-H borylation detailed in Ch. 4 led to the discovery of the 2,2'-dipyridyl(3-fluorophenyl)methane (**L4**)/Ir catalyst—a system which offers notable

improvements over conventional diimine/Ir and Cp*Ir or Rh catalysts (**Figure 5.1**).[7,8] The catalyst generated from **L4**/Ir was proven capable of atom-economic conversion of the diboron reagent B_2pin_2 into two equivalents of organoborane product, and provides for efficient sp^3 C-H borylation of a minimal excess of alkane substrate in hydrocarbon solvent.

As preliminary ^{19}F NMR studies point to the **L4**/Ir system having complex speciation behavior that evolves during catalysis, an array of *in-situ* ligand modifications and binding modes unique to the 2,2'-dipyridylarylmethane structure warrant consideration in the development of improved catalyst systems. This chapter details the examination of structural and mechanistic features of the 2,2'-dipyridylarylmethane/Ir catalyst for the purpose of guiding design of optimized ligand structures which engender highly efficient catalysts for alkane C-H borylation. Special attention is given to ligand structures which might mitigate formation of less-active catalyst species, affording greater catalyst lifetimes and improved concentration of active catalyst. Herein we report elucidation of structural features of the proposed **L4**/Ir resting state, and the preparation of new ligand variants informed by our mechanistic work which give improved catalysts for the C-H borylation of alkane in hydrocarbon solvent.

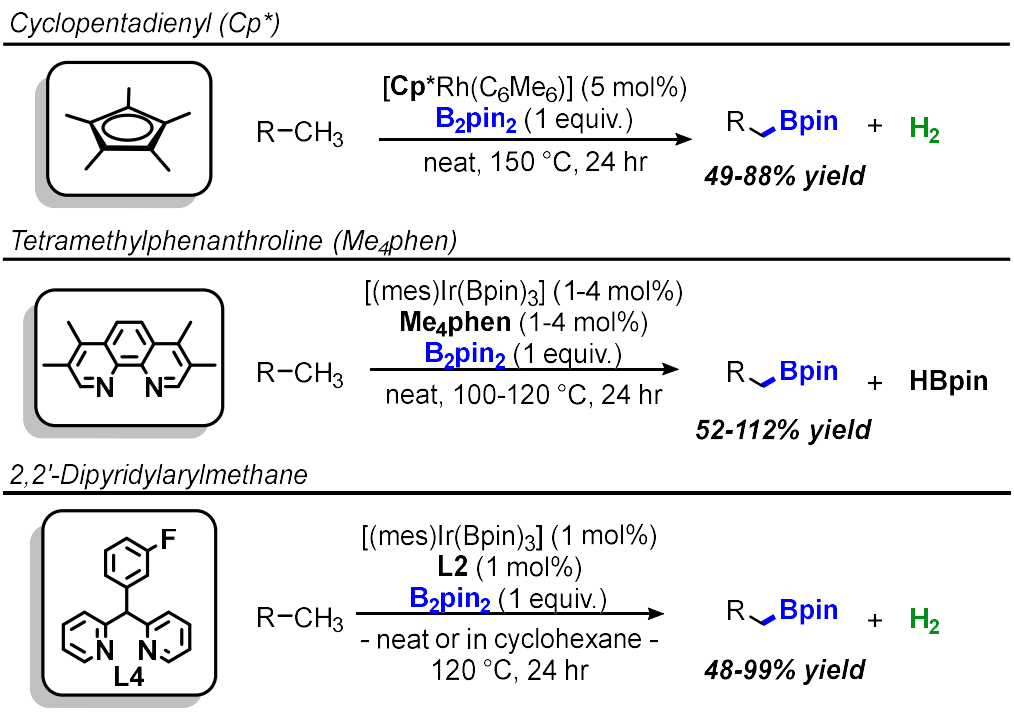

Figure 5.1: *Review of C–H borylation catalysts and ligands for the sp^3 C–H borylation*

of unactivated substrates with Cp,*[9,10] *Me_4phen,*[11,12] *and* ***L4.***[8] *Yields are reported relative to either 1 equiv. B_2pin_2 (Me_4phen) or total boron (Cp* and* ***L4****).*

5.1.1 Mechanistic Considerations Distinctive to L4/Ir-catalyzed C-H Borylation

Based upon the analogous accepted mechanism with diimine/Ir catalysts[6,12,13], a plausible mechanism for borylation with 2,2'-dipyridylarylmethane/Ir catalyst is depicted in **Figure 5.2**, including possible off-cycle or deactivation species. Initial catalyst activation involves displacement of mesitylene to give the N,N-bound **L4-**Ir complex (**A**), followed by proposed cyclometalation of the ligand aryl group (**B**) to give the active catalyst. Cyclometalation can give two distinct species, **B1** and **B2**; the relative activity of the two C-H bonds and propensity towards rollover cyclometalation is currently unknown, though it is expected that both would engender competent catalysts. Assuming resemblance to Me_4phen/Ir catalysts, rate-limiting C-H oxidative addition of substrate would give the Ir(V) complex **C**, followed by reductive elimination to generate organoborane product and **L4**/Ir(III) species **D**. Regeneration of the active catalyst **B** would occur by addition of another equivalent of B_2pin_2 **(E)** or HBpin **(F)** and extrusion of either HBpin or dihydrogen, respectively.

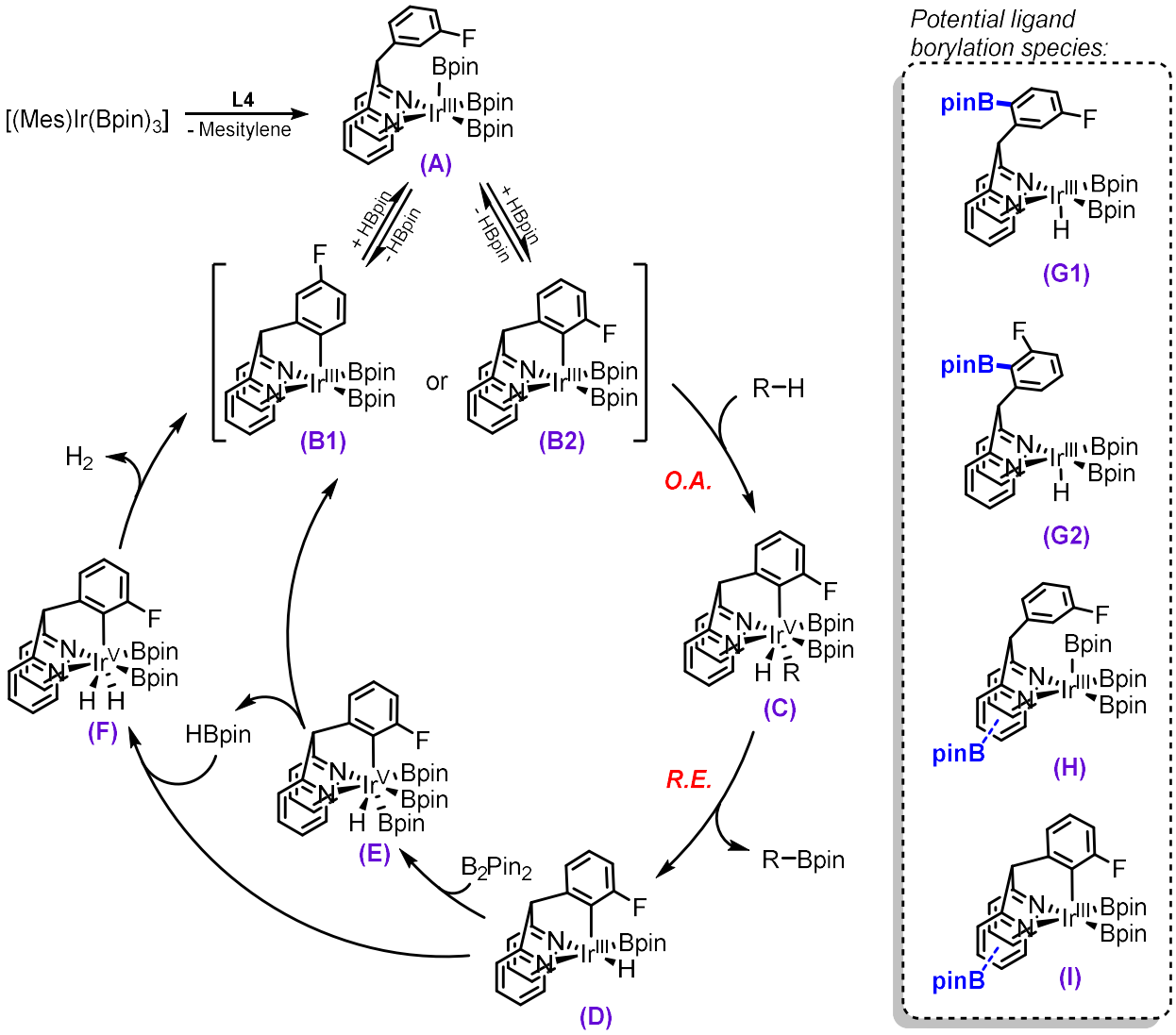

Figure 5.2: *Plausible mechanism for **L4**/Ir-catalyzed C-H borylation, and potential species involving borylation of the ligand. **C**-**F** rendered based on **B2**, the analogous **B1**-derived species of **C**-**F** are also plausible.*

Pathways which result in catalyst deactivation, off-cycle speciation, or *in-situ* modification of **L4** are also considered. Reductive elimination of the σ-aryl complex **E** would give **G1** or **G2,** similarly, products of reductive elimination from Ir(V) species **C** or **F** are also conceivable. Sp^2 borylation of either unbound ligand or complex **A** could also give rise to products of **L4** pyridine borylation (**H**). C-H borylation of pyridines has been shown to occur preferentially at the 2-position, resulting in steric inhibition of bipy and phen ligand coordination to the metal center.[3,5,6] The analogous borylation of **L4** is anticipated to similarly give decreased concentrations of active catalyst.

Catalyst activity is also anticipated to be highly dependent upon the composition of the complex with respect to boryl ligands, which can be replaced by hydrides as illustrated by comparison of **D**, **E**, and **F**; Especially at later phases of the reaction where HBpin acts as the boron source, **D** would necessarily constitute the active catalyst. Complexes **B** and **D** are presumed to have drastically different relative rates of C-H oxidative addition based on observations of varied kinetic regimes with borylating agents B_2pin_2 and HBpin.[8] Alternatively, this discrepancy could arise from inherent statistical favorability towards productive reductive elimination from the bis-boryl (**C**) relative to the monoboryl dihydride. Reductive elimination of hydride and **L4** σ-aryl is also likely, particularly at later phases in catalysis, though formation of this off-cycle species is presumably reversible and unlikely to have a large bearing on activity.

5.2 Results and Discussion

5.2.1 Ligand Structural Trends in the C-H Borylation of Neat *n*-octane

Initial insight into mechanism and coordination mode of the **L4**/Ir catalyst was garnered through survey of an expanded set of ligand derivatives in the C-H borylation of *n*-octane (**Figure 5.3**). As previously reported by our group, use of **L4** produces a catalyst which facilitates near-quantitative conversion of the diboron reagent to octyl-Bpin product and dihydrogen. Yields are calculated relative to B_2pin_2 for consistency with previous reporting methods for alkane borylation by diimine/Ir catalysts[11,12]; a percent yield in excess of 100% is representative of the uncommon case of conversion of byproduct HBpin to a second equivalent of organoborane product. Although the parent ligand **L1** gives an active catalyst for *n*-octane borylation, it significantly underperforms most aryl-functionalized derivatives. Surprisingly, substitution of methine proton with an isosteric fluorine substituent completely attenuates catalyst turnover in the case of **L2**. Modest activity is regained by 3-fluoro substitution of the aryl group in **L3**, however, unlike **L4**, boron incorporation is restricted to a single equivalent of octyl-Bpin product relative to B_2pin_2 reagent.

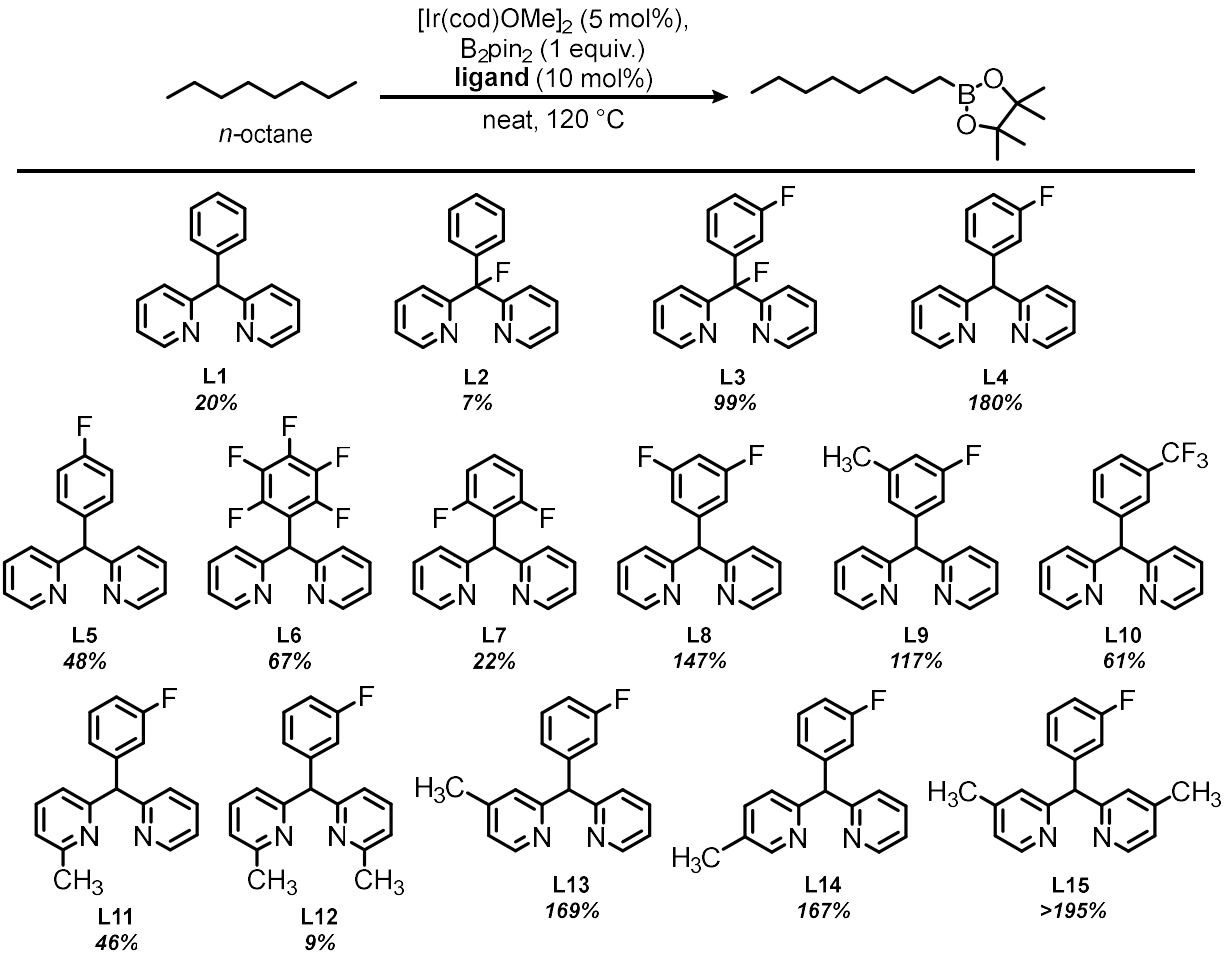

Figure 5.3: *Comparison of substituted 2,2'-dipyridylarylmethane ligands for n-octane borylation. [a]NMR yields reported relative to molar equivalents of B_2pin_2.*

An additional series of aryl-substituted derivatives (**L4**-**L10**) were prepared and explored in *n*-octane borylation, displaying several interesting features. **L6** and **L7**, which cannot undergo ortho C-H cyclometalation, show relatively poor performance when compared to **L4. L8** and **L9** structures only allow a single cyclometalation isomer ortho to fluorine (**Figure 5.2, B1**) and result in modestly reduced yield relative to **L4**. Disparate electronic characteristics, rather than catalyst structural features, may account for this decrease with **L8**. **L9** is more electronically similar to **L4**, while also sterically impeding both rollover cyclometalation and ligand aryl borylation (**Figure 5.2, G1**). Similarly, **L10** favors only a single site of C-H activation and contains a more electron-poor aryl substituent, factors which would both be anticipated to favor cyclometalation, however, **L10** underperforms relative to **L4**. These comparisons imply

a possible role for rollover cyclometalation or ligand aryl-borylation in the active catalyst and suggest that the 3-fluoro of **L4** provides optimal electron density about the aryl substituent.

Inspired by prior studies of the profound impact of substituent patterns[2,3] and *in-situ* borylation[4,5] on activity of diimine/Ir catalysts, we also prepared and screened a series of picoline derivatives of **L4** (**L11**-**L15**). 6-methyl and 6,6'-dimethyl derivatives **L11** and **L12** show substantially diminished performance relative to **L4**; This is presumably due to steric congestion about the metal center, evocative of similar observations in Ir-catalyzed arene borylation with bpy ligand derivatives.[3] Mono-methylation of pyridine at the 4- and 5- positions (**L13** and **L14**) give similar outcomes, with yields comparable to the predecessor **L4**. Bis-4-picoline derivative **L15** produced a highly effective catalyst, generating a quantitative amount of octyl-Bpin on a boron basis. Substitution at both 4-pyridyl sites is expected to enhance catalyst performance by increasing the electron-richness of the coordinating pyridines and by obstructing off-cycle ligand borylation pathways.

5.2.2 Investigation of Catalyst Speciation by ^{19}F NMR

The benchmark **L4**/Ir catalyst was initially examined by variable temperature ^{19}F NMR during the borylation of neat *n*-octane at 1 hr, a timepoint independently determined to constitute a highly active phase of catalysis with 55-65% conversion of B_2pin_2 (**Figure 5.4**). Interestingly, this revealed 3 major fluorine-containing species comprising the putative catalyst resting state, all of which appearing at a distinctively downfield chemical shift range near -69 ppm relative to the unbound ligand which resonates at -114 ppm. We hypothesized that such a dramatic change in chemical shift could only result from proximal interaction of the aryl substituent with the iridium center, supporting a role for ligand cyclometalation in the catalyst resting state. The observation of 3 similar signals, rather than a single resonance, is speculated to arise from borylation of the pyridine moieties, which would produce multiple regioisomers (**Figure 5.2, complex I**). Analysis of the signal separation is inconsistent with splitting of single resonance to a triplet indicating that each signal constitutes an individual fluorine-containing species.

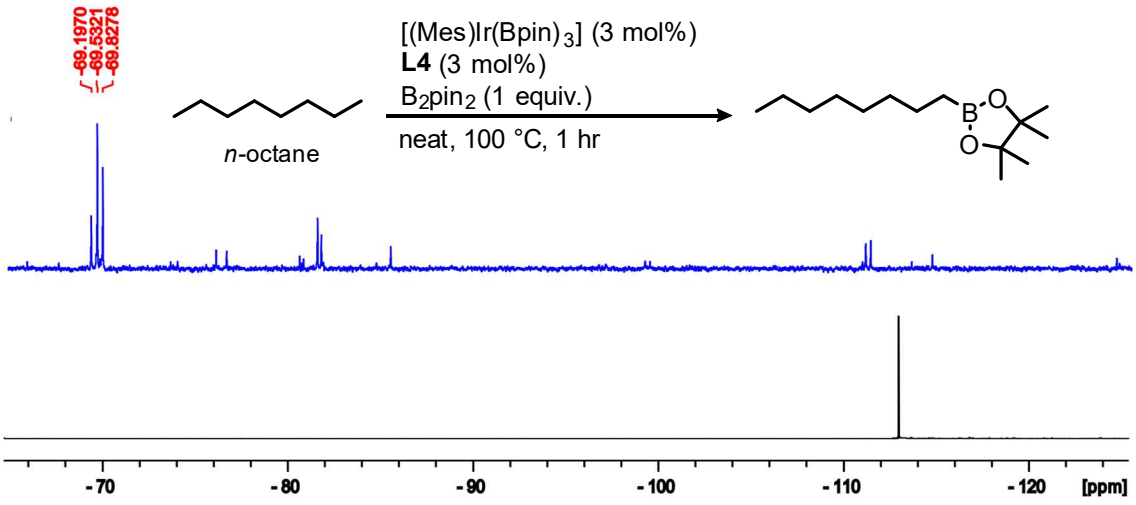

Figure 5.4: *^{19}F NMR during the borylation of n-octane at 1 hr (top) compared to free ligand **L4** (bottom). Carried out in a J. Young NMR tube fitted with C_6D_6 capillary.*

To evaluate whether *in situ* cyclometalation of **L4** might be responsible for the observed chemical shifts, 3-fluorobenzylpyridine (3-F-bnpy) Ir model complexes were prepared and assessed by ^{19}F NMR (**Figure 5.5**). Notable change in shift relative to free 3-F-bnpy (-113 ppm), and compared to previously characterized aryl-borylated derivatives of 3-F-bnpy (*o*-Bpin: -107 ppm; *p*-Bpin: -116 ppm),[14] was observed for both isomers **(1)** and **(2)**. However, deshielding of the fluorine was only observed in the complex metalated at the ortho-fluoro position **(2)**. While this chemical shift change is not as drastic as the species observed near -69 ppm during catalysis, it is expected that difference in chemical environment about the metal center significantly impacts the electronic nature of a σ-aryl group. These observations lead us to suspect the ortho-fluoro isomer of **L4** cyclometalation (complex **B2**, **Figure 5.2**) acts as the resting state, consistent with the kinetically favored product of aryl C-H activation. Unfortunately, analogous treatment of $[Cp^*IrCl_2]_2$ with **L4** does not give the corresponding κ^3-coordinated **L4** cationic iridium complex **(3)**. In this case, deprotonation of the ligand methine position rather than a second chloride abstraction generates the N,N'-bound amido complex **(4)** (**Figure 5.6**).

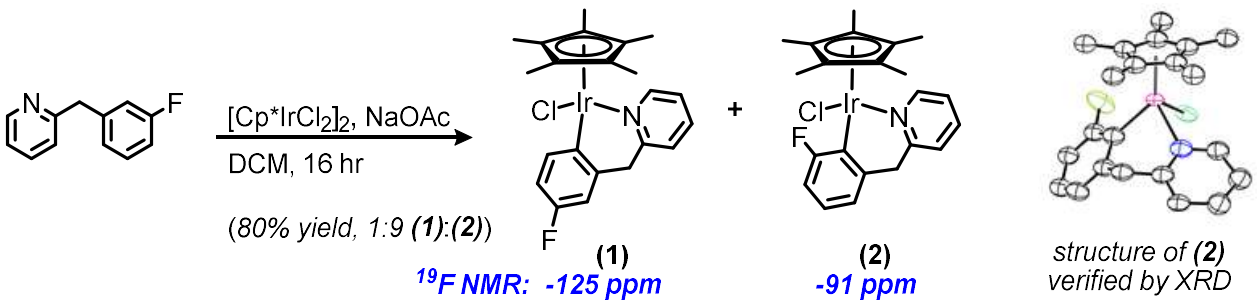

Figure 5.5: *Preparation of [Cp*Ir(3-F-bnpy)Cl], ^{19}F NMR characterization of isomers, and structural elucidation of* ***(2)*** *by x-ray diffraction*

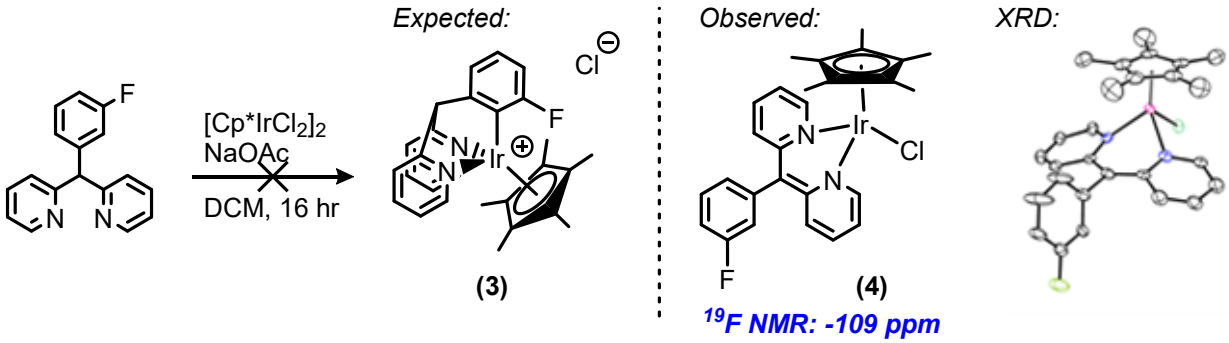

Figure 5.6: *Preparation of [Cp*Ir(**L4**)Cl], structure verified by x-ray diffraction.*

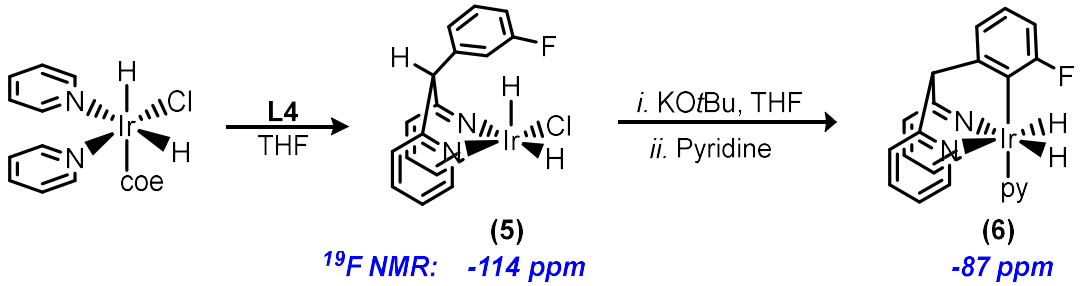

Figure 5.7: *Ir-dihydrido model complexes of **L4** coordination mode **(a)** [(**L4**)Ir(H)$_2$Cl] **(b)** [(**L4**)IrH$_2$(py)]*

Additional model complexes of ligand coordination were prepared from [(py)$_2$(coe)Ir(H)$_2$Cl] and **L4** (**Figure 5.7**). Initial displacement of the pyridines by **L4** readily gives the N,N'-bound structure **(5).** The ^{19}F NMR resonance of **(5)** at -114 ppm indicates that the chemical environment at fluorine relative to the parent unbound ligand is unperturbed by pyridine coordination to iridium. Abstraction of chloride from **(a)** encourages formation of the cyclometalated complex **(6)**, however, isolation of this

species was unsuccessful due to product instability. NMR data of the impure complex was sufficient to assign the purported structure [(**L4**)IrH_2(py)]; The downfield ^{19}F NMR resonance -87 ppm is consistent with the 3-fluorobenzylpyridine model complexes synthesized in **Figure 5.5.**

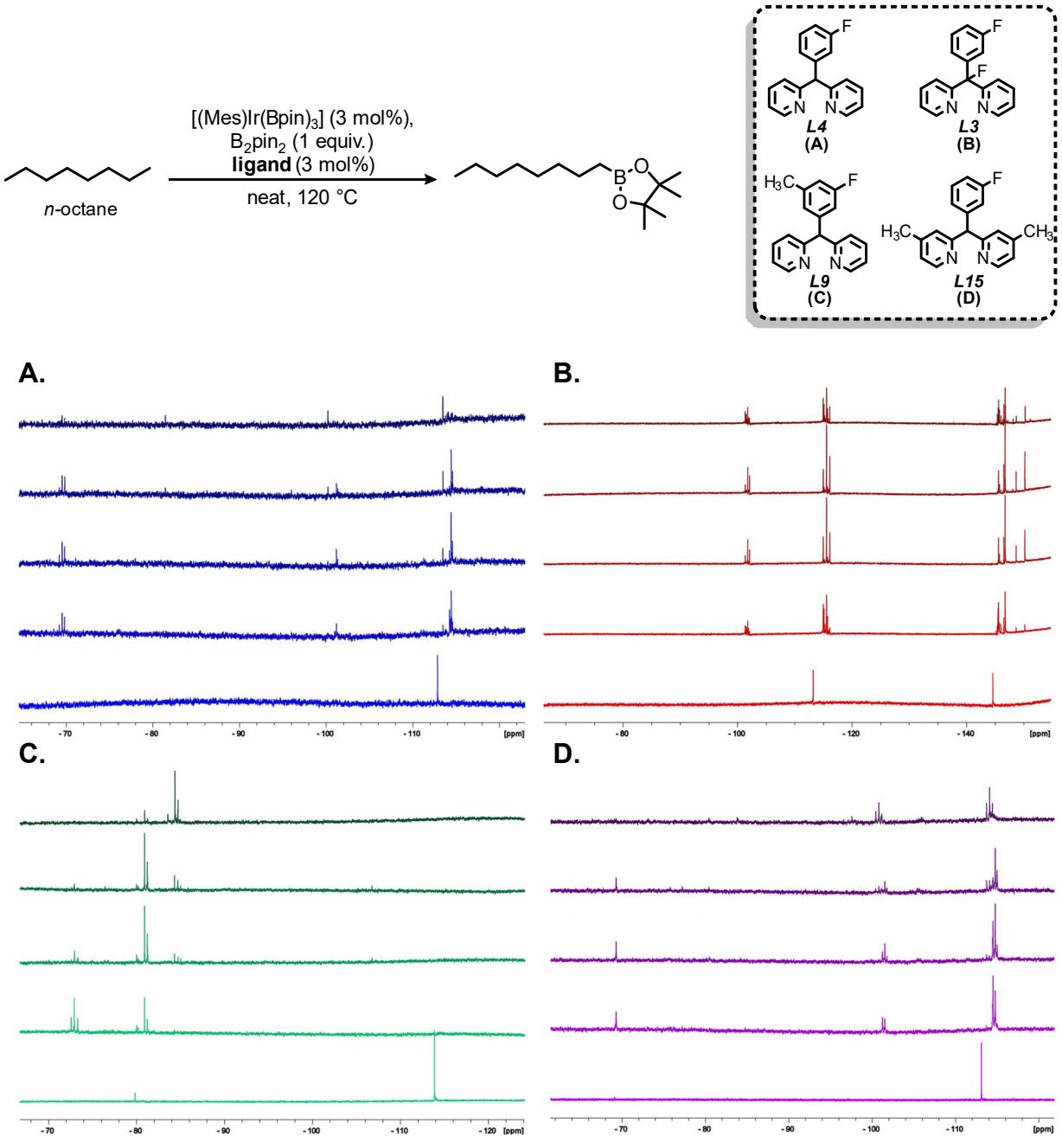

Figure 5.8: *^{19}F NMR monitoring of C-H borylation of n-octane catalyzed by ligand/[(Mes)Ir(Bpin)$_3$]; spectra collected at 0 hr, 0.5 hr, 1 hr, 3 hr, and 16 hr (bottom to top). A)* ***L4*** *B)* ***L3*** *C)* ***L9*** *D)* ***L15***

L3, **L9**, and **L15** were selected as a structurally representative subset of derivatives to further probe the impact of ligand structure on catalyst speciation. Each ligand was employed alongside [(Mes)Ir(Bpin)$_3$] pre-catalyst in the borylation of neat *n*-octane and the reaction monitored by ^{19}F NMR (**Figure 5.8**). In a previous report we demonstrated that when **L4**/Ir is used, complete conversion of B_2pin_2 occurs quickly within the first 3-5 hr of the reaction, followed by a period of much slower consumption of HBpin.[8] Accordingly, time points were chosen which represent each distinct active phase of the catalytic reaction.

By comparison of **Figure 5.8** time course **B** (**L3**) and **A** (**L4**), it is speculated that introduction of fluorine to the methine position attenuates catalyst activity via inhibition of cyclometalation. While ^{19}F NMR resonances in the appropriate downfield range indicate a σ-(2-fluoro)aryl are not present, the **L3**/Ir catalyst still produces a considerable 99% yield in the neat borylation of *n*-octane. Similarly, **L6** and **L7**, which are both directly inhibited from ortho-aryl C-H activation, still generate acceptable yields of organoborane product. Further evidence supporting the importance of methine substitution was observed during unsuccessful attempts to generate **L3**-cyclometalated analogs of the model compounds **(3)** and **(6)**. In both cases, **L3** gives exclusively the N,N'-bound product even under extended periods of heating. **(7)**, the **L2** analog of complex **(5)** proved similarly stable to cyclometalation and decomposition, allowing for growth of single crystals and structural analysis by x-ray diffraction (**Figure 5.9**).

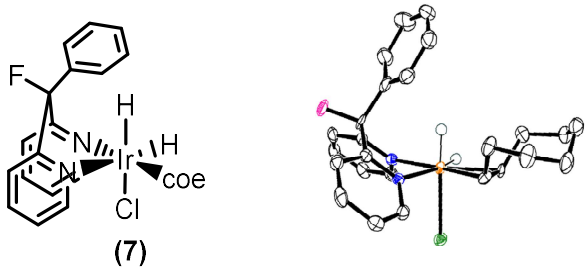

(7)

Figure 5.9: *Structure of [(**L2**)Ir(H)$_2$Cl(coe)]* ***(7)*** *verified by x-ray diffraction*

To examine the importance of the methine proton, we explored the role of added base in the borylation reaction (**Figure 5.10**). A previous literature report illustrated improved yields in alkane borylation, particularly of sterically hindered substrates, by Me$_4$phen/Ir catalysts through the addition of catalytic KO*t*Bu[15], however, addition of

KO*t*Bu to the **L4**/Ir-catalyzed borylation of *n*-octane severely inhibits catalyst performance. To account for issues of catalyst activation the pre-formed complex [(cod)Ir(**L4***)] **(8)** was also explored as catalyst, remarkably giving a yield of 98%, similar to that of **L3**. These experiments suggest the following: 1) The N,N-bound complex (**Figure 5.2, species A**) may be active in early stages of catalysis where B_2pin_2 incorporation occurs and 2) The presence of methine proton may modulate the ease of the cyclometalation process, and therefore be involved in generating more active catalyst species.

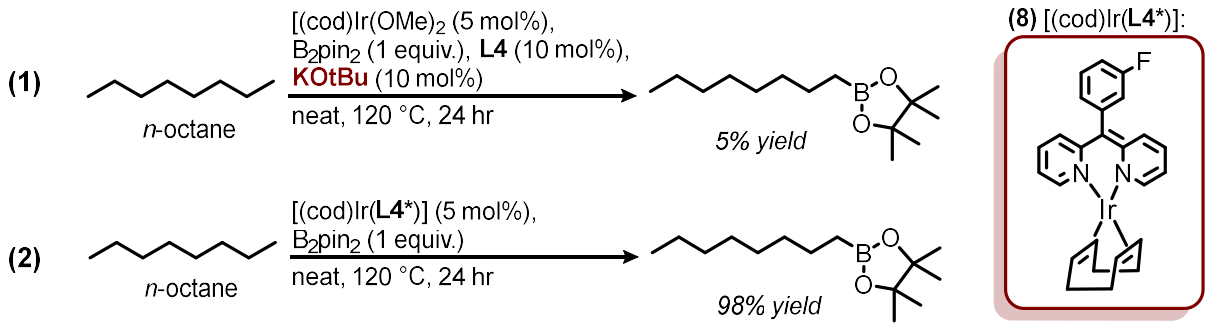

Figure 5.10: *Neat borylation of n-octane catalyzed by (1)* ***L4****/Ir with added KOtBu (10 mol%) or (2) [(cod)Ir(****L4*****)]* ***(8)***

5-methyl derivative **L9,** which contains only one accessible site for aryl C-H activation, was used for study of ligand aryl-group borylation and the impact of rollover cyclometalation on catalyst activity. ^{19}F NMR timecourse (**Figure 5.8C**) is consistent with the model system shown in **Figure 5.5** wherein only the *o*-fluoro σ-aryl produces a significant downfield shift in fluorine resonance. While species in the upfield range, likely corresponding to either N,N'-bound species, unbound ligand, or *p*-fluoro cyclometalation, are completely eliminated, a number of species persist. It is suspected that these signals represent various possible pyridine-borylated or bis-boryl, hydrido-boryl, and bis-hydride species, as described in **Figure 5.2**. Unfortunately, despite producing greater concentrations of the proposed active catalyst, **L9** gives diminished performance relative to **L4** in the borylation of neat *n*-octane with a yield of 117%. It has been proposed based on computational treatments that a rollover borylation-cyclometalation sequence may produce the most active species.[16] Our findings support a role for both sites of ligand aryl C-H activation in the active catalyst, though details of

this mechanism remain unclear experimentally. However, when 3 mol% [(Mes)Ir(Bpin)$_3$] is used as pre-catalyst, a near-quantitative 180% yield of octyl-Bpin is observed, indicating the importance of Ir pre-catalyst and possible differences in catalyst activation with the ligands **L4** and **L9**.

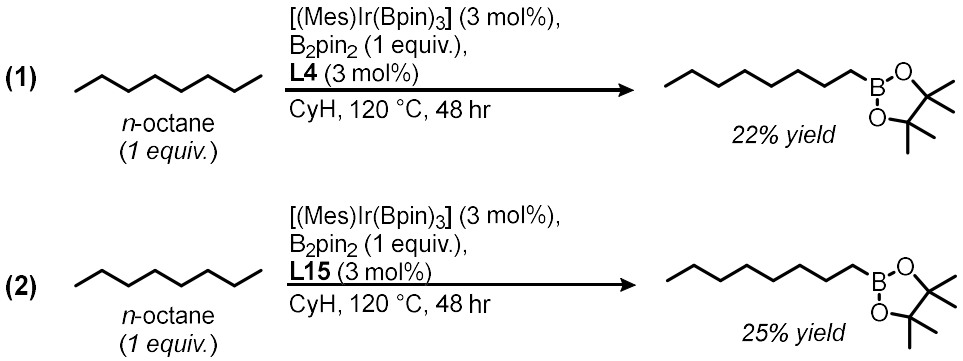

Figure 5.11: *Borylation of 1 equiv. n-octane in cyclohexane solvent catalyzed by (1)* ***L4****/[(Mes)Ir(Bpin)$_3$] (3 mol%) and (2)* ***L15****/[(Mes)Ir(Bpin)$_3$] (3 mol%)*

L15, which performs excellently in the borylation of neat *n*-octane, exhibits only a single downfield species at -69 ppm by ^{19}F NMR throughout the reaction (**Figure 5.8D**). This result is consistent with our speculation that multiple downfield resonances found with **L4** arise from borylation of the ligand pyridine moieties, and that 4,4'-methylation is an effective strategy to hinder this process. Just as in the case of **L4** (**Figure 5.8A**), when **L15** is used resonances appear in the -105 ppm range with increasing intensity at later time points in the catalytic reaction. Based on the effect of aryl-borylation on fluorine chemical shift noted with model 3-fluorobenzylpyridine compounds (**Figure 5.5**), it is speculated that these species result from reductive elimination of the *o*-fluoro σ-aryl to give complexes such as **G2** (**Figure 5.2**). While the postulated pathway would reduce concentration of the active catalyst, it is expected not to result in catalyst deactivation due to the reversible nature of arene borylation.[17]

To further explore the relative activity of the **L4**/Ir and L**15**/Ir catalysts, both were employed in the borylation of a single equivalent of *n*-octane in cyclohexane solvent (**Figure 5.11**). **L15**/Ir displayed comparable performance relative to **L4**/Ir, indicating *in situ* ligand borylation is unlikely to represent a catalyst deactivation pathway. Further study of the direct impact of ligand borylation of **L4** on catalyst activity is required,

however, this data supports the possibility of both parent and the borylated ligand generating productive catalysts. Interestingly, this feature would be unique to 2,2'-dipyridylarylmethane/Ir catalysts, as *in situ* ligand borylation has been shown to be detrimental to bpy/Ir and phen/Ir systems.[3,6] Further study of the direct impact of ligand borylation of **L4** on catalyst activity is required, however. Efforts to synthesize and characterize cyclometalated and ligand-borylated complexes representing ^{19}F NMR resonances observed in catalysis are ongoing.

5.2.3 Preparation and Study of Putative Resting State Species

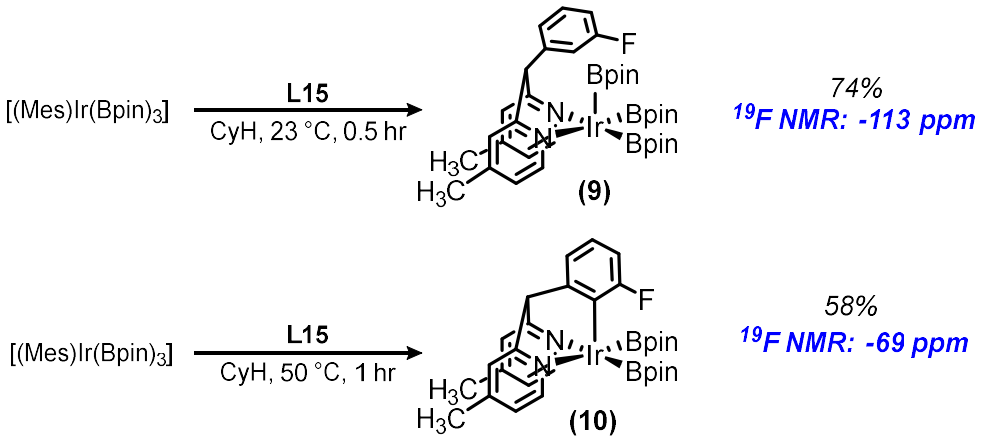

Figure 5.12: *Preparation of [(**L15**)Ir(Bpin)$_3$] **(9)** and cyclometalated ligand complex [(**L15**)Ir(Bpin)$_2$] **(10)** and characterization by NMR*

Initial efforts at preparing catalyst resting state species were aimed at mimicking methods used by Hartwig and coworkers in the syntheses of [(dtbpy)Ir(Bpin)$_3$(coe)][18] and [(Me$_4$phen)Ir(Bpin)$_3$(CO)][6], however, introduction of spectator ligands to solutions containing **L4**/Ir and **L15**/Ir derived compounds led to loss of catalytically-relevant ^{19}F signals and decomposition of the desired compounds. Treatment of [(Mes)Ir(Bpin)$_3$] with **L15** at ambient temperature readily gives the putative complex [(**L15**)Ir(Bpin)$_3$] **(9)**, which undergoes cyclometalation on standing in solution and is unstable with respect to further decomposition. Mild heating was found to give conversion to an isolable complex assigned as [(**L15**)Ir(Bpin)$_2$] **(10)**, identical to the downfield ^{19}F NMR resonance noted in the catalytic reaction (**Figure 5.12**). Analysis of the product **(10)** by ^{1}H NMR reveals two upfield resonances integrating to 12H relative to **L15**, signifying the two Ir-Bpin

moieties, and the disappearance of the *o*-fluoro proton at the site of cyclometalation. Borylation of a single equivalent of *n*-octane was carried out using the pre-generated species [(**L15**)Ir(Bpin)$_2$] (**Figure 5.13**). Enhanced performance relative to **L15**/[(Mes)Ir(Bpin)$_3$], giving a yield of 32%, demonstrates this species as an effective catalyst, and indicates the -69 ppm signal observed in ^{19}F NMR studies is catalytically relevant.

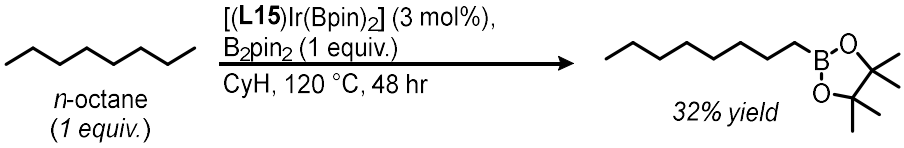

Figure 5.13: *Borylation of 1 equiv. n-octane catalyzed by [(**L15**)Ir(Bpin)$_2$] **(10)** (3 mol%)*

Preliminary investigation of ligand borylation was conducted by treatment of the complex assigned as [(**L4**)Ir(Bpin)$_2$] **(11)** with 1 equivalent of B_2pin_2 under moderate heating (**Figure 5.14**). This gave rise to 5 signals between -68 and -70 ppm in the ^{19}F NMR, analogous to the 3 close range resonances observed in the catalytic reaction. When the same experiment was conducted with **L15**, this phenomenon of multiple close range ^{19}F NMR signals was not observed. Analysis of the product mixture by ^{1}H NMR shows a complex mixture of inseparable isomers, speculated to constitute the illustrated ligand-borylated complexes **(12)**. Unfortunately, drastic signal broadening by ^{11}B NMR prevented further insight into speciation relative to boron atoms. Incomplete characterization of products of ligand borylation warrant further preparation and investigation of these species—studies aimed at structural analysis by either 2D NMR or x-ray crystallography are currently underway.

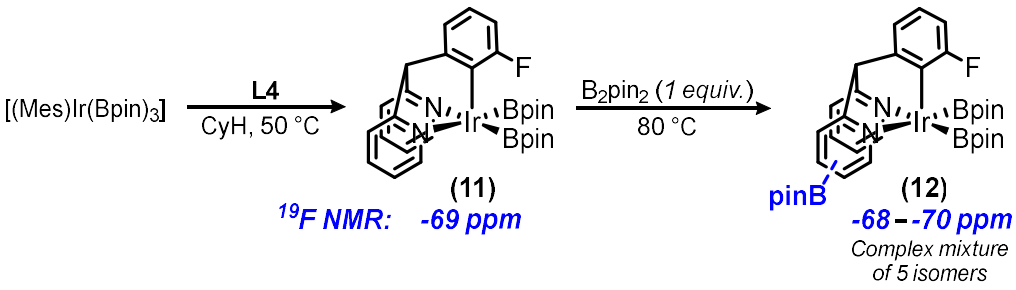

Figure 5.14: *Preparation of [(**L4**)Ir(Bpin)$_2$] **(11)** and treatment with B_2pin_2 to give 5 isomers of the putative ligand borylated complex **(12)**.*

5.3 Conclusions

In our initial report of 2,2'-dipyridylarylmethane ligands, we envisioned *in situ* cyclometalation might provide a facial κ^3 coordination mode, akin to seminal Cp*Ir and Rh catalysts for alkane C-H borylation. Following extensive examination of possible coordination modes, various strategically constructed ligand derivatives, and investigation of catalyst speciation and features, elucidation of the cyclometalation species [(**L**)Ir(Bpin)$_2$] as an active catalytic species has been achieved. While our mechanistic investigation remains ongoing, our current understanding was sufficient to guide the design of the **L15**/Ir catalyst, which is competent in the challenging borylation of a single equivalent of alkane substrate and gives a less complex catalyst speciation by ^{19}F NMR. Continued efforts will be directed towards the isolation, characterization, and study of additional catalyst species found by ^{19}F NMR, for the purpose of optimizing the concentration of active catalyst and mitigating catalyst degradation. Ultimately, these studies of mechanism will continue to inform the development of increasingly active 2,2'-dipyridylarylmethane/Ir platforms for efficient C-H borylation of alkanes.

Portions of this chapter have been adapted with permission from Jones, M.R., Schley, N.D.; Ligand-Driven Advances in Iridium-Catalyzed sp3 C–H Borylation: 2,2'-Dipyridylarylmethan. Synlett 2021; 32(09): 845-850. DOI: 10.1055/a-1344-1904 Georg Thieme Verlag KG Copyright 2021

This material is based upon work supported by the National Science Foundation under grant no. CHE-1847813.

5.4 Experimental

General Considerations. Syntheses and manipulations with organometallic reagents were carried out using standard vacuum, Schlenk, cannula, or glovebox techniques under N_2 in oven- or flame-dried glassware unless otherwise specified. Tetrahydrofuran, dichloromethane, toluene, pentane, and diethyl ether were degassed with argon and dried over activated alumina using a solvent purification system.

Spectroscopy. ^{1}H, ^{13}C{^{1}H}, ^{11}B, and ^{19}F NMR spectra were recorded on Bruker NMR spectrometers at ambient temperatures unless otherwise noted. ^{1}H and ^{13}C{^{1}H}

chemical shifts are referenced to residual solvent signals, ^{19}F chemical shifts are referenced to an external C_6F_6 standard. $^{13}C\{^1H\}$ resonances for boron-attached carbon atoms are not observed and are not included in the listings of spectral data.

Synthesis and Characterization of Products

Organometallic starting materials. Bis(1,5-cyclooctadiene)diiridium(I) dichloride $[(cod)IrCl]_2$,[19] Di-μ-chlorotetrakis(cyclooctene)diiridium(I) $[(coe)_2IrCl]_2$,[19] Bis(1,5-cyclooctadiene) diiridium(I) dimethoxide $[(cod)IrOMe]_2$,[19] Di-μ-dichlorobis (η^5-pentamethylcyclopentadienyl) diiridium(III) $[Cp^*IrCl_2]_2$,[20] $[(coe)Ir(H)_2Cl(py)_2]$,[21] (η^5-indenyl)(1,5-cyclooctadiene)iridium [(Ind)Ir(cod)],[22] and (η^6-mesitylene)(tris-pinacolboryl) iridium $[(Mes)Ir(Bpin)_3]$,[23] were prepared according to published procedures. $IrCl_3 \cdot 3H_2O$, pinacolborane and bispinacolatodiboron were purchased from chemical vendors and used as received.

***Ligand syntheses*.** Syntheses and characterization of **L1**-**L15** are described in chapter 2 of this document.

[Cp*Ir(κ^2-(3-fluorobenzylpyridine))Cl] (1) & (2) These compounds were synthesized according to a reported literature procedure[24] with the following modifications: In an inert-atmosphere glove box, a 20 mL vial was charged with $[Cp^*IrCl_2]_2$ (0.025 g, 0.031 mmol) and sodium acetate (0.015 g, 0.19 mmol). To the vial was added dichloromethane (10 mL) and 2-(3-fluorobenzyl)pyridine (0.014 g, 0.075 mmol). The resulting solution was stirred at ambient temperature for 24 hr, followed by removal of salts by filtration. The supernatant was concentrated in vacuo to a solid, and the solid extracted with hexane to remove excess unbound benzylpyridine. The solid was recrystallized by diffusion of pentane into dichloromethane, giving a 1:9 mixture isomers **(1)** and **(2)** as a yellow crystalline solid. 33 mg, 80% combined yield. Fractional crystallization repeated under the conditions above resulted in purification of the major isomer **(2)**

(1) ^1H NMR ($CDCl_3$, 400 MHz): δ 8.65 (d, *J* = 5.8 Hz, 1H), 7.49 (td, *J* = 1.6 Hz, 7.7 Hz, 1H), 7.20-7.35 (m, 2H), 7.00 (m, 1H), 6.87-6.75 (m, 2H), 3.84 (d, *J* = 14.6 Hz, 1H), 3.75 (d, *J* = 14.6 Hz, 1H), 1.56 (s, 15H). $^{19}F\{^1H\}$ NMR ($CDCl_3$, 376 MHz): δ -124.7

(2) ^{1}H NMR ($CDCl_3$, 400 MHz): δ 9.03 (d, *J* = 5.8 Hz, 1H), 7.59 (td, *J* = 1.6 Hz, 7.7 Hz, 1H), 7.34 (d, *J* = 7.7 Hz, 1H), 7.08 (t, *J* = 6.5 Hz, 1H), 6.92 (d, *J* = 6.7 Hz, 1H), 6.84-6.76 (m, 2H), 3.95 (d, *J* = 14.4 Hz, 1H), 3.85 (d, *J* = 14.4 Hz, 1H), 1.63 (s, 15H). ^{19}F{^{1}H} NMR ($CDCl_3$, 376 MHz): δ -91.6

[Cp*(L4)IrCl] (4) In an inert-atmosphere glove box, a 20 mL vial was charged with $[Cp^*IrCl_2]_2$ (0.010 g, 0.013 mmol) and sodium acetate (0.013 g, 0.16 mmol). To the vial was added dichloromethane (5 mL) and **L4** (0.007 g, 0.025 mmol). The resulting red solution was stirred at ambient temperature for 24 hr, followed by removal of salts by filtration. The supernatant was concentrated in vacuo to dryness, and the solid triturated 3x with diethyl ether. The solid was recrystallized by diffusion of pentane into toluene to give **(4)** as a red crystalline solid. 15 mg, 96% yield.

^{1}H NMR (C_6D_6, 400 MHz): δ 8.94 (d, *J* = 5.6 Hz, 1H), 8.65 (t, *J* = 6.5 Hz, 1H), 8.02 (t, *J* = 6.8 Hz, 1H), 7.83 (t, *J* = 7.5 Hz, 1H), 7.67 (dd, *J* = 7.8, 13.8 Hz, 1H), 7.35 – 7.48 (m, 4H), 7.26 (t, *J* = 8.9 Hz, 1H), 7.18 (m, 1H), 6.88 (t, *J* = 8.4 Hz, 1H), 1.41 (s, 15H).

^{19}F{^{1}H} NMR (C_6D_6, 376 MHz): δ -109.2

[(L4)Ir(H)$_2$(Cl)(coe)] (5) In an inert-atmosphere glove box, a 20 mL vial was charged with $[(coe)Ir(H)_2Cl(py)_2]$ (0.019 g, 0.038 mmol) and **L4** (0.010 g, 0.038 mmol). THF (1 mL) was added to the vial and the solution stirred at ambient temperature for 15 minutes, resulting in the formation of a precipitate. Diethyl ether (3 mL) was layered into the vial to encourage further precipitation, and the solid collected by filtration. The precipitate was then extracted with an additional portion of diethyl ether to give the product as a white crystalline solid with poor solubility in organic solvents. 0.018 g, 79% yield.

^{1}H NMR (CD_3CN, 400 MHz): δ 9.52 (d, *J* = 6.3 Hz, 1H), 9.24 (d, *J* = 5.4 Hz, 1H), 8.05 (td, 7.5, 1.8 *J* = Hz, 1H), 8.00 (td, *J* = 7.5, 1.8 Hz, 1H), 7.84 (d, *J* = 7.9 Hz, 1H), 7.81 (d, *J* = 7.9 Hz, 1H), 7.53 (ddd, *J* = 7.3, 5.7, 1.3 Hz, 1H), 7.33 (ddd, *J* = 7.3, 5.7, 1.3 Hz, 1H), 7.22 – 7.30 (m, 2H), 6.99 (td, *J* = 8.6, 2.6 Hz, 1H), 6.57 (d, *J* = Hz, 1H), 6.02 (s, 1H), 3.86 (ddd, *J* = 12.1, 8.8, 3.7 Hz, 1H), 3.07 (ddd, *J* = 12.1, 8.8, 3.7 Hz, 1H), 2.22 (m, 1H), 1.18 – 1.65 (m, 11H), -20.5 (d, *J* = 6.9 Hz, 1H), -26.0 (d, *J* = 6.9 Hz, 1H).

^{19}F{^{1}H} NMR (CD_3CN, 376 MHz): δ -115.2

[(L4)Ir(H)$_2$] (6) In an inert-atmosphere glove box, a 20 mL vial was charged with **(5)** (0.010 g, 0.020 mmol) and THF (1 mL). KO*t*Bu (0.003 g, 0.026 mmol) was added to the suspension, inducing immediate color change to a deep red homogenous solution. The solution was stirred at ambient temperature for 3 hr. The solution was filtered to remove salts, and the concentrated *in vacuo*. The solid was extracted with cold pentanes to give the product as a red, highly-soluble, solid. The resulting impure product was characterized by NMR in the crude form to avoid further decomposition by the addition of spectator ligands or reaction with solvent, therefore product yield was not obtained.

^{1}H NMR (C_6D_6, 400 MHz): δ 8.79 (d, *J* = 5.5 Hz, 2H), 6.88 (d, *J* = 8.0 Hz, 2H), 6.79 (td, *J* = 7.6, 1.2 Hz, 2H), 6.56 (t, *J* = 7.8 Hz, 2H), 6.11 (t, *J* = 6.7 Hz, 1H), 6.00 (d, *J* = 9.3 Hz, 1H), 5.82 (t, *J* = 6.1 Hz, 1H), 5.31 (s, 1H), -19.7 (d, *J* = 11.5 Hz, 2H).

^{19}F{^{1}H} NMR (C_6D_6, 376 MHz): δ -87.0

[(L2)Ir(H)$_2$(Cl)(coe)] (7) In an inert-atmosphere glove box, a 20 mL vial was charged with [(coe)Ir(H)$_2$Cl(py)$_2$] (0.019 g, 0.038 mmol) and **L2** (0.010 g, 0.038 mmol). THF (1 mL) was added to the vial and the solution stirred at ambient temperature for 15 minutes, resulting in the formation of a precipitate. Diethyl ether (3 mL) was layered into the vial to encourage further precipitation, and the solid collected by filtration. The precipitate was then extracted with an additional portion of diethyl ether to give the product as a white solid. The product was taken up in a minimal volume of toluene and 0.10 mL coe was added to the solution, then recrystallized by vapor diffusion of pentane. 0.015 g, 66% yield.

^{1}H NMR (CD_3CN, 400 MHz): δ 9.53 (d, *J* = 5.9 Hz, 1H), 9.21 (d, *J* = 5.9 Hz, 1H), 8.18 (d, *J* = 8.0 Hz, 1H), 8.14 (m, 2H), 8.10 (td, 7.9, 1.6 *J* = Hz, 1H), 7.58 (td, *J* = 5.5, 3.2 Hz, 1H), 7.36 – 7.44 (m, 2H), 7.31 (t *J* = 8.0 Hz, 2H). 6.90 – 6.94 (m, 2H), 3.79 (ddd, *J* = 12.1, 8.8, 3.7 Hz, 1H), 3.03 (ddd, *J* = 12.1, 8.8, 3.7 Hz, 1H), 2.19 (m, 1H), 1.14 – 1.60 (m, 11H), -21.0 (d, *J* = 6.7 Hz, 1H), -25.6 (d, *J* = 6.7 Hz, 1H).

^{19}F{^{1}H} NMR (CD_3CN, 376 MHz): δ -123.7

[(cod)Ir(L4*)] (8) In an inert-atmosphere glove box, a 20 mL vial was charged with **L4** (0.010 g, 0.038 mmol) and KO*t*Bu (0.005 g, 0.044 mmol). THF (1 mL) was added to the

vial, giving an immediate color change to red, and the solution stirred at ambient temperature for 15 minutes. The volume of the solution was reduced and 2 mL cold diethyl ether was added to precipitate the K(**L4**) salt. The precipitate was collected by filtration and charged to a separate 20 mL vial containing $[(cod)IrCl]_2$ (0.013 g, 0.020 mmol (dimer basis)). THF (1 mL) was added, giving a deep purple solution which was allowed to stir at ambient temperature for 16 hr. The solution was then filtered to remove KCl and concentrated *in vacuo* to a dark purple solid. 0.016 g, 76% yield.

^{1}H NMR (C_6D_6, 400 MHz): δ 7.65 (dd, *J* = 1.6 Hz, 6.5 Hz, 2H), 6.91 (dd, *J* = 6.3 Hz, 7.7 Hz, 1H), 6.79 (m, 2H), 6.68 (td, *J* = 2.7 Hz, 8.6 Hz, 1H), 6.35 (ddd, *J* = 1.6 Hz, 6.6 Hz, 9.2 Hz, 2H), 6.16 (dd, *J* = 1.1 Hz, 9.0 Hz, 2H), 5.63 (td, *J* = 1.4 Hz, 6.4 Hz, 2H), 3.56 (d, *J* = 3.0 Hz, 4H), 2.01 (m, 4H), 1.29 (m, 4H).

^{19}F{^{1}H} NMR (C_6D_6, 376 MHz): δ -112.1

[(L15)Ir(Bpin)$_3$] (9) In an inert-atmosphere glove box, a 20 mL vial was charged with [(Mes)Ir(Bpin)$_3$] (0.010 g, 0.014 mmol), **L15** (0.005 g, 0.017 mmol), and cyclohexane (1 mL). The solution was stirred slowly at ambient temperature for 0.5 hr, then placed immediately the freezer. The solution was then lyophilized to an off-white solid, which was noted to decompose readily within 2-3 hr in solution of cyclohexane or THF at ambient temperature under an inert atmosphere. The cyclometalated complex **(10)** was present by ^{19}F NMR in a ratio of 1:7 relative to **(9)**, and the calculated yield adjusted to account for presence of this compound. 0.005 g, 74% yield.

^{1}H NMR (d_8-THF, 400 MHz): δ 9.19 (d, *J* = 5.8 Hz, 2H), 7.50 (s, 2H), 6.99 (d, *J* = 7.1 Hz, 1H), 6.71 (d, *J* = 5.2 Hz, 2H), 6.62 (td, *J* = 7.7, 5.2 Hz, 1H), 6.38 (dd, *J* = 7.2, 6.8 Hz, 2H), 5.63 (s, 1H), 2.33 (s, 6H), 1.36 (s, 6H), 1.20 (s, 12H), 1.01 (s, 6H), 0.99 (s, 12H).

^{19}F{^{1}H} NMR (C_6D_6, 376 MHz): δ -113.0

[(L15)Ir(Bpin)$_2$] (10) In an inert-atmosphere glove box, a 20 mL vial was charged with [(Mes)Ir(Bpin)$_3$] (0.010 g, 0.014 mmol), **L15** (0.005 g, 0.017 mmol), and cyclohexane (1 mL). The vial was sealed with a PTFE-lined cap, removed from the glove box and was heated in a 50 °C oil bath for 1 hour to give a bright yellow solution. The solution was then flash-frozen, returned to the glove box, and lyophilized. The resulting yellow

powder was extracted with 3 x 3 mL portions of pentane, the extracts combined, and the total volume reduced *in vacuo* to ~2 mL. The resulting pentane solution was cooled to -35 °C, to precipitate the product as a yellow semi-crystalline solid. 0.004 g, 58% yield.

^{1}H NMR (d_8-THF, 400 MHz): δ 9.18 (d, *J* = 5.8 Hz, 2H), 7.43 (s, 2H), 7.26 (dd, *J* = 7.9, 6.4 Hz, 1H), 7.05 (s, 1H), 6.72 (d, *J* = 5.2 Hz, 2H), 6.36 (dd, *J* = 7.8, 6.3 Hz, 1H), 2.20 (s, 6H), 1.36 (s, 12H), 1.21 (s, 12H).

^{19}F{^{1}H} NMR (C_6D_6, 376 MHz): δ -69.2

[(L4)Ir(Bpin)$_2$] (11) In an inert-atmosphere glove box, a 20 mL vial was charged with [(Mes)Ir(Bpin)$_3$] (0.010 g, 0.014 mmol), **L4** (0.004 g, 0.016 mmol), and cyclohexane (1 mL). The vial was sealed with a PTFE-lined cap, removed from the glove box and was heated in a 50 °C oil bath for 1 hour to give a bright yellow solution. The solution was then flash-frozen, returned to the glove box, and lyophilized. The resulting yellow powder was extracted with 3 x 3 mL portions of pentane, the extracts combined, and the total volume reduced *in vacuo* to ~2 mL. The resulting pentane solution was cooled to -35 °C, to precipitate the product as a yellow semi-crystalline solid. 0.006 g, 63% yield.

^{1}H NMR (d_8-THF, 400 MHz): δ 9.49 (d, *J* = 5.4 Hz, 2H), 7.73 – 7.80 (m, 4H), 7.40 (dd, *J* = 8.0, 6.5 Hz, 1H), 7.32 (d, *J* = 1.1 Hz, 1H), 7.00 (td, *J* = 5.7, 2.9 Hz, 2H), 6.50 (dd, *J* = 7.9, 6.3 Hz, 1H), 1.48 (s, 12H), 1.35 (s, 12H).

^{19}F{^{1}H} NMR (C_6D_6, 376 MHz): δ -69.0

[(pinB-L4)Ir(Bpin)$_2$] (12) In an inert-atmosphere glove box, a 20 mL vial was charged with [(Mes)Ir(Bpin)$_3$] (0.010 g, 0.014 mmol), **L4** (0.004 g, 0.016 mmol), B_2pin_2 (0.004 g, 0.014 mmol) and cyclohexane (1 mL). The vial was sealed with a PTFE-lined cap, removed from the glove box and was heated in a 50 °C oil bath for 1 hour to give an orange solution. The solution was then flash-frozen, returned to the glove box, and lyophilized. The resulting orange powder was extracted with 3 x 3 mL portions of pentane, the extracts combined, and the total volume reduced *in vacuo* to ~2 mL. The resulting pentane solution was cooled to -35 °C, to precipitate the product as an orange

powder. 0.006 g, 51% yield.

*Combined yield of 5 isomers by ^{1}H and ^{19}F NMR; product ratio by order of ^{19}F resonances 2.6:2.2:3:1.3:1). ^{1}H NMR gives multiple sets of overlapping aryl and Bpin signals with similar chemical shifts to **(11)**; individual isomers are indistinguishable*.

$^{19}F\{^{1}H\}$ NMR (C_6D_6, 376 MHz): δ -69.3, -69.5, -69.7, -69.8, -70.0

General procedures

Procedure for ligand comparisons (Figure 5.3). In an inert-atmosphere glove box, a 4 mL vial was charged with $[Ir(COD)OMe]_2$ (0.0030 g, 0.010 mmol (Ir basis), 10 mol % Ir) and B_2pin_2 (0.026 g, 0.10 mmol). *n*-octane (1.0 mL, 200 mM) was added and the solution stirred for 3 min. The resulting solution was transferred to a separate 4 mL vial charged with ligand (0.010 mmol, 10 mol %). The vial was sealed with a PTFE-lined phenolic cap, removed from the glove box, and heated to 120 °C in an oil bath with stirring for 24 hr. At this point the reaction was cooled to room temperature and the crude mixture analyzed by ^{1}H NMR. Yields were obtained using an internal tetrachloroethylene standard.

Procedure for catalytic borylation of 1 equiv. n-octane in cyclohexane solvent (Figure 5.11, 5.13). In an inert-atmosphere glove box, a 4 mL vial was charged with $[(Mes)Ir(Bpin)_3]$ (0.0032 g, 4.5 μmol, 3 mol %) and ***ligand*** (4.5 μmol, 3 mol %), and B_2pin_2 (0.039 g, 150 μmol). The mixture was taken up in 2.7 mL cyclohexane and allowed to stir for 2-3 min at room temperature to give a pale yellow-orange solution, followed by the addition of *n*-octane (0.024 mL, 150 μmol, 1.0 equiv). The vial was sealed with a PTFE-lined cap, removed from the glove box and was heated in a 120 °C oil bath for 48 hours to give a deep red solution. The crude mixture was cooled to room temperature, concentrated *in vacuo*, and analyzed by ^{1}H NMR with a tetrachloroethane standard to obtain NMR yields.

Procedure for ^{19}F NMR monitoring of the borylation of neat *n*-octane (Figure 5.5). In an inert-atmosphere glove box, a 4 mL vial was charged with $[(Mes)Ir(Bpin)_3]$ (0.0021 g, 3.0 μmol, 3 mol %), ***ligand*** (3.0 μmol, 3 mol %), and B_2pin_2 (0.026 g, 100 μmol). The mixture was then taken up in 1 mL of *n*-octane, stirred briefly, and 0.5 mL of the resulting

solution was added to a J. Young NMR tube equipped with a sealed capillary containing a C_6D_6 lock and $PhCF_3$ standard. The sealed tube was then removed from the glove box and an initial ^{19}F NMR spectrum was collected at room temperature. The J. Young tube was then heated in a 120 °C oil bath. The tube was removed from heat after 1, 3, 5, and 18 hours for analysis by ^{19}F NMR. NMR spectra were collected at 23 °C after which the tube was returned to the oil bath.

5.5 References

(1) Larsen, M. A.; Oeschger, R. J.; Hartwig, J. F. Effect of Ligand Structure on the Electron Density and Activity of Iridium Catalysts for the Borylation of Alkanes. *ACS Catal.* **2020**, *10* (5), 3415–3424.

(2) Oeschger, R.; Su, B.; Yu, I.; Ehinger, C.; Romero, E.; He, S.; Hartwig, J. Diverse Functionalization of Strong Alkyl C–H Bonds by Undirected Borylation. *Science* **2020**, *368* (6492), 736–741.

(3) Ishiyama, T.; Takagi, J.; Hartwig, J. F.; Miyaura, N. A Stoichiometric Aromatic C-H Borylation Catalyzed by Iridium(I)/2,2′-Bipyridine Complexes at Room Temperature. *Angew. Chem. Int. Ed.* **2002**, *41* (16), 3056–3058.

(4) Preshlock, S. M.; Ghaffari, B.; Maligres, P. E.; Krska, S. W.; Maleczka, R. E.; Smith, M. R. High-Throughput Optimization of Ir-Catalyzed C–H Borylation: A Tutorial for Practical Applications. *J. Am. Chem. Soc.* **2013**, *135* (20), 7572–7582.

(5) Sadler, S. A.; Tajuddin, H.; Mkhalid, I. A. I.; Batsanov, A. S.; Albesa-Jove, D.; Cheung, M. S.; Maxwell, A. C.; Shukla, L.; Roberts, B.; Blakemore, D. C.; Lin, Z.; Marder, T. B.; Steel, P. G. Iridium-Catalyzed C–H Borylation of Pyridines. *Org. Biomol. Chem.* **2014**, *12* (37), 7318–7327.

(6) Oeschger, R. J.; Larsen, M. A.; Bismuto, A.; Hartwig, J. F. Origin of the Difference in Reactivity between Ir Catalysts for the Borylation of C–H Bonds. *J. Am. Chem. Soc.* **2019**, *141* (41), 16479–16485.

(7) Jones, M. R.; Schley, N. D. Ligand-Driven Advances in Iridium-Catalyzed Sp^3 C–H Borylation: 2,2′-Dipyridylarylmethane. *Synlett* **2020**. 24

(8) Jones, M. R.; Fast, C. D.; Schley, N. D. Iridium-Catalyzed Sp3 C–H Borylation in Hydrocarbon Solvent Enabled by 2,2′-Dipyridylarylmethane Ligands. *J. Am. Chem. Soc.* **2020**, *142* (14), 6488–6492.

(9) Chen, H.; Schlecht, S.; Semple, T. C.; Hartwig, J. F. Thermal, Catalytic, Regiospecific Functionalization of Alkanes. *Science* **2000**, *287* (5460), 1995–1997.

(10) Lawrence, J. D.; Takahashi, M.; Bae, C.; Hartwig, J. F. Regiospecific Functionalization of Methyl C−H Bonds of Alkyl Groups in Reagents with Heteroatom Functionality. *J. Am. Chem. Soc.* **2004**, *126* (47), 15334–15335.

(11) Liskey, C. W.; Hartwig, J. F. Iridium-Catalyzed Borylation of Secondary C–H Bonds in Cyclic Ethers. *J. Am. Chem. Soc.* **2012**, *134* (30), 12422–12425.

(12) Li, Q.; Liskey, C. W.; Hartwig, J. F. Regioselective Borylation of the C–H Bonds in Alkylamines and Alkyl Ethers. Observation and Origin of High Reactivity of Primary C–H Bonds Beta to Nitrogen and Oxygen. *J. Am. Chem. Soc.* **2014**, *136* (24), 8755–8765.

(13) Zhong, R.-L.; Sakaki, S. Sp^3 C–H Borylation Catalyzed by Iridium(III) Triboryl Complex: Comprehensive Theoretical Study of Reactivity, Regioselectivity, and Prediction of Excellent Ligand. *J. Am. Chem. Soc.* **2019**, *141* (25), 9854–9866.

(14) Yang, Y.; Gao, Q.; Xu, S. Ligand-Free Iridium-Catalyzed Dehydrogenative Ortho C−H Borylation of Benzyl-2-Pyridines at Room Temperature. *Adv. Synth. Catal.* **2019**, *361* (4), 858–862.

(15) Ohmura, T.; Torigoe, T.; Suginome, M. Iridium-Catalysed Borylation of Sterically Hindered C(Sp^3)–H Bonds: Remarkable Rate Acceleration by a Catalytic Amount of Potassium Tert-Butoxide. *Chem. Commun.* **2014**, *50* (48), 6333–6336.

(16) Zhang, M.; Wu, H.; Yang, J.; Huang, G. A Computational Mechanistic Analysis of Iridium-Catalyzed C(Sp^3)–H Borylation Reveals a One-Stone–Two-Birds Strategy to Enhance Catalytic Activity. *ACS Catal.* **2021**, *11* (8), 4833–4847.

(17) F. Hartwig, J. Regioselectivity of the Borylation of Alkanes and Arenes. *Chem. Soc. Rev.* **2011**, *40* (4), 1992–2002.

(18) Boller, T. M.; Murphy, J. M.; Hapke, M.; Ishiyama, T.; Miyaura, N.; Hartwig, J. F. Mechanism of the Mild Functionalization of Arenes by Diboron Reagents Catalyzed by Iridium Complexes. Intermediacy and Chemistry of Bipyridine-Ligated Iridium Trisboryl Complexes. *J. Am. Chem. Soc.* **2005**, *127* (41), 14263–14278.

(19) Herde, J. L.; Lambert, J. C.; Senoff, C. V.; Cushing, M. A., Cyclooctene and 1,5-Cyclooctadiene Complexes of Iridium(I). *Inorg. Synth*. **1974**, 18-20

(20) White, C.; Yates, A.; Maitlis, P. M.; Heinekey, D. M. (η^5-Pentamethylcyclopentadienyl) Rhodium and − Iridium Compounds. *Inorg. Synth.* **2007**, 29, 228−234.

(21) Iali, W.; Green, G. G. R.; Hart, S. J.; Whitwood, A. C.; Duckett, S. B. Iridium Cyclooctene Complex That Forms a Hyperpolarization Transfer Catalyst before Converting to a Binuclear C–H Bond Activation Product Responsible for Hydrogen Isotope Exchange. *Inorg. Chem.* **2016**, *55* (22), 11639–11643.

(22) Merola, J. S.; Kacmarcik, R. T. Synthesis and Reaction Chemistry of (.Eta.5-Indenyl)(Cyclooctadiene)Iridium: Migration of Indenyl from Iridium to Cyclooctadiene. *Organometallics* **1989**, *8* (3), 778–784. https://doi.org/10.1021/om00105a031.

(23) Chotana, G. A.; Britt A. Vanchura, I. I.; Tse, M. K.; Staples, R. J.; Robert E. Maleczka, J.; Milton R. Smith, I. I. I. Getting the Sterics Just Right: A Five-Coordinate Iridium Trisboryl Complex That Reacts with C–H Bonds at Room Temperature. *Chem. Commun.* **2009**, No. 38, 5731–5733.

(24) Li, L.; Brennessel, W. W.; Jones, W. D. C−H Activation of Phenyl Imines and 2-Phenylpyridines with [Cp*MCl2]2 (M = Ir, Rh): Regioselectivity, Kinetics, and Mechanism. *Organometallics* **2009**, *28* (12), 3492–3500.